Valorization of waste cooking oils through conversion processes into biodiesel catalyzed by [HMIM][HSO_4]

Fábio Júlio Santos Monteiro

Dissertation presented to the Escola Superior de Tecnologia e Gestão of the Instituto Politécnico de Bragança to the fulfilment of requirements to obtain the Master Degree in Renewable Energy and Energy Efficiency

Supervised by

Professora Doutora Ana Maria Alves Queiroz da Silva

Professor Doutor António Manuel Esteves Ribeiro

Professor Doutor Paulo Miguel Pereira de Brito

Bragança, October 2021

“If my mind can conceive it and my heart can believe it, then I can achieve it .”

Muhammad Ali

Acknowledgments

A master's work is a long journey, which includes a trajectory permeated by countless challenges, sadness, uncertainty, joy and many setbacks along the way, but despite the process that any researcher is destined to, it brings together contributions from several people, indispensable for find the best course at every moment of the journey. Treading this path was only possible with the support, energy and strength of several people, one to whom I especially dedicate this life project.

To my advisors, Professor Ana Queiroz, Professor António Ribeiro and Professor Paulo Brito, for their enormous patience, attention and availability, constructive criticism and friendship towards me, especially Professor Ana, who has always believed in me, I am grateful for the exemplary guidance provided by my first year at the Polytechnic Institute of Bragança, a permanent and fruitful interest, a critical and timely vision, an unsurpassed and healthy demanding commitment, which contributed to enrich, with great dedication, step by step, all the stages underlying the work carried out.

To my friend forever, Fretson Almeida, I am grateful for the support and unconditional motivation that aims to make this work valid and a pleasant learning experience. I am grateful for our friendship.

To my friends, Giovanni Afonseca, Fábio Vieira, Elvino Gonçalves, Vera Silva, Edilone da Luz, Igor David, Luís Brito, Ricardo Barros, Christopher St' Aubyn, Pedro Cruz, Domingos Duarte, Keila Fatuda Emanuel Marta and Renato Barros, thank you very much for all the experiences, for all the support and joy shared between us during all these years.

My girlfriend Krisley Costa for her unconditional support throughout all these years, for her love, for the companionship and for always motivating me in the most difficult moments.

Finally, but most importantly, a huge thank you to my parents and my brother, for making this day happen, for all the love, trust and unconditional support, for the possible and impossible things I did so that I would never miss anything throughout my academic and personal path. Without you none of this would be possible and thanks are not enough to express gratitude for all that you have done for me since the day I was born.

Finally, my deep and heartfelt thanks to all the people who contributed to the realization of this dissertation, stimulating me intellectually and emotionally.

Abstract

Biodiesel is a renewable alternative to fossil diesel, produced from vegetable oils, animal fats and residual oils. In the present work, the influence of the application of the ionic liquid 1-methylimidazolium hydrogen sulfate [HMIM]HSO_4 in the catalysis of transesterification/esterification reactions in a simulated acidic oil, obtained through the incorporation of oleic acid in a waste cooking oil, was studied at 65 °C. The effect of the selected parameters: reaction time (2 h, 4 h and 8 h), catalyst dosage (5 % wt, 10 % wt and 15 % wt), molar ratio oil: methanol (1:5, 1:15 and 1:20) and mass percentage of incorporation of oleic acid (20%, 40% and 60%) was studied using a Response Surface Methodology (RSM) from an experimental design based on a Box-Behnken 3^4. Three responses were evaluated: the conversion in terms of reduction of the acidity of the simulated oil (R1), the Fatty Acid Methyl Esters (FAME) mass content of the biodiesel produced (R2) and the yield in terms of mass of FAME obtained at the end of reaction in relation to the initial mass of the simulated oil (R3). In the analysis of the experimental results obtained, it is concluded that for all responses, the least relevant factor is the catalyst dosage, while the other factors are significant for the model. The most favorable reaction conditions for the conversion response in terms of acidity reduction correspond to a reaction time of 6 h, catalyst dosage of 5% wt, molar ratio oil/methanol 1:20, incorporation of 20% oleic acid, temperature of 65 ºC, with an average conversion of 76.70%. The most favorable reaction conditions for the FAME content and yield response are similar, corresponding to a reaction time of 6h, catalyst dosage 5% wt, oil/methanol molar ratio of 1:20, incorporation of 60% oleic acid and temperature of 65 ºC, with an average conversion of 42.52% and 37.70%, respectively.

Additionally, the recovery and reuse of the ionic liquid was studied in two reaction cycles, at the optimum conditions corresponding to FAME content and Yield, already mentioned. The reaction conversion in terms of acidity reduction, FAME content and Yield remained practically constant during the two cycles. In terms of acidity reduction, it was obtained for the first cycle, 69.81% and for the second cycle, 69.39%. FAME content of 42.44% was obtained for the first cycle and 42.60% for the second cycle. Finally, the yield in the first cycle was 35.91% and for the second, a value of 39.50% was obtained. The achieved results indicate that, for the selected operational conditions, IL promotes only the esterification reaction. Thus, the possibility of using this IL to treat oils with high acidity values is viable, and subsequently a transesterification reaction with basic catalysts can be carried out.

Keywords: Biodiesel; Waste cooking oils; Esterification; Response Surface Methodology (RSM); Ionic liquids.

Resumo

O biodiesel é uma alternativa renovável ao diesel fóssil, produzido através de óleos vegetais, gorduras animais e óleos residuais. No presente trabalho, estudou-se a influência da aplicação do líquido iónico 1-metilimidazólio hidrogenossulfato, [HMIM]HSO_4, na catálise de reações de transesterificação/esterificação num óleo ácido simulado através da incorporação de ácido oleico num óleo alimentar usado. A influência dos parâmetros: tempo de reação (2 h, 4 h e 8 h), dosagem de catalisador (5 % m/m, 10 % m/m e 15 % m/m), razão molar óleo: metanol (1:5, 1:15 e 1:20) e percentagem mássica de incorporação de ácido oleico (20 %, 40 % e 60 %) foi estudada utilizando uma Metodologia de Superfície de Resposta (RSM) a partir de um planeamento experimental baseado num Box-Behnken 3^4, mantendo uma temperatura de 65 °C. A conversão em termos de redução da acidez do óleo simulado (R1), o conteúdo mássico em FAME do biodiesel produzido (R2) e o rendimento em termos de massa de FAME obtido no final da reação em relação ao inicialmente presente no óleo simulado (R3) foram as três respostas estudadas. Na análise dos resultados experimentais obtidos, conclui-se que para todas as respostas, o fator menos relevante é a dosagem de catalisador, enquanto os outros fatores são significativos para o modelo. As condições reacionais mais favoráveis para a resposta conversão em termos de redução de acidez correspondem a um tempo de reação de 6 h, dosagem de catalisador de 5 % (m/m), razão molar óleo/metanol 1:20, incorporação de ácido oleico de 20 %, temperatura de 65 ºC, com uma conversão média de 76,70 %. As condições reacionais mais favoráveis para a resposta conteúdo em FAME e do rendimento são semelhantes, correspondendo a um tempo de reação de 6 h, dosagem catalisador 5 % (m/m), razão molar óleo/metanol de 1:20, incorporação de ácido oleico de 60 % e temperatura de 65 ºC, com uma conversão média de 42,52 % e 37,70 %, respetivamente.

Adicionalmente, a recuperação e reutilização do líquido iónico foi estudada em dois ciclos, para as condições dos pontos ótimos do FAME e do rendimento, já referidos. Obteve-se uma taxa de conversão em termos de redução de acidez, de FAME e de Rendimento, praticamente constante durante os dois ciclos. Em termos de redução de acidez obteve-se para o primeiro ciclo, 69,81 % e para o segundo 69,39 %, enquanto para o conteúdo em FAME, obteve-se para o primeiro 42,44 % e para o segundo 42,60 %, e para o rendimento no primeiro ciclo obteve-se 35,91 % e para o segundo 39,50 %. Os resultados obtidos indicam que, para as condições operacionais selecionadas, o IL promove apenas a reação de esterificação. Assim, pode ser considerada a possibilidade de usar esse IL para tratar óleos com alto valor de acidez, e posteriormente realizar uma reação de transesterificação com catalisadores básicos.

Palavras-chave: Biodiesel; Óleos alimentares usados; Esterificação; Metodologia de Superfície de Resposta (RSM); Líquidos Iónicos.

Table of Contents

FIGURE INDEX

TABLE INDEX

NOMENCLATURE

ASTM	American Society of Testing and Materials
AV	Acidity value
BBD	Box-Behnken Design
BD	Biodiesel phase
BRs	Stirred batch reactors
CEN	Européen de Normalisation Committee
CSTRs	Continuous stirred tank reactors
ETBE	Ethyl Tertiary Butyl Ether
FAME	*Fatty acid methyl ester*
FFA	*Free fatty acids*
FT-IR	*Fourier Transform Infrared Spectroscopy*
GC-FID	Gas Chromatography with Flame Ionization Detector
GL	Glycerol phase
HEFA	Hydrotreated esters and free fatty acids
HVO	Hydrotreated vegetable oil
IL	Ionic Liquids
OA	Oleic Acid
REN21	Renewable Energy Policy Network for the 21st Century
RSM	Response surface methodology
SDPs	Small dedicated producers

U.S. EPA	U.S. Environmental Protection Agency
WCO	Waste cooking oils

CHEMICAL FORMULAS

NaOH	Sodium hydroxide
KOH	Potassium hydroxide
$AlCl_3$	Aluminum chloride
NaCl	Sodium chloride
Na_2SO_4	Anhydrous Sodium sulphate
HCl	Hydrochloric acid
H_2SO_4	Sulfuric acid
$C_{18}H_{34}O_2$	Oleic Acid
CH_3OH	Methanol
$C_4H_{10}O$	Diethyl Ether
$Na_2B_4O_{7.}10H_2O$	Borax
CH_3OH	Methanol
SO_4^{2-}	Sulfate ion
NO^{3-}	Nitrate ion
PF_6^-	Hexafluorophosphate ion
PF_4^-	Tetrafluorophosphate ion
PH_4^+	Phosphonium ion
$C_4H_9N^+$	Pyrrolidinium ion
BF_4^-	Tetrafluoroborate ion
TBHQ	Tert-butylhydroquinone

$CH_3CH_2NH_2$	Ethylamine
$[EtNH_3]$ $[NO_3]$	Ethylammonium nitrate
$[CF_3SO_3]^-$	Tri-fluoromethanesulfonate
[BMIM]Cl	1-butyl-3-methylimidazolium chloride
$[HMIM][HSO_4]$	1-methylimidiazolium hydrogen sulfate
$[BMIM][HSO_4]$	1-butyl-3-methylimidiazolium hydrogen sulfate
$[BSMBIM][CF_3SO_3]$	3-methyl-1-(4-sulfo-butyl)-benzimidazole
[BMIM]OH	1-butyl-3-methylim-idazolium hydroxide salt
Fe_3O_4 [*β-CD-6-Im-$(CH_2)_3HSO_3$] $[HSO_4]$-Fe_3O_4	Brønsted acidic ionic liquid supported on magnetic
$[C12\text{-}DMAPH][HSO_4]_2$	1-dodecyl-(4-dimethylammonium)-pyridinium bisulfate.

1. INTRODUCTION

Energy and clean air are two of the most basic human necessities, and they are both necessary for socio-economic progress. Rapid population increase, industrialization and urbanization have led to rising energy and clean air need (Mahlia T.M.I *et al*., 2020).

To date, fossil fuels predominate as the primary source of energy, with a high consumption in transport and industries, which makes them a major problem for our planet, given its weak environmental sustainability as the case of its high greenhouse gas emissions to the atmosphere and also because there are limited reserves (Mahlia T.M.I *et al*., 2020).

According to REN21 (Renewable Energy Policy Network for the 21st Century) report published in 2020, the consumption of final energy in 2019 came mainly from fossil fuels with about 80 %, the other 20% is distributed among modern renewable energies (Wind, Solar, Geothermal, Hydroelectric, Biomass, etc.), nuclear energy and the traditional use of biomass. To circumvent these high percentages of fossil fuels, alternatives must be found to avoid serious consequences for our ecosystem.

Biodiesel emerges as a biofuel, biodegradable, environmentally sustainable and less toxic when compared to fossil diesel. That has been acquiring much attention over the years being used already in some countries in a pure or mixed way with diesel, also having a by-product that can be valued and applied in several areas such as the chemical and cosmetic industry. Chemically it can be defined as fatty acid esters *(fatty acid methyl ester* – FAME), produced through transesterification reactions of a raw material, normally vegetable oils or animal fats, with an alcohol, usually methanol, in the presence traditionally of basic catalysts or acids, catalysts that are highly corrosive and difficult to recover (Wu, Q. *et al.,* 2007).

Thus, biodiesel production is subdivided into three generations that have been developed over time to obtain better use and efficiency in the production process in order to have fewer environmental, social, and economic consequences. Biodiesel 1st Generation consists essentially of its production through raw materials from edible vegetable oils such as palm oil, sunflower oil, rapeseed oil, among others, which has caused socio-economic conflicts since these oils compete directly with the food sector, thus reducing the quantities available and consequently increasing their prices. The 2nd Generation came to get around these problems caused, being now produced through inedible oils such as *Jatropha Curcas oil, salmon* oil, tobacco seeds, among others, becoming more environmentally and economically efficient raw materials, however, new problems have appeared, such as the case of large tracts of land, the

intensive cultivation of these crops and consequent deforesting of conflicting land also with their use for agriculture. Then appears the 3rd Generation to overcome these problems associated with other generations, which consists of the use, on the one hand, microalgae which is a very efficient raw material with higher yields, and on the other hand, the use of waste cooking oils (WCO), because it is a residue that can be reused and with high energy content. However, these processes still need better studies, due to the problems associated with the production processes through transesterification, with regard to the high content of Free Fatty Acids (Mahlia T.M.I *et al*., 2020).

Conventional catalysts present several problems for the environment, and for this reason, there is a need to develop more environmentally friendly catalysts. Ionic Liquids (IL) have attracted a lot of attention in recent decades, presenting themselves as the main alternative to traditional catalysts, being green, non-toxic and non-flammable solvents (Ullah Z. , *et al.*, 2017).

IL's can be defined as liquids of organic salts at room temperature, with a melting point of less than 100 ºC, consisting essentially of cations and anions, acting as catalysts for different reactions, endorsed with unique properties, such as their thermal stability, low vapor pressure, ability to dissolve a wide variety of organic and inorganic components, easy to separate and the availability of highly purified products (Ullah, Z. *et al.*, 2018).

Through the literature review, it can be observed that IL's used in biodiesel production, under optimal conditions, allow to obtain high yields, with approximate values of 98 %, revealing that the application of these "green" catalysts in the productive system will have a highly positive impact, and since it is also possible to recover and reuse, thus reducing the associated costs (Ullah, Z. *et al.*, 2018).

1.1. Objective

The main objective of this work is the study of the application of 1-methylimidiazolium hydrogen sulfate ionic liquid ([HMIM][HSO_4]) in the catalysis of esterification/transesterification reactions of a waste cooking oils with high free fatty acids contents.

1.1.1. Specific Objectives

- Evaluate the effect of the ionic liquid over the conversion of the esterification reaction of waste cooking oil with methanol, for biodiesel production;
- Apply a Response Surface Methodology (RSM) based in a Box-Behnken Design (BBD) to determine the optimal reaction conditions (reaction time, catalyst dosage, molar ratio methanol: oil and incorporation of oleic acid in waste cooking oil to simulate an oil with high acidity) for the esterification reaction of waste cooking oil with methanol using a suitable ionic liquid.

1.2. Document Structure

This Dissertation report is organized into 6 chapters. In the first chapter, a brief introduction of the study is carried out and its objectives are presented. The second chapter is focused on the theoretical review of studies already done related to biodiesel production, starting whit a brief history, the current situation in the world for the renewable energy and biodiesel itself: properties, raw materials used in its production, production processes, advantages and disadvantages, and the production on an industrial scale. The third chapter introduces brief concepts about ionic liquids: the main characteristics, properties and advantages associated with their application in the context of biodiesel production. Fourth chapter consists in a description of the methodology, reagents, standards and materials used in the experimental work. In the fifth chapter the results are presented, discussed, related to the established objectives, and compared with results available in the literature. The last chapter presents the main conclusions and suggestions for future work to be carried out.

2. BIODIESEL

Biodiesel is defined as a natural and renewable substitute for fossil fuels and can be produced through the transesterification reaction of a vegetable oil or animal fat, or by the esterification reaction of free fatty acids, with an alcohol usually methanol or ethanol, in the presence of homogeneous, heterogeneous or enzymatic catalysts (Ramos, L. *et al.*, 2011).

The use of vegetable oils for biodiesel production began in 1853, by Duffy and Patrick, through the conversion of vegetable oils or animal fats into Biodiesel. In 1893, through inventor Dr. Rudolph Diesel, the diesel engine appeared, which was originally designed to operate with vegetable oils. Peanut oil was used in 1900 in one of its engines at an exhibition in Paris, and it was found that due to high temperatures, the engine operated with different types of vegetable oils, including peanut oil and hemp. "The diesel engine can be powered with vegetable oils and will greatly help the development of agriculture from countries that use it," a phrase uttered in 1911 by Dr. Diesel. It was proposed in the early 1980s to use vegetable oils in the production of an alternative renewable fuel due to concerns about energy supply in the 1970s, and its commercial production began only in the 1990s (Demirbas, 2008).

2.1. Current Scenario of Renewables Energy in the World

The use of energy from renewable sources has been intensifying year after year to combat the various climate problems resulting from the use of fossil fuels. However, despite the increasing deployment of this clean energy worldwide, its share of final energy consumption in 2018 according to the REN21 report, saw only a moderate increase in which modern renewable energy (excluding traditional biomass use) represented an estimated 11 % of final energy consumption, with only a slight increase of 9.6 % compared to 2013, with the largest share of renewable electricity (5.7 %), followed by renewable heat (4.3 %) and transport biofuels (1.0 %) as shown in Figure 1.

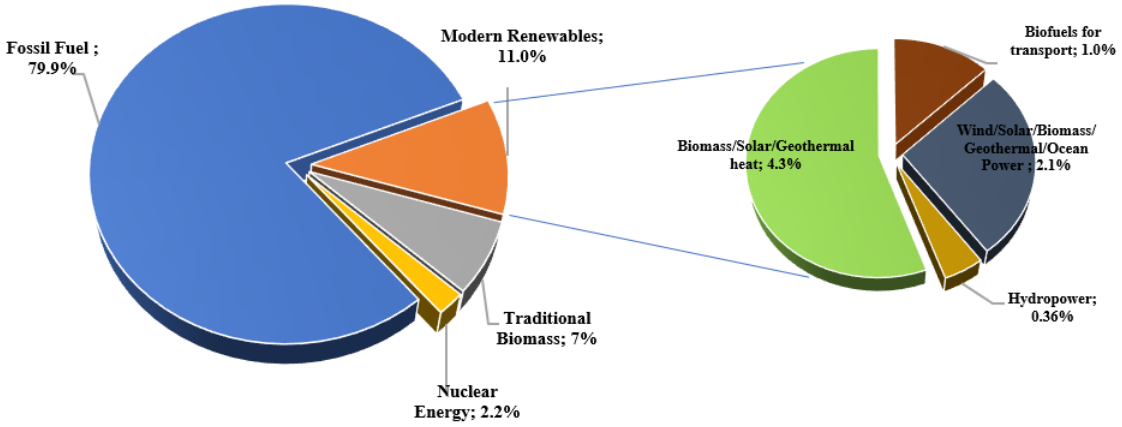

Figure 1 - Estimated renewable share of total final energy consumption Worldwide in 2018.

Source: Adapted from REN21, 2021.

Total demand for modern renewables (i.e., biomass, geothermal, solar, hydro, wind, and biofuels) grew strongly (7.3 EJ) between 2013 and 2018, rising by about 4.0 % per year. Almost half of this growth (48 %) was due to the consumption of wind and photovoltaic solar energy. During the period 2013-2018, total final energy consumption rises by around 1.4 % per year, so renewable energy increased almost three times the rate of total final energy consumption, representing 29 % of the total increase in energy demand. However, this means that other energy sources (predominantly fossil fuels, growing at a rate of 1.3 % per year) accounted for 71 % of the total increase in energy demand. The largest share of renewable energy use is connected to the electricity sector (27.1 %), however the final use accounted for only 17 % of final energy consumption in 2017. The use of energy for transport represented about 32 % and had the lowest share of renewables (3.4 %). The rest of the thermal uses of energy, which include space cooling and heating, water heating and industrial process heat, accounted for more than half (51 %); of this, about 10.2 % were supplied by renewables, as represented in Figure 2.

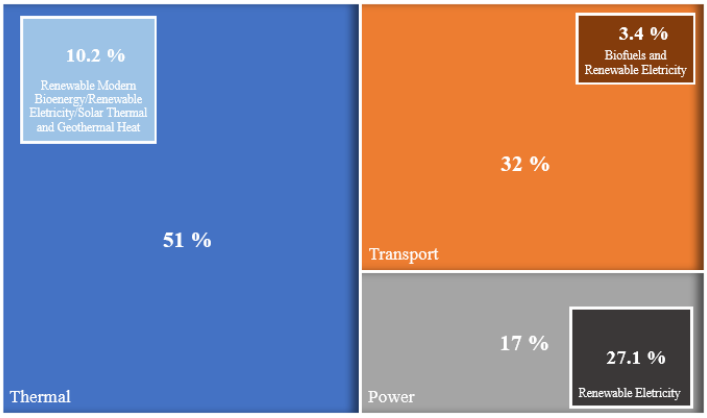

Figure 2 - Renewable portion of total final energy consumption, by final energy use, 2017.

Source: Adapted from REN21, 2021.

Global production of liquid biofuels increased by 5 % in 2019 to 161 billion liters (equivalent to 4 EJ). The United States continued to be the main producer, with a 41 % share, despite the fall in U.S. ethanol and biodiesel production. The next largest producers were Brazil (26 %) and, farther, Indonesia (4.5 %), China (2.9 %) and Germany (2.8 %). The main biofuels are ethanol (produced mainly from corn, sugarcane and other crops) and biodiesel (produced from vegetable oils and fats, including waste such as used food oil). In addition, the production capacity increased for other diesel substitute fuels, made by treating animal and vegetable oils and fats with hydrogen, hydrotreated vegetable oil or HVO, hydrotreated esters and free fatty acids or HEFA. In 2019, ethanol accounted for about 59 % of biofuel production (in energy terms), biodiesel (FAME), to 35 % and HVO/HEFA by 6 %, represented in Figure 3, with biofuel production including biomethane and a range of advanced biofuels, but its production remained low, estimated at less than 1 % of total biofuel production.

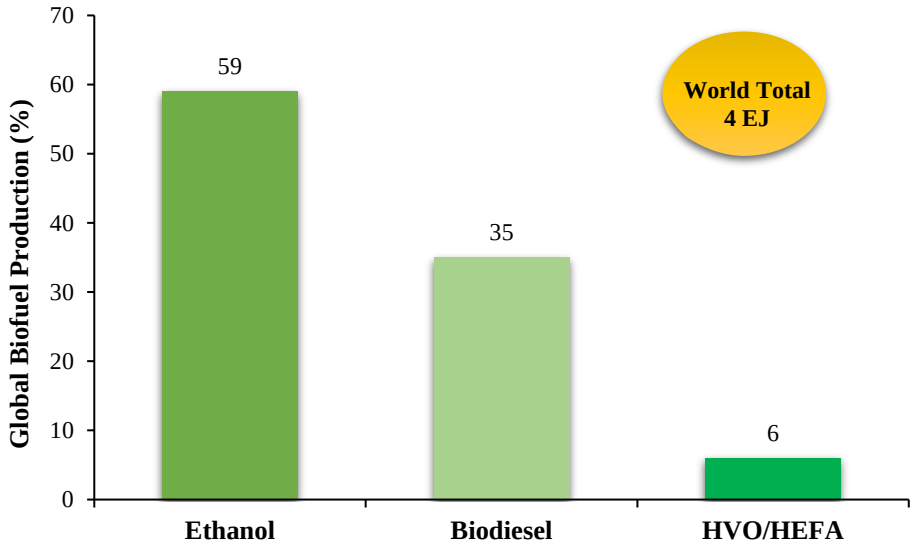

Figure 3 - Global Production of Ethanol, Biodiesel and L HVO / HEFA, by Energy Content, 2019.

Source: Adapted from REN21, 2021.

Global biodiesel production increased by 13 % in 2019 to 45.9 billion liters, with this biofuel being more geographically diversified than ethanol production, and the top five countries in 2019 accounted for 57% of global production. Indonesia took the lead as the country's largest producer (17 % of global production), surpassing the United States (14 %) and Brazil (12 %). The next largest producers were Germany (8 %), France (6,3 %) and Argentina (5.3 %). Indonesia's biodiesel production nearly doubled in 2019 to 7.9 billion liters, compared to 4 billion liters in 2018. Figure 4 shows global biodiesel consumption globally for 2019.

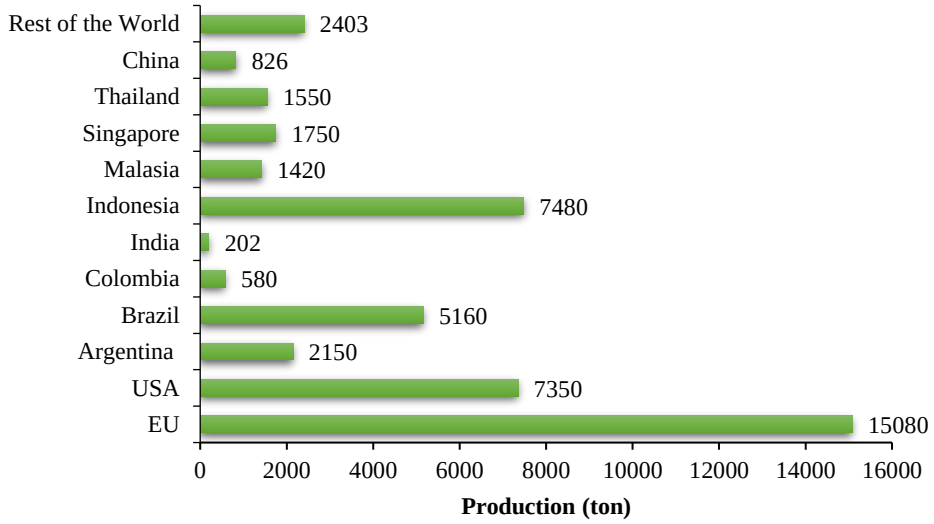

Figure 4 - Global biodiesel consumption in by countries in 2019 (ton).

Source: Adapted from: UFOP, 2021

2.2. Current Scenario in Portugal

The biofuel market in Portugal consists mainly of biodiesel with small percentages of use of Hydrotreated Vegetable Oils or ETBE (Ethyl Tertiary Butyl Ether), incorporated into diesel and gasoline, respectively, and in Portugal, diesel is by far the most popular fuel for road transport (GAIN, 2017).

Since 2015, when the overall quota for biofuels was set at 7.5 percent for transport fuels, the market has adjusted to avoid exceeding the limits for volumetric mixing hitherto achieved by biodiesel and bioethanol, B7 and E10, respectively and the use of third generation raw materials such as WCO, was maximized. Another alternative is the increased use of HVO and bio-ETBE in their diesel or gasoline mixtures, respectively. These measures resulted in lower-than-expected growth in biodiesel sales in 2015 and consequently a reduction in biodiesel consumption in 2016 (GAIN, 2017).

Production

The production of biodiesel by medium / large producers has increased steadily over the years until 2012 after collapsing, and its production decreased further in 2013 and in 2014 it recovered in parallel with the trend of the conventional diesel. Although the quota increased from 5.5 in 2014 to 7.5 percent in 2015, the production growth, was just over 10 percent. In 2016, biodiesel production in Portugal decreased by almost 15 percent. The slowdown in growth and subsequent reduction in production levels in 2015 and 2016 respectively, are a direct consequence of the alternatives put in place to fulfill the mandates without exceeding the

limits of volumetric mixing. In Table 1 shows mainly the fluctuation of production capacity, the production of biodiesel, the capacity used, the production, by small dedicated producers from the year 2012 to 2017, with the values estimated for 2017 (GAIN, 2017).

Table 1 - Biodiesel Production and Capacity Use by M/L Producers in Portugal (1000 m^3).

Source: Adapted from GAIN, 2017.

Year	2012	2013	2014	2015	2016	2017e
Capacity (1000 m^3)	711	742	742	742	742	742
Production Medium/Large Producers (1000 m^3)	351	323	342	380	329	350
Capacity used (%)	49	44	46	51	44	47
Production SDP (1000 m^3)	5	6	7	6	4	5
Total Biodiesel Production (1000 m^3)	566	329	349	386	333	355
Overall Mandate (%)	5	5.5	5.5	7.5	7.5	7.5

e-estimated

Feedstock

The biodiesel sector in Portugal depends heavily on imported raw materials. The national production of oilseeds is essentially based on olive oil and sunflower oil, which are practically all destined for the food market (GAIN, 2017).

In the country, the supply for the production of biodiesel is summarized in animal fats and WCOs, markets that are fragmented and, until 2015, the acquisition of Animal Fats and WCO was only feasible for SDPs (Small Dedicated Producers) (GAIN, 2017).

The deficit in national oilseed production for the biodiesel industry is normally offset by imports of oilseeds to be processed in the country or imports of vegetable oils as shown in Figure 5. In 2016, extensive imports of WCO were observed, which not only resulted in reduction in all imports of crude oil, but also in the reduction of imports of oilseeds for grinding in 2016 as shown in Figure 6, most significantly affecting rapeseed grinding, which until then had traditionally been the preferred oilseed for oilseed crushers oriented towards biodiesel, this due to its higher oil content, compared, for example, with soy (GAIN, 2017).

Consumption and Marketing

With all other incentives eliminated, the consumption mandates are the only drivers of the biofuels market, therefore, the consumption quotas together with the evolution of the demand for formal reformulation define the dimension of the Portuguese biofuel market. (GAIN, 2017)

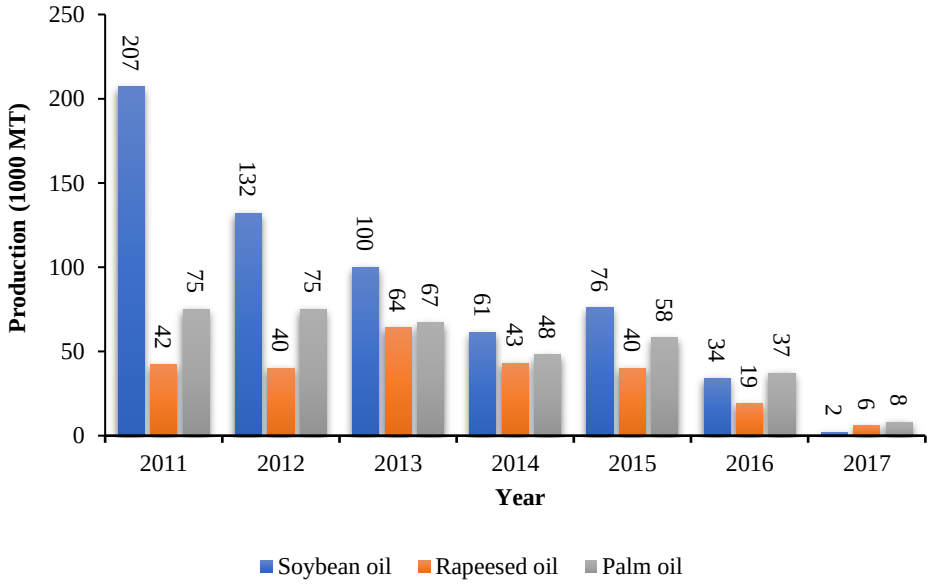

Figure 5 - Portugal Oilseed Imports (1,000 MT)

Source: Adapted from GAIN, 2017.

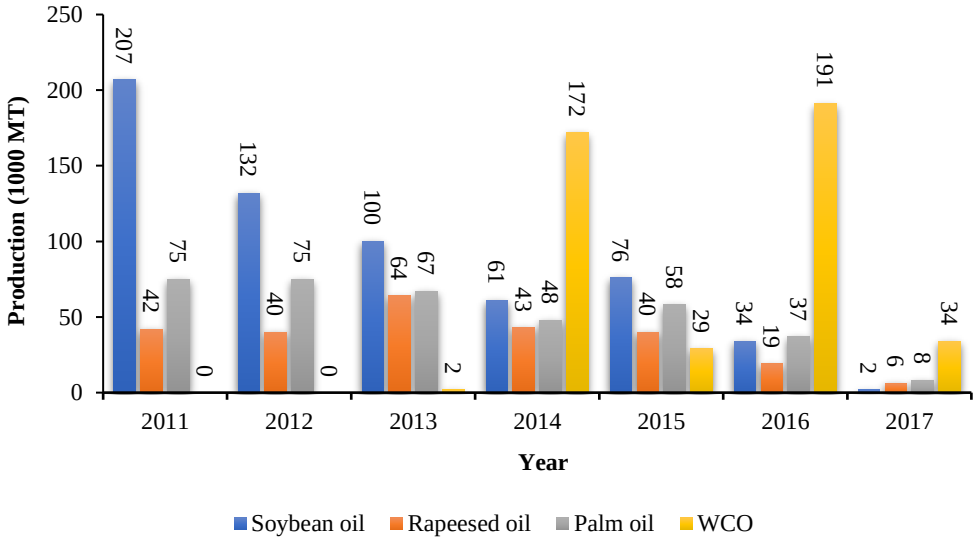

Figure 6 - Portugal Oil Imports (1,000 MT).

Source: Adapted from GAIN, 2017.

As in the vast majority of EU Member States, diesel is the main transport fuel in Portugal. However, while the average EU diesel-gasoline ratio is 2:1, in Portugal it is 4:1, which means the potential for ethanol and gasoline to contribute to meeting the 10 % incorporation target is very lower than in the case of the EU-wide fuel market. The consumption of diesel and gasoline in road transport has shown a downward trend since 2008, due to lower economic activity, but since 2014, as statistical information shows a slight recovery in the use of diesel, while gasoline consumption continues to decrease as shown in Table 2 (GAIN, 2017).

Table 2 - Fuel Consumption for Road Transport in Portugal.

Adapted source from: (GAIN, 2017).

Year	2012	2013	2014	2015	2016	2017e
Bioethanol (1000 m^3)	5	8	4	50	55	10
Gasoline** (1000 m^3)	1521	1466	1462	1449	1412	1375
Diesel* (1000 m^3)	5007	4885	4993	5172	5199	5250
Biodiesel (1000 m^3)	354	322	350	353	322	351
HVO*** (m^3)	2	6	1	59	7	40
Biodiesel + HVO (m^3)	356	328	351	412	329	391

*Includes diesel plus biodiesel; ** Includes bioETBE; ***Assuming TdB-D issued to imported biofuels consist entirely of HVO.

In 2016, the use of WCO as raw material for biodiesel increased even more and the use of soy and palm oil decreased dramatically in the same year, with some biodiesel companies opting for the extensive use of raw materials such as WCO, in total reduction in sales of biodiesel, since produced from raw materials from 3rd generation, contributed to meet the required quotas without increasing the volume of biofuel consumed but, on the other hand, the vast majority of the WCO used for the production of biodiesel in Portugal, it is imported from outside the EU, a situation that further increases Portugal's dependence on imported raw materials (GAIN, 2017).

2.3. Biodiesel as a Renewable Energy Source

Biodiesel, a renewable alternative to diesel, is defined as a biofuel consisting of alkyl esters of long-chain fatty acids, which have combustion properties like those of diesel. The use of biodiesel in diesel engine presents better degradation characteristics and lower emissions of carbon monoxide (CO), carbon dioxide (CO_2), hydrocarbons, particulate matter and volatile organic compounds, but produces higher NOx emissions, being these the most harmful parameters that affect the environment through acid rains, human diseases, and other. CO and NO are the primary pollutants in the formation of the tropospheric zone, which is an important greenhouse gas. Biodiesel is the most widely accepted alternative fuel for diesel engines due to its technical, environmental and strategic advantages and was the first alternative fuel that passed the Health Effects testing requirements required by the U.S. EPA. Therefore, biodiesel in place of diesel, provides a safe environment, and provides energy diversification and sustainable replacement of oil fuel and is an insurance policy against geopolitical risks and government insecurity on fossil fuel costs and fuel safety in the near future (Ajala E., *et al.*, 2015).

2.4. Raw Materials

Biodiesel can be produced using raw materials like vegetable oils, which may be or may not be edible, animal fats and also through waste oils such as waste cooking oils.

The chemical structure of vegetable oils and animal fats are basically similar, composed mainly of triglycerides, with a small fraction of diglycerides and monoglycerides. Vegetable oil also typically contains long chains of carbon and hydrogen atoms, with functional groups of esters. Molecules of vegetable oils are almost three times larger than normal diesel molecules, a large structure called triglycerides. The atomic size and structure of the triglyceride cause it to freeze at low temperatures, which means that its direct use in engines is complicated. The common atomic structure of triglycerides is shown in Figure 7 (Ruhul, *et al.*, 2015).

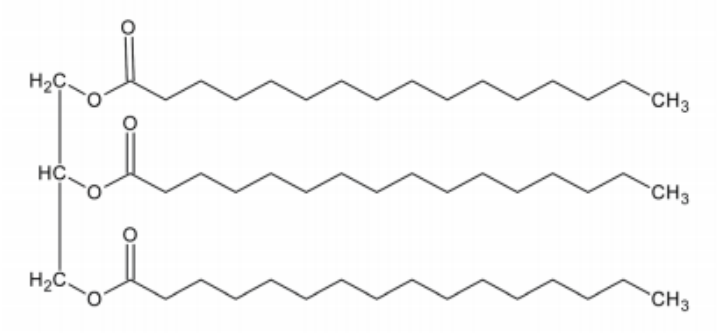

Figure 7 - Triglycerides.

Source: Ruhul, *et al.*, 2015.

Biodiesel production and, as a result, feedstock demand, has increased over the world. The total amount of feedstock used in 2019 increased by more than 11% over the previous year, to almost 46 million tons. Palm oil accounts for 39% of the worldwide resource basis, soybean oil for 25%, and rapeseed oil for 14%, while utilized culinary fats, animal fats, and other fats account for the remaining 11%. Palm oil increased by 4% in 2019, while soybean and rapeseed oil both experienced modest decreases of 1 and 2 percentage points, respectively. Figure 8 shows the portion of each raw material worldwide and in European Union (UFOP, 2021).

In the European Union the production was up to 14.9 million tons in which rapeseed oil is the most common feedstock for biodiesel manufacturing, but its share is decreasing. It dropped to 38% in 2019, down from 46% in 2016. On the other hand, since policy continues to support its usage, the use of waste cooking oil has expanded considerably. Biofuels from waste and residues count double towards national quota commitments in the EU. International competition from low-cost feedstocks, on the other hand, barely rose in 2019. Palm oil's share of the market increased by only 1% to 30%. Imported palm oil is the most common feedstock

in biodiesel fuel production in nations like Italy, Spain, and the Netherlands, but rapeseed oil is the most common feedstock in Germany and France (UFOP, 2021).

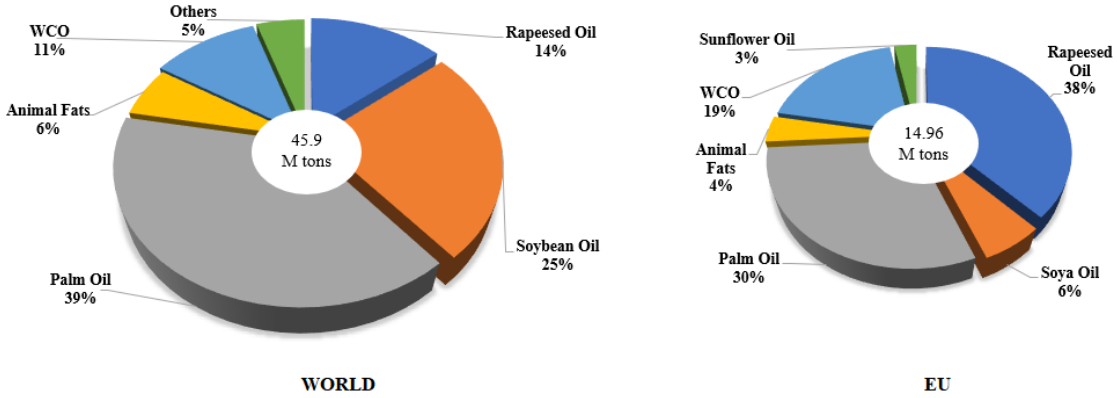

Figure 8 - Raw Materials used in Europe and in the World for Biodiesel Production in 2019.

Source: Adapted from UFOP, 2021.

Table 3 shows some of the various sources used for biodiesel production, including the percentage of oil content of each source.

Table 3 - Different sources of oil for biodiesel production.

Source: Adapted from Ambat I. *et al.*, 2018.

Raw Material	Oil Type	Oil Content (%)
Sunflower Oil	Edible Oils	25-35
Soybean Oil		15-20
Rapeseed Oil		38-46
Palm Oil		30-60
Jatropha Oil	Non-Edible Oils	30-40
Beaver Oil		45-40
Chinese tallow oil		44.15
Karanja Oil		27-39
Mutton fat	Animal Fats and Other Sources	30-70
Waste Cooking Oil		
Microalgae		

Based on Table 3, the raw materials with the highest oil content are palm oil, beaver oil, animal fats and other sources such as microalgae, while soybean and sunflower oil have lower oil content. The conversion of edible oils into biodiesel was considered a process that directly affects the food sector since they are used essentially for food production. This imbalance is a cause for concern, as competition with the food market can also negatively affect the price of biodiesel (Ambat, I. *et al*., 2018).

In this sense, inedible oils and animal fats become attractive since they have a high growth potential such as microalgae, cattle fats, which in the case of the last-mentioned raw material, require intensified pretreatment since they are solid sources (Tadevosyan A., 2017).

The use of inedible oils and waste raw materials for the production of biodiesel have several advantages, including reducing the price of the material and avoiding competition with the food market (Ambat, I. *et al*., 2018).

2.4.1. Vegetable Oils

Conventionally biodiesel is produced through the transesterification of edible vegetable oils such as soybean oil, beaver oil, palm oil, among others, and these are of primary need in biodiesel production, since they have high yields and low percentages of *free fatty acids* (FFA). One of the major disadvantages of edible food oils is certainly the high costs associated with obtaining them and being directly linked to the food industry (Gupta, J. *et al.*, 2016).

Due to these obstacles, attention should be focused on inedible vegetable oils since these are not used in human food and can be grown in arid fields. Oil from the Jatropha plant is one of the most promising inedible oils for biodiesel production and is one of the most developing raw materials in some countries such as India and can be grown easily without needing intensive care (Banković-Ilić *et al.*, 2012).

The great disadvantages associated with inedible vegetable oils are related to the high levels in FFA, high viscosity, insufficient quantities available for use in the industry, thus leading to problems of self-sufficiency of them for biodiesel production (Gupta, J. *et al.*, 2016).

Table 4 shows the fatty acid composition of 4 types of vegetable oils used as raw material in biodiesel production.

Table 4 - Fatty acids present in vegetable oils used as raw material in biodiesel production.

Source: Adapted from Sajjadi, B. *et al.*, 2016.

Vegetable Oils	Composition in fatty acids (%)						
	C14:0[a]	C16:0[b]	C18:0[c]	C18:1[d]	C18:2[e]	C18:3[f]	C20:0[g]
Soybean Leo	---	12.13	3.49	23.41	54.18	6.5	---
Palm Oil	---	39.83	5.33	41.9	11.46	0.15	---
Rapeseed Oil	---	3.36	1.12	63.33	22	8.11	---
Jatropha Oil	1,4	14.62	7.36	41.43	35.42	0.2	0.3

[a] Myristic acid methyl ester [b] Palmitic acid methyl ester, [c] Stearic acid methyl ester [d] Oleic acid methyl ester, Elaidic acid methyl ester [e] Linoleic acid methyl ester, Linolelaidic acid methyl ester [f] Linolenic acid methyl ester [g] Arachidic acid.methyl ester

As seen in Table 4, the content in methyl esters of fatty acids varies from oil to oil and soybean oil, palm and rapeseed esters are essentially composed of methyl esters of palmitic

acid, stearic, oleic, linoleic and linolenic, while for jatropha oil the presence of myristic acid methyl esters and araquidic acid methyl ester is also found. Soybean oil has a higher content in oleic acid methyl esters and in a lesser percentage the linoleic acid methyl ester. For palm oil, rapeseed oil and jatropha oil the ester present in higher percentages is the oleic acid methyl ester, while the methyl esters with lower presence are respectively, linolenic acid methyl ester, stearic acid methyl ester and linolenic acid methyl ester.

2.4.2. Waste Cooking Oil

As already mentioned, one of the biggest obstacles to the development of biodiesel production is related to the high costs of its raw materials. Therefore, the exploitation of waste materials is extremely important in order to reduce their costs and make the production process economically viable. Waste Cooking Oil (WCO) is a waste that can be converted into biodiesel, which will help reduce pollution, since it is discarded in the environment, and this conversion will be very valuable due to the addition of energy in the existing energy network (Sahar, *et al.*, 2018).

One of the major obstacles to the use of WCO as a raw material in biodiesel production is certainly the unwanted presence of FFA that can lead to the saponification process; the unwanted presence of water that can lead to the hydrolysis process and other solid impurities, resulting consequently in low reaction yields (Yaakob, Z. *et al.*, 2013).

Therefore, WCO requires physical treatment processes that essentially include filtration for removal of suspended solids and repeated washes for separation of water-soluble impurities, and also needs chemical treatment processes that encompass acid esterification and distillation for a reduction in FFA content (Banerjee, A. *et al.*, 2009).

2.5. Biodiesel Production Processes

Conventionally, biodiesel is mainly produced via transesterification of triglycerides with alcohol. The source of triglycerides for transesterification can vary widely, including animal fats, vegetable oils, used food oils, microalgae oil and others. Biodiesel can be produced using homogeneous, heterogeneous catalysts, biocatalysts and ionic liquids (Tran, DT. *et al.*, 2017).

2.5.1. Transesterification

Transesterification reaction for biodiesel production is widely described as the addition of an alcohol, usually methanol or ethanol with raw materials such as vegetable oil, algae oil or animal fats, in the presence of a acid or base catalysts. The general equation for

transesterification reactions of fatty acid methyl esters (FAME) are shown in Figure 9, where R1, R2 and R3 represent mixtures of long chains of fatty acids (Ruhul, *et al.*, 2015).

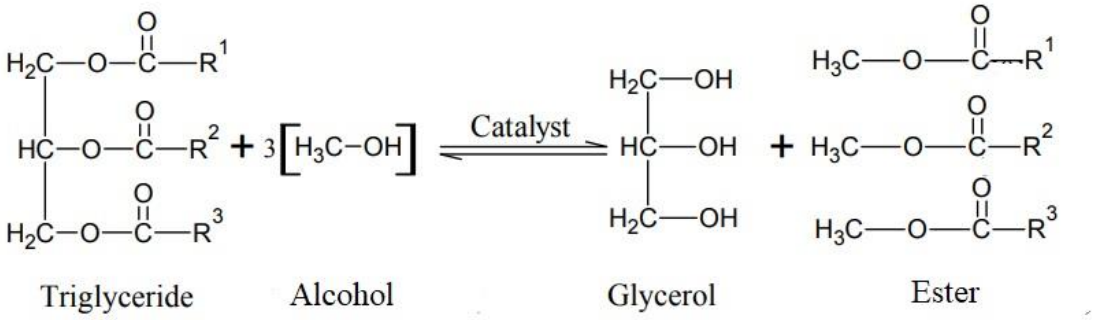

Figure 9 - General scheme for the transesterification reaction.

Source: Adapted from Ruhul, *et al.*, 2015.

2.5.2. Esterification

An esterification reaction is one in which an ester is produced from one or two other organic substances and the most common method for producing esters is by chemically reacting an organic acid with an alcohol, usually methanol, with the help of an acid catalyst. The general esterification reaction is shown in Figure 10, where R represents small alkyl groups and R1 the fatty acid chains, which can be carried out in vegetable oils or animal fats (triglycerides), with methanol or ethanol (short-chain alcohols) to produce biodiesel, especially where considerable amounts of free fatty acids are present, such as residual oils, non-edible oils, animal oils and refined vegetable oils, having a high amount of saturated fatty acids, like stearic acid, which contains 18 atoms of carbon. In some cases, the homogeneous reaction catalyzed by an acid is not viable as it can cause corrosion and consequently environmental problems. In contrast, heterogeneous reactions do not show corrosive behavior, being easier to use given the ease of dividing products, reducing the amounts of wastewater and reducing instrumentation of processes, expenses, time and environmental problems, demonstrating that the heterogeneous reaction catalyzed by acid is preferred for these types of reactions (Ruhul, *et al*., 2015).

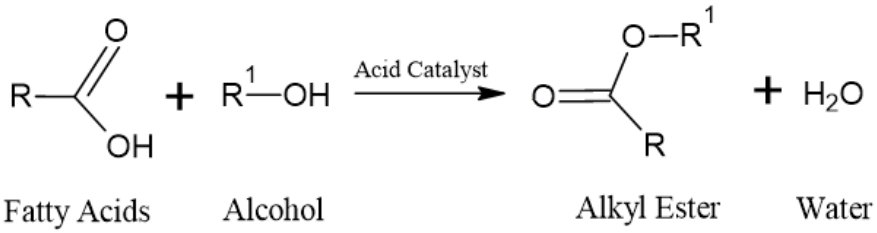

Figure 10 - - General scheme for the esterification reaction.

Source: Adapted from (Ruhul, et al., 2015).

2.6. Catalysts used in Biodiesel Production

The use of green resources as raw material and the type of catalyst are the main criteria to influence the yield and sustainability in the production of biodiesel. To produce biodiesel, in terms of catalysis it is necessary to have triglycerides, an alcohol and the aid of basic or alkaline, acid or enzymatic catalysts (Tran, DT. *et al.*, 2017).

Catalyst is a substance that, without being consumed during the reaction, increases its speed. The catalyst is used in the first stage of the chemical reaction and in the next stage it can be regenerated (Silva, J., 2008).

Potassium hydroxide and sodium hydroxide are the most common homogeneous catalysts and the transesterification process using these catalysts is more commercially used because they are easier to find and due to their low cost. When these catalysts are used, the process is carried out in environments of low temperature and pressure, not requiring large amounts of alcohol and the yield is high without resorting to intermediate steps. However, homogeneous alkaline catalysts have disadvantages because they are highly hygroscopic, due to the absorption of water from the air during storage and because they form water when dissolved in alcohol, affecting their performance (Leung, Y.C., *et al.*, 2010).

Several catalysts are associated with biodiesel production technology. Based on previous reviews, catalysts can be classified as homogeneous catalysts (acids or bases), heterogeneous catalysts (acids or bases), and biocatalysts (enzymes). These catalysts and their subtypes are listed in Figure 11.

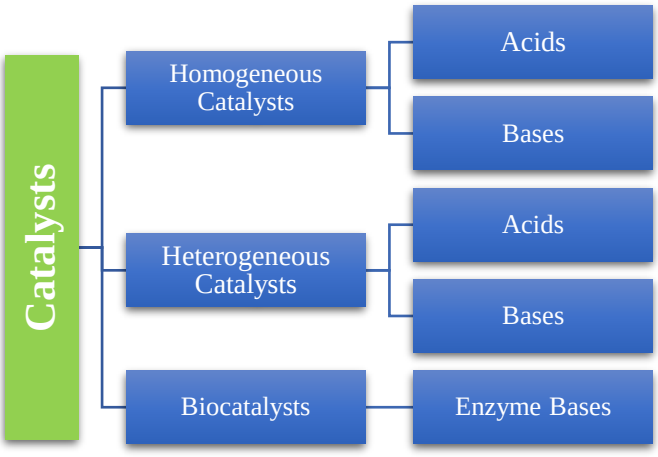

Figure 11 - Catalysts used in biodiesel production technology.

Source: Adapted from (Ruhul, *et al.*, 2015).

2.6.1. Homogeneous Catalysts

Homogeneous catalysis involves a sequence of reactions that includes a catalyst of the same phase as the reagents. For the most part, a homogeneous catalyst is dissolved or co-dissolved in the solvent with all reagents. Sodium hydroxide (NaOH) or potassium hydroxide (KOH) are currently the most popular homogeneous catalysts for the production of biodiesel. However, some researchers suggest that these homogeneous base catalysts are only suitable for raw materials with a low content of free fatty acids. If the FFA content is greater than 6 wt %, the base catalyst process is unsuitable for biodiesel synthesis. Thus, some scientists recommend that the content of free fatty acids be less than 2 wt %. The homogeneous base catalyst is gradually gaining popularity in the industrial production since it requires a low reaction temperature to synthesize biodiesel at atmospheric pressure and it offers a high yield under ideal conditions. The limitations of the use of a homogeneous catalyst for biodiesel synthesis are directly linked to the generation of water throughout the acid esterification, which slows down the process, it is almost impossible to reuse due to its associated costs and the corrosive nature of these catalysts (Ruhul, *et al.*, 2015).

2.6.2. Heterogeneous Catalysts

Catalysts with a different phase or state than the reactants are considered heterogeneous catalysts, being a practical material that regularly creates active sites with their reagents under the reaction atmosphere. Its application will result in simpler and less expensive separation processes and the disadvantages associated with these catalysts include high temperatures and higher proportions of alcohol to oil than those required in the homogeneous catalytic procedure. Some of these catalysts have demonstrated good performance even under the reaction conditions used for homogeneous catalysts. Separation, purification and reuse of the catalyst are among the most attractive features of the heterogeneous catalytic process. Some examples of heterogeneous catalysts are alkali metal carbonates and hydrocarbons, alkali metal oxides, anionic alkali metal hydroxide resins, and basic zeolites (Ruhul, *et al.*, 2015).

2.6.3. Enzyme Catalysts

The enzymatic process has also been used in the production of biodiesel due to its benefits over the use of chemical catalysts. Although this method has been reported in numerous literatures, the use of this process in the industrial and commercial production of biodiesel is still at an experimental stage. Enzymatic catalysts have a high catalytic activity and can simultaneously catalyze the transesterification of triglycerides and the esterification of free fatty acids. Lipases have attracted significant interest due to their efficiency over other catalysts, such as in the

separation of glycerol during the production process. The use of lipases as a catalyst has a positive effect on the transesterification process, as they require less intense reaction conditions, can be unlinked without difficulty, and are reused for several cycles without getting lost during the process. However, the biggest drawback to using such catalyzed processes includes its high cost and deactivation of the enzyme under higher operating conditions (Alajmi, S.M.D.A *et al.*, 2017).

2.7. Physicochemical Properties of Biodiesel

In order to guarantee good quality of biodiesel, it is necessary to establish quality parameters, which aim to set limit rates of contaminants, so that it does not harm the performance, the quality of CO_2 emissions, the integrity of the engines, and in order to guarantee good security in transport, handling, and monitoring of possible product degradation in the storage process must also be done. The first country to define and approve the quality standards for biodiesel applied to colza methyl esters was Austria and other countries were also setting these standards. The quality standard of biodiesel is currently established by standards, the most used is the European Union, EN 14214 of 2003 from the European Committee for Standardization - Européen de Normalisation Committee - CEN, and the American quality standard, which is the ASTM D6751 of 2002, carried out by ASTM - American Society of Testing and Materials (Lôbo, P. *et al.*, 2009).

The quality of biodiesel can be characterized by its viscosity and density, by the number of cetane, by its acidity, pour point, by the distillation rate, sulfur content, among other parameters. One of the most important factors that affect the yield during the transesterification reaction is related to the alcohol / raw material molar ratio and the reaction temperature. There is a big setback in relation to the values of density and viscosity of the methyl esters of vegetable oils and the values of viscosity and flash point of FAME's are regular (Demirbas, 2008).

Table 5 shows some of the most relevant characteristics to consider corresponding to the characterization of biodiesel according to EN 14214 - 2003.

Table 5 - Main Properties of Biodiesel in the determination of Quality Parameters.

Source: EN14214, 2003.

Properties	Units	Biodiesel
Viscosity at 40 ºC	mm^2/s	3.50 – 5.00
Density at 15 ºC	kg/m^3	860 - 900
Flash Point	ºC	120
Carbon Waste	% (wt/wt)	0.30
Sulphur Content	% (wt/wt)	0.02
Cetane's No.	------	51
Ester content	% (wt/wt)	96.5
Acidity Index	mg KOH/g	0.50
Free Glycerin	% (wt/wt)	0.02
Total Glycerin	% (wt/wt)	0.25

Viscosity

Viscosity is one of the important parameters to consider when determining the quality of biodiesel. Some engines require a minimum viscosity value because of potential energy losses caused by the injection pump and injector leakage. High viscosities can cause poor fuel combustion, forming deposits, as well as greater penetration into the pulverized fuel cylinder, resulting in greater dilution of the diesel engine oil (U.S Department of Energy, 2016)

Flash Point

This parameter is defined by the minimum temperature where the release of vapors from a liquid is observed, in sufficient quantity to form a flammable mixture with the air. The flash point value of pure biodiesel is considerably higher than that of mineral diesel (Lôbo, P. *et al.*, 2009).

The Flash Point and fuel volatility are inversely related, and this parameter is specified in fuels in order to protect it against highly volatile impurities and contaminations, methanol being the main reason, after the product removal process (Hoekman, K. *et al.*, 2012).

Cetane Number

The cetane number is the indicative value of the delay time in the ignition of fuels for diesel engines, reflecting the ignition quality of the fuel. The greater the number of cetane, the

shorter the ignition time and the longer the unbranched carbon chain, the greater the number of cetane. Compared to diesel, biodiesel has higher values for the number of ketones. While in the European Standard EN14214 - 2003, the minimum number of cetane for diesel and biodiesel is fixed at 51, for the American standard the values of cetane numbers for diesel and biodiesel adopt different values, which are 40 respectively and 47 (Lôbo, P. *et al.*, 2009).

Carbon Waste

This parameter is characterized by the tendency of deposits to form in the combustion chambers. The values of carbon residues can be determined by the formation of soaps, residual glycerides, free water, FFA, the residue from catalysts and unsaponifiable from the raw material (Lôbo, P. *et al.*, 2009).

Table 6 shows the physical and chemical properties of some raw materials used in the production of biodiesel.

Table 6 - Physical-chemical properties of some raw materials used in biodiesel production.

Source: Adapted from Karmakar A. *et al.*, 2010.

Oils or Fats	Density (kg/m^3)	Kinematic viscosity at 40°C (mm^2/s)	Cetane N°	Flash point (°C)
Soybean Oil	913.8	28.87	37.9	254
Sunflower Oil	916.1	35.84	37.1	274
Palm Oil	918.0	44.79	42.0	267
Peanut Oil	902.6	39.60	41.8	271
Cotton	914.8	33.50	------	234
Jatropha Oil	940	33.90	------	225

As shown in Table 6, the properties of the raw materials do not vary significantly from each other. Palm oil has a high viscosity when compared to other raw materials, being a disadvantage since high viscosities can cause combustion deficient in fuel. For the cetane number, sunflower oil has relatively low values, resulting in a shorter ignition time compared to the others. Jatropha oil has a significantly lower flash point than the others, which means that fumes are released faster for combustion.

2.8. Advantages and disadvantages of Biodiesel

Biodiesel has numerous advantages and some disadvantages both in production and for the environment. One of the major problems associated with the production of this biofuel is, without a doubt, the high cost of its raw materials and many of them are inserted in the food

sector, making their production unfeasible in socio-economic terms. Thus, waste cooking oils and animal fats appear as an excellent way to overcome the inconveniences caused in the food industry (Lam K. *et al.*, 2010).

Table 7 shows some advantages and disadvantages related to the production of biodiesel.

Table 7 - Advantages and disadvantages of biodiesel compared to fossil diesel.

Advantages	Disadvantages
➢ It is renewable, biodegradable and less toxic than diesel (Lam, K *et al.*, 2010). ➢ Better emission properties compared to diesel (Johnston & Holloway, 2007). ➢ Compatibility with existing engines (Johnston & Holloway, 2007). ➢ Compared to diesel, biodiesel has higher cetane number values (Lôbo, P. *et al.*, 2009). ➢ The flash point of pure biodiesel is considerably higher than that of diesel (Lôbo, P. *et al.*, 2009).	➢ High costs for its production due to the high costs of its raw materials (Lam, K. *et al*,, 2010). ➢ Higher emissions of nitrogen oxide (NO_x) compared to diesel (Demirbas, 2008). ➢ Lower energy content compared to diesel (Demirbas, 2008). ➢ Engine speed and power are lower than diesel (Demirbas, 2008). ➢ Biodiesel cleans dirt from the engine, which can be an advantage of biofuels, but it is possible that this dirt is collected in fuel filters and clogged (Hoekman, K. *et al.*, 2012).

2.9. Biodiesel Production on an Industrial Scale

The global biodiesel industry has grown significantly over the past decade. One of the main drivers of this tremendous growth is due to the reduction of dependence on oil, which is an ecologically more viable alternative to diesel, allowing the reduction of greenhouse gas emissions. All types of vegetable oils, animal fats, among others, can be adopted as raw material for the production of biodiesel, but for their long-term production, the cost of refined vegetable oils can be prohibitive (Li, Q. *et al.*, 2008).

Vegetable oils for the production of biodiesel must be pre-treated before entering the transesterification process, whenever their quality and refinement are not guaranteed, as identified in Figure 12, which means that the oil sometimes goes through treatments already implemented in previous stages.

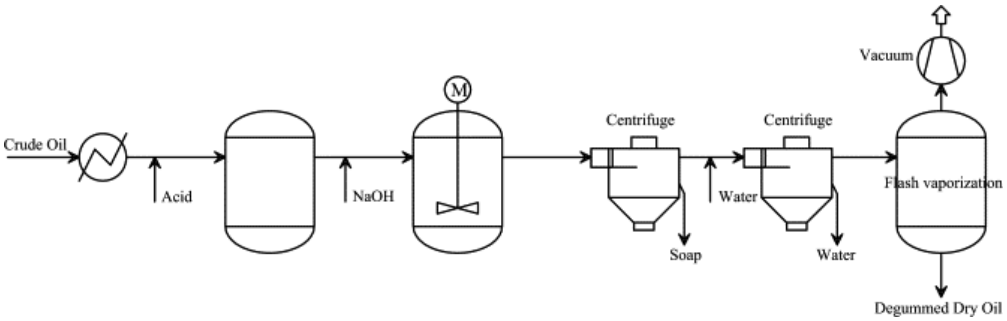

Figure 12 - Vegetable oils neutralization process for biodiesel production.

Source: Santori, G. *et al.*, 2012.

The first step is to heat the oil to about 90 °C which is then mixed with a strong mineral acid, acting as a flocculant clarifier of the oil. Acid treatment is used to remove any hydrophobic particles that may be contained in the raw material. This conditioning step is completed with the mixture parked in a tank for about 10 min. In the next step, vegetable oil is mixed with NaOH (usually 0.1–0.2 % wt) for neutralization. This catalyst allows the removal of FFA that would cause problems in subsequent biodiesel production. Then, the centrifugation follows to separate the soap formed from the previous step. Subsequently, water is added, and the solution goes through a centrifugation process in order to remove traces of impurities. The washing water is then separated from vegetable oil by means of an instantaneous vaporization process conducted with the oil at 116 °C and at a pressure of 0.8–0.9 bar, which makes it possible to reduce the water content to less than 0.1 % wt. The oil is often sent to the reactor at a temperature range between 40 °C and 50 °C. After this, the oil is filtered to ensure that no solid particles enter the biodiesel production section. So as long as its fatty acid content is adequate (< 2.5 % wt), the oil can be sent to the transesterification step (Santori, G. *et al.*, 2012).

In order to prevent the complete formation of soap in the transesterification reactor, the maximum amount of FFA allowed in a system with an alkaline catalyst should be less than 0.5 % wt. If this is not the case, a preliminary step of esterification is required (Santori, G. *et al.*, 2012).

The reaction is catalyzed by several compounds, that can be alkaline or acidic or using biochemical compounds. Homogeneous alkaline catalysts like NaOH or KOH are typically used in industrial processes because of their high conversion rate, low associated cost, lower required temperature, lower amounts of alcohol, low corrosive power of intermediate products when compared to acid catalysis, and a fairly rapid reaction, about 2 h for balance (Santori, G. *et al.*, 2012).

Many installations have based to the block diagram shown in Figure 13 for processing or stages used in biodiesel production.

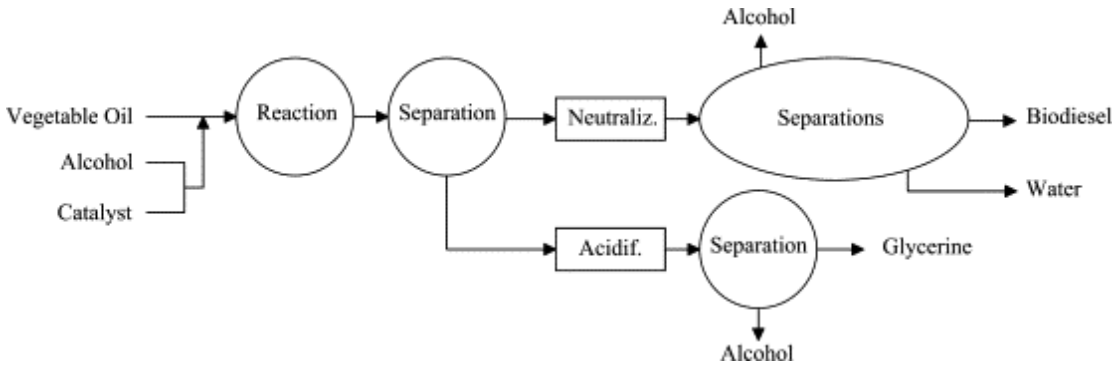

Figure 13 - Block diagram for biodiesel production process.

Source: Santori, G. *et al.*, 2012.

Transesterification reactors

The most important factors to consider in a reactor are the degree of conversion of a reagent and the selectivity of the reaction to the products. The main variables that govern the degree of conversion and selectivity in transesterification are temperature, residence time and mixing rate, although for transesterification, the temperature is limited by the evaporation of the alcohol used as a reagent and the residence time is limited due to the conversion rate the most changes significantly after the first few minutes. The agitation inside the reactor helps in immiscibility between the reagents and assists in the reaction speed. The two main chemical reactor types, used in the large-scale plants, are the stirred batch reactors (BRs) and the continuous stirred tank reactors (CSTRs) (Santori, G. *et al.*, 2012).

Stirred batch reactors

The batch reactor is typically a stirred vessel in which its main function is to first be filled with unreacted material in which the reaction proceeds and later the reaction mixture is removed. For the production of biodiesel, the tank is filled with reagents, that is, oil and alcohol, and catalyst, and this reaction mixture is then heated and stirred for a certain period. After the necessary time has elapsed, the contents of the tank are drained, the FFA and glycerol are separated, and the two products are further processed. Batch reactors are generally used in small biodiesel production plants but are relatively inflexible in terms of productivity. To increase production, it may be necessary to reduce the cycle time, configure other tanks or replace it with a larger one (Tabatabaei & Aghbashlo, 2018).

Continuous-Flow Reactors

The most common continuous-flow system in biodiesel production is the continuous stirred-tank reactor (CSTR) in which the reactor is conventionally a vessel with agitation, set up in a continuous-flow system where the reactants are added continuously, and an equal mass flow of the product mixture is continuously withdrawn. Adequate agitation is required to

increase the interphase area between the two phases as well as to ensure uniform chemical composition and temperature in all volume elements of the reaction mixture (Tabatabaei & Aghbashlo, 2018)

The characteristic for the operation of a CSTR is related with the incoming stream of reactants that becomes mixed with the reaction mixture contained in the vessel. When a CSTR is operated at steady state, the concentration of reactants, intermediaries, and products is even in all volume elements of the vessel and with time. The chemical composition of the reaction mixture at the reactor outlet is equal to the composition in the reaction mixture and because of this is called back-mixing of the reaction mixture, there is always a certain concentration of unreacted reactants and intermediaries at the outlet of the reactor. To address this issue, the percentage of conversion can be raised by increasing the reactor size and, hence, the residence time of the reaction mixture inside the vessel. To increase the conversion, more than one reactor can be used in a cascade as represented in Figure14 in which the process often involves an arrangement of two consecutive CSTRs, the first reactor, the oil is reacted with approximately 80 % of the alcohol. Then, the outlet stream goes through a glycerol removal step before entering the second reactor. The remaining 20 % of the alcohol is then added to this reactor. As a result, this system generates higher conversions of the biodiesel. A lower excess of alcohol is needed compared to a process involving a single CSTR (Tabatabaei & Aghbashlo, 2018).

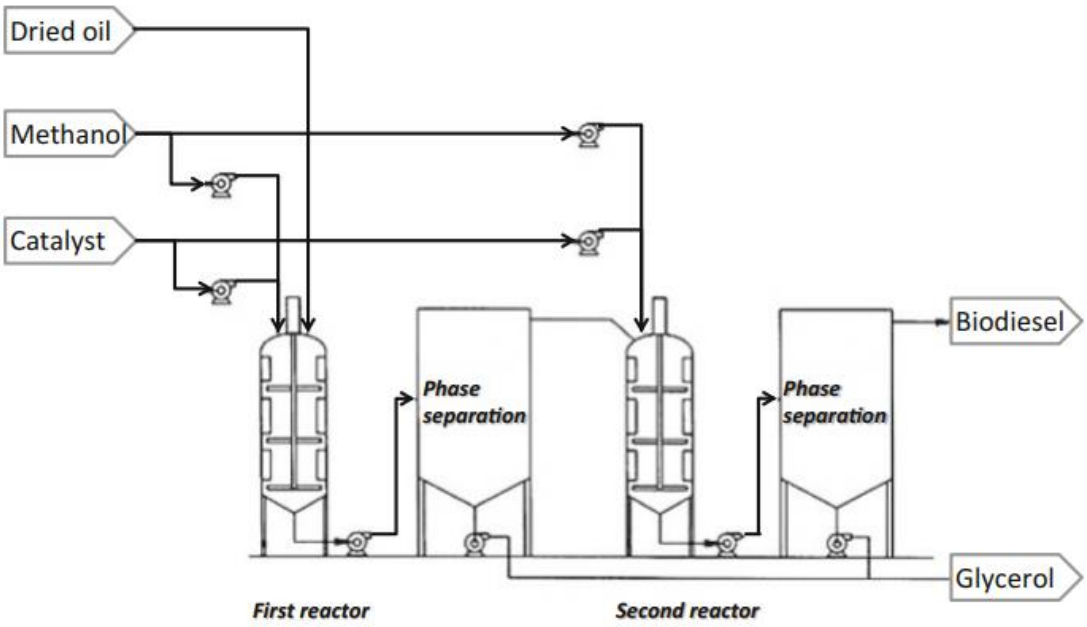

Figure 14 - Biodiesel production in a process with a cascade of two continuous stirred-tank reactors.

Source: Tabatabaei & Aghbashlo, 2018.

Separation of the phase rich in esters (BD) from the glycerol-rich phase (GL)

Products that emerge from a transesterification reactor can easily form an emulsion, especially if they are in contact with water, and these problems can be reduced with the use of volumetric gear pumps. The presence of significant amounts of mono-, di- and triglycerides in the final mixture can lead to the formation of an emulsion layer at the interface between the BD and GL phases and this layer will result in the loss of products if it is not recovered and separated and the final biodiesel may not comply with the stipulated legislation (Santori, G. *et al.*, 2012).

After the reaction, the GL phase is removed from the BD phase and the closer to neutral pH the reaction mixture is, the faster the coalescence of the GL phase will be. Given the low solubility of glycerol in esters, general separation does not require much time and can be done directly in the reactor or by centrifugation in the case of continuous installations. The presence of methanol in both phases increases the solubility of the ester and glycerol. The BD phase is quickly separated from the GL phase. The centrifuge completes this operation in a mixture with a temperature of 50–60 °C and can also separate the solids that accumulate on the outer edge of the centrifuge drum. Excess methanol tends to act as a solvent, slowing down the separation process, but excess methanol is not normally derived from the product flow before GL and BD are separated to avoid reversing the transesterification reaction. Once separated from the GL, the BD goes into a neutralization phase (Santori, G. *et al.*, 2012).

Recovering excess alcohol from biodiesel

After separating a GL phase and neutralization, the BD enters the methanol separation phase, which is usually a vacuum flash vaporization process. The alcohol recovery process can be preceded by an acidification process to remove any soap from biodiesel. The remaining free fatty acids in the BD phase and the salts will be removed later by washing with neutral water. Removing the methanol in the flash separation tank can also cause the soap remaining in the BD phase solution to precipitate, clogging the filters and sieves (Santori, G. *et al.*, 2012).

Ester washing

The water used in the ester washing process is at 50–60 °C and has a slightly acidified pH to remove any soap that might form during the reaction and to neutralize any contaminants. The salts will be removed by the water, and the free fatty acids will remain in the BD. This rinsing with water also enables any residual methanol and free glycerin to be extracted from the BD, although this methanol will need to be removed from the water before the washing stage to prevent it from getting into the wastewater. The neutralizing process adopted before the washing cycle reduces the washing water consumption and minimizes any formation of

emulsions in subsequent purification stages. The BD phase then undergoes water separation, which is often done by a centrifuge operating at a temperature of bigger than 40 °C and capable of separating any solids accumulating on the outer edge of the drum as well. Then the BD, consisting by now almost entirely of esters, can come into contact with clean water again (which must still be separated). Later in the washing process, any remaining water is eliminated from the BD by drying process, thus obtaining biodiesel. The methanol is recovered from the washing water using a distillation column (Santori, G. *et al.*, 2012).

The water used in the ester washing process must be in the temperature range of 50 to 60 °C and must have an acidified pH to remove any soap that may form during the reaction and to neutralize any contaminants. The salts will be removed by the water and the free fatty acids will remain in the BD. This water wash also allows any residual methanol and free glycerin to be extracted from the BD, although this methanol will need to be shipped from the water before the wash step to prevent it from entering the wastewater. The neutralization process adopted before the washing cycle reduces the consumption of washing water and minimizes the formation of emulsions in the subsequent purification steps. The BD phase then passes through the water separation, which is usually done by a centrifuge operating at a temperature above 40 °C and capable of separating any solids that accumulate on the outer edge of the tank and not ending the BD, now consisting almost entirely of esters, it can come into contact with clean water again, which must later be separated. After the washing process, all the remaining water is eliminated from the BD by the drying process, thus obtaining biodiesel. Methanol is recovered from the wash water using a distillation column (Santori, G. *et al.*, 2012).

Adding oxidation inhibitors

Biodiesel contains a large number of molecules with double bonds, so it is susceptible to oxidation and this effect is increased mainly when esters are exposed to light and air or even contain traces of free fatty acids so effective additives are used, usually for use in food, which is tert-butylhydroquinone (TBHQ) (Santori, G. *et al.*, 2012).

GL phase acidification

At the end of the reaction, the alcohol content in the GL phase is much higher than in the BD phase. The GL phase that leaves the separator is only 50-60 % glycerol and contains some of the excess methanol and most of the catalyst and soap, making its value limited and difficult to dispose of. The first refining stage of the GL phase generally involves adding acid to convert the soap into free fatty acids and salts, these FFA's being insoluble in the GL phase, which can be separated, removed and recycled. The fraction rich in free fatty acids accumulates

on the surface of the GL phase and can be removed and recycled in the esterification process and these must be less than 1% of the biodiesel obtained (Santori, G. *et al.*, 2012).

Separation of the alcohol from the GL phase

After acidification and separation of free fatty acids, methanol can be removed from the GL phase and is carried out after acidification, as removing methanol while the GL phase still contains soap leads to solidification. First, the liquid mixture is heated to 90-120 °C, and then the heated liquid is sent through a pressure reducing valve to a tank. The pressure drop induced by the valve causes the most volatile part of the liquid to evaporate. This occurs in a vacuum. At that point, the GL phase would consist of glycerin with a purity close to 85 %, which can be sold as crude glycerin and the glycerin refining process can be carried out, aiming at a purity of more than 95.5-97.7 %, by other methods. Methanol removed from the BD phase and GL phase flows tends to collect all the water that may have entered the process, so that water must be removed in a continuous distillation column before this alcohol is recycled in the process. The recovered methanol should have a water content of less than 0.1% wt, so that the water in the reagent mixture is minimal during transesterification (Santori, G. *et al.*, 2012).

Alcohol purification

In case of methanol continuous distillation is the separation technique used for the purification before the reaction. This is the component with higher thermal power requirement and also the bulkier. Typically, the residual methanol content in water is below the 5 % wt and this flow rate of wastewater can be mixed with the final glycerin stream to adjust the purity at some levels. This solution allows a high-saving on-disposal costs (Santori, G. *et al.*, 2012).

3. IONIC LIQUIDS

By definition, ionic liquids (IL's) are salts composed exclusively of ions (cations and anions) with low melting temperatures, negligible vapor pressure, exceptional thermal and chemical stability. They are liquid at room temperature and can be combined using different sets of cations and anions (Fauzi, M. *et al.*, 2012).

The IL study began in 1914 in a publication by Paul Walden, in which the author reported the physical properties of ethyl ammonium nitrate [$EtNH_3$] [NO_3] (melting point 13-14 ºC), which is formed by neutralizing ethylamine ($CH_3CH_2NH_2$) with concentrated nitric acid (HNO_3). IL's reemerged after World War II, where applications of mixtures of aluminum chloride ($AlCl_3$) and N-ethyl pyridinium bromide are described for aluminum electrodeposition, which was an important discovery. The study was complicated since systems are based on chemically complex solvent bromide and chloride salts. This problem was overcome after 25 years, when Osteryoung's group in 1975, assisted by Bernard Gilbert, studied the physical-defined properties of IL's in detail. This study was a significant advance, but the system they developed had serious limitations, being that it was liquid at room temperature, but in only a narrow range of composition and the cation was very easily reduced. In 1992, Wilkes and Zaworotko published in a publication a preparation and classification of a new class of IL's, which contained the cation 1-ethyl-3-methylimidazolium and a variety of anions. Since this date, many IL's have been developed incorporating several types of anions such as hexafluorophosphate (PF_6^-), sulfate (SO_4^{2-}) or nitrate (NO^{3-}). Gratzel and his co-workers developed IL's more based on hydrophobic anions such as tri-fluoromethanesulfonate $[CF_3SO_3]^-$ and these attracted a lot of attention due to their low reactivity with water and also for their excellent electrochemical properties. Over the years, new classes of cations have been developed, cations based on phosphonium (PH_4^+) and pyrrolidinium ($C_4H_9N^+$), with over one million simple ionic liquids being known to be synthesized (Plechkovaa & Seddonab, 2007).

One of the most important characteristics of IL's is related to the great variety of its physicochemical properties such as polarity, hydrophobicity, viscosity, miscibility in the solvent, among others, making its use advantageous instead of common organic solvents. Despite the many advantages that IL's have over conventional solvents, they are expensive. Its efficient recovery, product isolation and reuse will be the key to its development at an industrial level (Muriell, G., 2009)

The use of IL's as catalysts for the production of biodiesel has as main focus to develop more economical and environmental aspects throughout the process. In addition to its excellent

properties, the catalysis using IL's reduces the number of reaction and purification steps necessary for the preparation and separation of biodiesel, making the process more economical and producing greater purity of esters (Lin, YC *et al.*, 2013).

From the Web of Science website, a study was carried out on the publications made about the Ionic Liquids from the year 2000 to 2020, represented in Figure 15 and in the same way a study was made of the publications made about the use of IL's for production biodiesel represented in Figure 16.

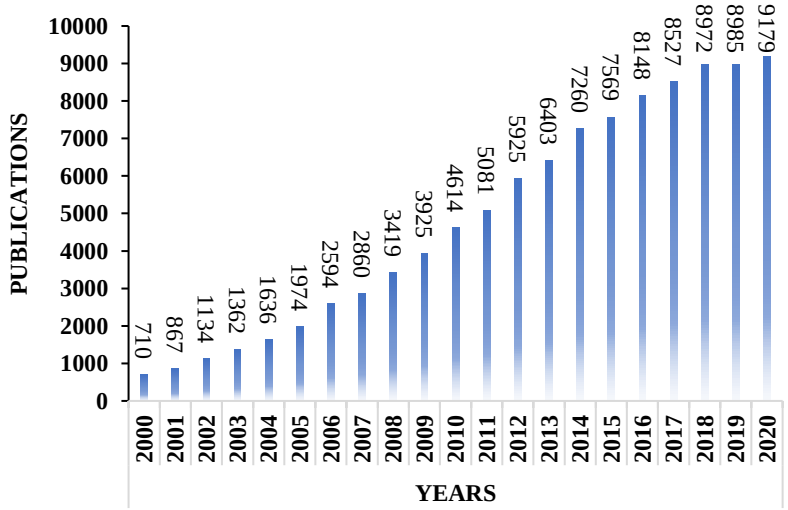

Figure 15 - IL's publications on Web Science website (2000-2020); Consultation held on 23 February 2021.

Source: Own authorship.

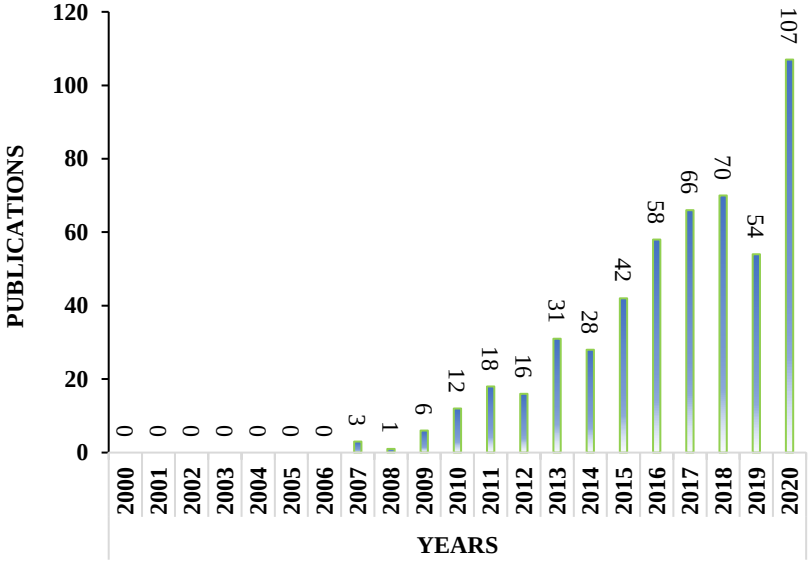

Figure 16 - IL's for biodiesel production publications on Web Science website (2000-2020). Consultation held on 23 February 2021

Source: Own authorship.

As it can be seen through Figure 15, over the 20 years, the number of studies carried out on ionic liquids has been increasing year after year, demonstrating the high interest of the scientific community in these catalysts, which, in the last 3 years, studies have intensified further, reaching around 9179 publications in 2020. In Figure 16, we can see that the publications about IL's for biodiesel production started in 2007, with a reduced number of publications, but which increased year after year, reaching its peak in 2020, with about 107 publications.

3.1. Structure of Ionic Liquids

Similar to all salts, IL's are made up of cationic and anionic species, but are differentiated by their low tendency to crystallize, due to their bulky and asymmetric cationic structure. The countless combinations that we can have of cations and anions, lead to the possibility of adapting the properties of IL, with the anion being responsible for qualities such as, air and water stability and the cation is responsible for the melting temperature and organic solubility (Mohammad & Inamuddin, 2012).

IL's are known as “designer solvents”, because they offer the opportunity to adjust their specific properties to a particular need, for example, researchers can design a specific IL, choosing small negatively charged anions like PF_6^- or PF_4^- and large positively charged cations of imidazole, pyridinium, pyrrolidinium or phosphonium, since these specific IL's can be used to dissolve a certain chemical or to extract a certain material from a solution, concluding that the adjustment of the structure provides properties designed under measure to satisfy specific application requirements (Mohammad & Inamuddin, 2012).

The anions and cations already mentioned, and their possible combinations have been studied over the years, but more and more cations and anions appear, which consequently have been reported by the scientific community (Mohammad & Inamuddin, 2012).

In Figures 17 are represented, respectively, the structures of the cations and anions most commonly used in IL's.

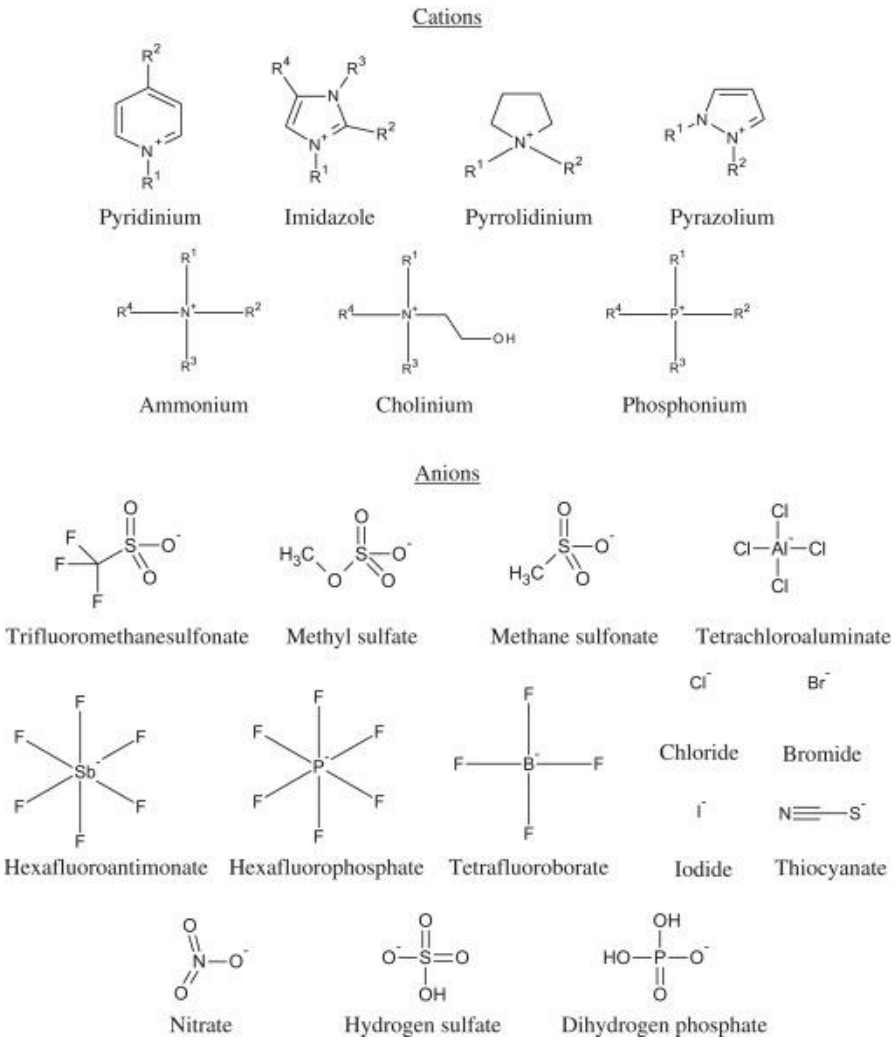

Figure 17 - Commonly used cations and anions in ionic liquids.

Source: (Fauzi, M. *et al.*, 2012).

For imidazolium-based cations, the larger the size and asymmetry of the cation, the lower the melting point of the IL, and consequently, an increase in branching in the alkyl chain, increases the melting point (Mohammad & Inamuddin, 2012).

Anions have a great importance in determining the properties available by each IL, since the introduction of different anions gives rise to IL's with different properties. For example, the combination of the 1-n-butyl-3-methylimidazolium cation with the PF_6^- anion is immiscible in water, while the combination of the same cation with the BF_4^- anion gives IL water solubility. Anions can be divided into 4 essential groups. (Mohammad & Inamuddin, 2012).

- The first, based on aluminum chloride $AlCl_3$ and organic salts, such as 1-butyl-3-methylimidazolium chloride [BMIM]Cl, in which IL's can be Lewis acids or bases, if they contain excess organic salts, or Lewis neutral liquids if they contain equimolar amounts of organic salts and $AlCl_3$;

- The second, based on anions such as PF_6^- and BF_4^-, which are almost neutral and stable in air, although they have disadvantages since they react with strong Lewis acids;
- The third, based on anions such as $CF_3SO_3^-$, $(CF_3SO_2)2N^-$ and similar, which in turn are more stable for some reactions, presenting specific properties, such as low melting point, low viscosity and high conductivity.
- The fourth, based on anions such as sulphates and sulphonates, which are relatively inexpensive and do not contain fluorine atoms, in which the corresponding IL's that originate, can often be easily prepared under ambient conditions, the same being characterized by their vast electrochemical properties and their stability in air.

3.2. Properties of Ionic Liquids

The various ionic liquids have extraordinary properties, making them of great interest to the scientific community, due to the thermodynamics and the kinetics of the reactions they offer, being different from the conventional molecular solvents (Koel, M., 2008)

The use of ionic liquids to the solution of common solvents is very advantageous, since they have properties such as polarity, hydrophobicity, viscosity, miscibility in the solvent, among others, in which they can be modulated using an appropriate combination of anion and alkyl substituents on the cation and these are possible combinations between cations and anions, which give IL a wide range of extremely important characteristics because by manipulating the desired properties, an ionic liquid can be synthesized for specific reaction conditions (Muriell, G., 2009).

The presence of small fractions of water or any organic solvent as an impurity, has major impacts on the physical and chemical properties of IL's, in which small amounts of traces of water present in IL will have a great influence on biocatalytic activity, acidity, density, viscosity, electrical conductivity, enthalpy and many other parameters. In addition, the presence of water in IL's has strong intermolecular interactions, such as that of Van der Waals, hydrogen bonds, electrostatics and others, and when the amount of water is given in elevated supplies, the initials of IL's to dissociate ion pairs or individual ions (Singh & Savoy, 2020)

Density

Generally, most IL's are denser than water, with values ranging from 1 for typical IL's to 2.3 $g.cm^{-3}$ for fluorinated IL's (Koel, 2008). Consequently, if an ionic liquid does not mix with water, it will install itself in the lower phase when there is a mixture of two liquids. The density depends strictly on the size of the cation ring, the length of the cation's alkyl chain, the

symmetry of the ions and the forces of interaction between the cation and the anion. IL's with an aromatic ring, that is, those with less bulky cations, in general, have higher densities than IL's with longer chains or more bulky cations. The density increases with the increase in the symmetry of its cations. The increase in the alkyl chain (less bulky cations) systematically decreases density. IL's with functional groups show higher densities than those of alkyl chains (Freemantle, M., 2010).

Viscosity

Viscosity is a measure of a liquid resistance to flow. Liquids with lower viscosity, flow more easily. Centipoise (cP) is commonly used as a physical viscosity unit. In general, ionic liquids are more viscous than molecular solvents. The viscosities of IL's at room temperature are typically in the range of 10 to more than 500 cP, being higher in comparison, for example, with acetone, water and ethanol, which have viscosities of 0.31, 0.89 and 1.07 cP, respectively, at 25 °C. The viscosity of ethylene glycol at room temperature is 16.1 cP and that of glycerol is 934 cP. The viscosities of IL's generally increase with the increasing of the cation size particularly with the increase in the length of the alkyl chain and the viscosities of IL's decrease with increasing temperature and the changes can be dramatic (Koel, M., 2008).

Steam pressure

The insignificant vapor pressure is one of the most important properties of IL's, as they generally do not evaporate in reaction systems and cannot contribute to air pollution or cause health problems in this context. However, it is possible to distill certain IL’s at high temperatures and low pressure. In general, the vapor pressures of IL's with short and cationic alkyl chains are negligible at room temperature and pressure. Consequently, IL's may show little or no evidence of distillation below their thermal decomposition temperatures (Freemantle, M., 2010).

Conductivity

Ionic liquids, by definition, exhibit ionic conductivity, that is, electrical conductivity. Conductivity has Siemens units per meter (S/m). The conductivity of an IL is a measure of the liquid's ability to conduct electrical current, with ions acting as charge carriers (Freemantle, M., 2010).

Solubility and miscibility

The solubility, miscibility and immiscibility properties of ionic liquids vary widely, depending on the nature of the cations and anions. IL's at room temperature can dissolve organic and covalent compounds, making them attractive for the separation and extraction of materials

from solutions and mixtures, thus having a very significant impact in the course of a chemical reaction (Koel, M., 2008).

Fusion Point

The melting points of ionic liquids, at room temperature, tend to decrease as the size of the anion or cation increases. The symmetry of the cation also significantly influences the melting point. As the symmetry increases, the ions accumulate more efficiently and the melting point of the IL increases. The melting point of an IL can be reduced by adding another salt to form a eutectic mixture (Koel, M., 2008).

High thermal stability

Another essential property of ionic liquids is their thermal stability, in which they generally have high thermal stability when compared to other conventional solvents, which means that IL are less susceptible to decomposition at high temperature (Fauzi, M. *et al.*, 2012).

Acidity and basicity

The characteristic of IL as a green solvent can be highlighted by its nature of having acidic or basic properties, in which they can be modified, changing a combination of cations and anions. The factors that determine the acidity of an IL are the presence of different nitrogen groups, the length of the hydrocarbon chain and the existence of anions in the system. The acidity and basicity of IL are one of the reasons why they are suitable to be used as catalysts in reactions and their suitability as catalysts depends on the nature of the reagents used and the operational conditions of the processes (Fauzi, M. *et al.*, 2012).

3.3. Ionic Liquids in Biodiesel Production

IL's due to their excellent properties such as low corrosivity and ease of recovery, have attracted a lot of attention and have been applied as ecologically beneficial catalysts for biodiesel production reactions, reducing the number of reactions and consequent purification steps required in their preparation and separation allowing a much more economical process and obtaining high percentages of pure esters (Lin, YC *et al.*, 2013).

Table 8 shows the compilation of some recent results obtained by several researchers regarding the use of different ionic liquids as catalysts for biodiesel production.

Yue, S. *et al.*, 2015, use N-methylimidazole and concentrated sulfuric acid as raw materials, a novel Brønsted acidic ionic liquid [HMIM][HSO_4] synthesized and used as catalyst in the esterification reaction of oleic acid and methanol. The chemical structure of [HMIM][HSO_4] was characterized by FTIR and the oleic acid methyl oleate was qualitatively

analyzed by GC-MS. The results showed that the optimal synthesis conditions of oleic acid methyl oleate catalyzed by ionic liquid [HMIM][HSO_4] were obtained as follows: molar ratio of oleic acid to methanol 1:4 (0.04 mol oleic acid), catalyst dosage 3.5 mL and reaction time 6 h. Under these conditions, the esterification rate of oleic acid reached 92.5 %. The esterification rate of oleic acid was still above 85% when ionic liquid [HMIM][HSO_4] had been reused for nine times. Therefore, the ionic liquid [HMIM][HSO_4] showed good catalytic activity and was easily separated from product, which overcame the shortcomings of traditional inorganic acid catalysis.

Ullah, *et al.*, 2015, studied the use of acidic IL's as catalysts for the production of biodiesel using WCO as raw material. Due to the high levels of FFA's contained in waste cooking oils, the direct use of alkaline catalysts to catalyze the transesterification reaction will not be possible due to the phenomenon of saponification and separation of layers. Biodiesel production was carried out in two stages, involving the esterification and transesterification processes. Due to its long side chain, IL 1-butyl-3-methylimidiazolium hydrogen sulfate, [BMIM][HSO_4], proved to be the most effective and with a catalyst dosage of 5 % (wt/wt), methanol / oil molar ratio 15:1, 1 hour of reaction, temperature of 160 ºC and a stirring speed of 600 rpm, the best performance was achieved, and the acidity value of WCO was reduced to values below 1.0 mg KOH/g. The second stage of transesterification was catalyzed by KOH with a catalyst dosage of 1.0 % wt, temperature of 60 ºC and a reaction time of 1 hour, resulting in a final yield of 95.65 %.

Ullah Z. *et al.*, 2017, studied the production of biodiesel using WCO as a raw material using trifluoro methane sulfonate 3-methyl-1-(4-sulfo-butyl)-benzimidazole [BSMBIM][CF_3SO_3] as IL. The WCO was characterized using gas chromatography linked to the flame ionization detector GC-FID (Gas Chromatography - Flame Ionization Detector), being able to determine the different fatty acids present. The efficiencies of these IL were studied in one- and two-step reactions. When the ionic liquid [BSMBIM] [CF_3SO_3] was used as a catalyst for the WCO esterification reaction, an efficiency of 78.13 % was obtained in just one reaction step, and potassium hydroxide was used in the second step, with an efficiency of 94.52 %. The catalyst was reused seven times, maintaining a high yield of biodiesel production.

Wei, X. *et al.*, 2015, used ionic liquids as catalysts for transesterification reaction of castor oil and methanol. The product was characterized using mass spectrometry. The efficiencies of four different catalysts, 1-methyl imidazole hydrogen sulfate salt [HMIM][HSO_4], 1-butyl-3-methylimidazolium hydroxide salt [BMIM]OH, NaOH, and H_2SO_4 were compared. The effect of the methanol/castor oil mole ratio, reaction temperature, reaction

time, and catalyst dosage on the MR content was investigated by single factor experiments. Based on single factor experiments and the Plackett–Burman design, the transesterification of castor oil and methanol was optimized using the response sur-face methodology. The results showed that the most effective catalyst was the ionic liquid [HMIM][HSO_4]. The optimal conditions were as follows: methanol/castor oil mole ratio 6:1, reaction time 4 h, reaction temperature 77 °C and [HMIM][HSO_4] dosage 12 %. Under these conditions, the MR content reached 89.82 %. The catalytic activity of [HMIM][HSO_4] still remained high after 4 cycles.

Mohammadi, F. *et al.,* 2018, used an alkaline ionic liquid, choline hydroxide (ChOH), as a catalyst for the transesterification reaction of soybean oil into biodiesel in a microchannel reactor. The optimization of the reaction temperature (ºC), catalyst dosage (wt %) and the total flow rate (mL/min), in FAME's content, was done using the Box-Behnken method. The optimum conditions obtained were: reaction temperature of 53.53 ºC, catalyst dosage 2.6 % wt and total flow rate of 11.82 mL/min. In these conditions, the predicted FAME content was 96.45 % and the experimental FAME content was obtained as 97.6 %, showing that the regression model is significant. The reuse of this IL was also studied, revealing excellent performances after several cycles without noticing many losses during the catalytic activity.

Ding H., *et al.,* 2018, used three acidic imidazolium ionic liquids were synthesized and employed to the production of biodiesel from palm oil under microwave irradiation. Among the three ionic liquids, ([HSO_3-BMIM] HSO_4) was proved to be the most suitable catalyst because of the excellent catalytic performance. Single factor experiments and response surface methodology (RSM) were conducted to investigate various reaction conditions to obtain the optimal condition, and the results indicated that ionic liquid dosage was the most significant variable. A maximal yield of 98.93 % was obtained while mole ratio of methanol to oil, ionic liquid dosage, microwave power and reaction time were 11: 1, 9.17%, 168 W and 6.43 h, respectively. In addition, the ionic liquid catalyst showed excellent operational stability with biodiesel yield of 84.76% after six cycles.

Bölük & Sönmez, 2020, used 1-butyl-3-methylimidazolium hydrogen sulfate [BMIM][HSO_4] ionic liquid and microwave heating to esterify oleic acid and methanol. Other catalyst such as H_2SO_4 and 1-methyl imidazole hydrogen sulfate [HMIM][HSO_4] were also used in the esterification of oleic acid and their catalytic activities were compared to that of [BMIM][HSO_4]. The effects of the amount of catalysts, reaction temperature, time, and methanol-to-oleic acid molar ratio were investigated. The experimental results indicated that the reaction temperature and amount of catalysts have a significant impact on the esterification of oleic acid. Optimized reaction conditions were reached when the concentration of catalysts

was 10 wt %, the methanol-to-oleic acid molar ratio was 9:1, the reaction time was 30 min, and the temperature was 120 °C. Under these optimum conditions, the methyl oleate yield and conversion were 85.7 % and 94 %, respectively. There was only a small decrease in the catalytic activity of [BMIM][HSO_4] after four successive applications.

Roman, *et al.*, 2019, used IL 1-metimidazolium hydrogen sulfate, [HMIM][HSO_4], as a catalyst for the reaction of esterification of oleic acid with methanol, to optimize the experimental conditions of the reaction using the Box–Behnken method, based on maximizing the conversion of oleic acid and the FAMES content in the biodiesel samples obtained. It was concluded that the most important parameters were the molar ratio between oleic acid/methanol and the dosage of catalyst, and for this model the optimal conditions for maximum conversion were fixed at 15 % (m/m) of catalyst, time reaction time of 8 hours, temperature of 110 ± 2 ºC and methanol / oil molar ratio of 15:1, with a 95 % yield, while the yield in terms of FAME's content was 90 %. It was confirmed that IL [HMIM][HSO_4] is an excellent alternative to conventional catalysts for the esterification process in the production of biodiesel.

Chang & Zhou, 2020, used Brönsted acidic ionic liquid supported on magnetic Fe_3O_4 [*β-CD-6-Im-$(CH_2)_3HSO_3$] [HSO_4]-Fe_3O_4 to catalyze the high-acidic untreated Jatropha carcass L. seed crude oil for biodiesel production in a single pot. The results showed that 94.70% yield of FAME was obtained under the optimized reaction conditions of temperature of 130 °C, 10:1 molar ratio of methanol to oil, 3 wt % of catalyst dosage, 3 h reaction time. In addition, the catalyst activity was not significantly decreased after five recycles.

Bian, Y. *et al.*, 2019, use a novel Brønsted acid poly ionic liquid (PIL-M) was synthesized for the transesterification of oleic acid. The optimal reaction condition was as follows: 6 wt% catalyst amount, reaction temperature 80 °C, the ratio of methanol to oleic acid 9:1 and reaction time 3 h. Under the optimal condition, the yield of methyl oleate was up to 95.9%. The excellent catalytic activity of PIL-M in the product of biodiesel benefit from its excellent properties such as high surface area (301.1 m^2/g) and hierarchical nanopores. Compared with commercial resin (Amberlyst 15) and other catalysts, PIL-M showed better catalytic activity. The yield of methyl oleate was still over 90% after four times reuse. The structure of PIL-M kept stable after four times reuse, which was confirmed by the FT-IR spectrum.

Cai, D. *et al.*, 2021, prepared a series of novel amphipathic ionic liquids based on the 4-dimethylaminopyridine (DMAP) for the transesterification of soapberry oil and methanol. C12-DMAPH][HSO_4]$_2$ was proven to be amphipathic, and the corresponding catalytic mechanism was proposed. Under the conditions of molar ratio (methanol to oil) 25.5:1, catalyst amount of

0.38 mmol/g (based on oil mass), reaction time 6 h and reaction temperature 112 ºC. The biodiesel yields decreased from 98.02% to 92.34% when [C12-DMAPH][HSO_4]$_2$ was used for 5 times, therefore, the decrease of biodiesel yield may be caused by catalyst loss in the recycling process.

Bian, Y. *et al.,* 2021, In their study, IL monomer with phenolic hydroxy was synthesized. And the FCPIL was synthesized by phenolic condensation. For the purpose of investigating the catalytic performance of FCPIL, the esterification between oleic acid and methanol was performed. In order to obtain the maximum yield, four parameters (reaction time, amount of methanol, temperature and catalyst amount) were considered. In the optimum condition (5 wt% catalyst amount, 9:1 methanol/oleic acid ratio at 80 °C for 1.5 h), the ester yield was up to 93.3%. After four cycles of use, the catalytic activity of FCPIL did not exhibit significant decline.

Fan, M. *et al.,* 2018, use different Brønsted-acid ionic liquid as catalysts for the reaction of rapeseed oil with methanol. 1-butylsulfonate-3-methyl ([BSO_3HMIM][HSO_4]) shows a better catalytic activity when compared to the others. The highest content in FAME (85 %) was achieved under mild reaction conditions: reaction temperature 130 °C, 2 wt % catalyst, molar ratio methanol to oil, 12:1, and reaction time 3h.

Table 8 - Bibliographic review on the use of ionic liquids as catalysts in the production of biodiesel.

Source: Own authorship.

Raw Materials	IL	Catalyst dosage (% wt / % wt)	Time (h)	Temperature (ºC)	Molar Ratio alcohol:oil (mol/ mol)	Conversions (%)	IL Reuse	Ref.
Oleic Acid	[HMIM][HSO_4]	3.5	6	----	4:1	92.5	9	Yue S., *et al.*, 2015
WCO	[BMIM][HSO_4]	5	1	160	15:1	95,65	5	Ullah Z. *et al.*, 2015
WCO	[BSMBIM][CF_3SO_3]	4	4	120	12:1	94.2	7	Ullah Z. *et al.*, 2017
Castor Oil	[HMIM][HSO_4]	12	4	77	6:1	89.8	4	Wei X. *et al.*, 2015
Soybean Oil	ChOH	2.6	----	53.53	9:1	97.6	4	Mohammadi F. *et al.*, 2018
Palm Oil	[HSO_3-BMIM][HSO_4]	9.17	6.43	108	11:1	98.93	6	Ding H., *et al.*, 2018
Oleic Acid	[BMIM][HSO4]	10	0.5	120	9:1	94	4	Bölük S. & Sönmez Ö., 2020,
Rapeseed Oil	[BSO_3HMIM][HSO_4]	2	130	180	12:1	85	6	Fan M. *et al.*, 2017
Oleic Acid	[HMIM][HSO_4]	15%	8	110 ± 2	15:1	90	---	Roman F. *et al.*, 2019
Jatropha carcass	[β-CD-6-Im-$(CH_2)_3HSO_3$] [HSO_4]-Fe_3O_4	3	3	130	10:1	94.7	5	Chang F. & Zhou Q., 2020
Oleic Acid	PIL-M	6	3	80	9:1	95.9	4	Bian Y. *et al.*, 2019
Soapberry Oil	[C12-DMAPH][HSO_4]$_2$	---	6	112	25.5:1	98.02 ± 0.36	5	Cai D., et al., 2021
Oleic Acid	FCPIL	5	1.5	80	9:1	93.3	4	Bian Y. *et al.*, 2021

3.4. Choose of the ionic liquid

1-Methylimidazolium hydrogen sulfate ([HMIM][HSO_4]) was chosen as the catalyst for this work, an ionic liquid that is acidic and is composed of the imidazolium cation, represented in Figure 18.

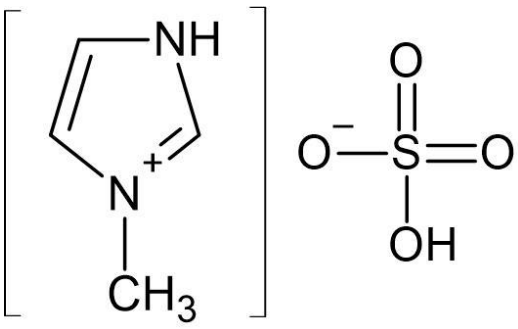

Figure 18 - Structure of the ionic liquid [HMIM][HSO_4].

Source: Adapted from Shaterian & Mohammadnia, 2013.

The choice of the ionic liquid was made based on the studies previously done in the LQA (Laboratório de Química Analítica, in ESTIG/IPB), conducted by Goes H., 2018, Roman F., 2018 and Diniz H., 2020.

Goes, 2018, studied the influence of the application of the ionic liquid 1-methylimidazolium hydrogen sulfate [HMIM][HSO_4], in the catalysis of the transesterification reaction of mixtures of triglycerides present in a simulated oil by incorporating oleic acid in a waste cooking oil. The most favorable reaction conditions for the FAME content response correspond to an incorporation of 40 % oleic acid, reaction time of 8 h, molar ratio oil/methanol 1:20, temperature of 90 ºC and a catalyst dosage of 10 % wt, with an average conversion of 36.5 %. The recovery and reuse of the ionic liquid was studied in five consecutive essays.

Diniz H., 2020, studied the influence of IL [HMIM][HSO_4] as a catalyst for an esterification reaction of a simulated high acid oil. The selected reaction conditions were: temperature of 65 °C, reaction time of 4 hours, molar ratio 1:10 of raw material / methanol and 10% (m / m) of IL in relation to the raw material. When using the simulated oil as raw material, an initial conversion of 45.6% is obtained and after nine reaction cycles the conversion decreased to 27.2%, while the content of FAMEs without biodiesel decreased from 24.1% to 14.0%. The results choose that, for the selected conditions, IL promotes only the esterification reaction. The correspondence between the FTIR spectra that relate the LI after the last reaction cycle and the initial LI was 99.3% for the reactions using AO and 90.0%.

3.5. Purification and Recovery of Ionic Liquids

As the cost of producing biodiesel is a major concern, the purification and recyclability of the catalysts used in the biodiesel process must be considered. The recycling of ionic liquids reduces the cost of producing biodiesel and minimizes its disposal as waste, as well as its environmental impacts. The obtained IL's are contaminated with generated side products such as water, salts, acids or organic solvents during the reaction therefore purification steps are necessary. Purification and/or recovery of IL's at both low scales and large scales are a major hurdle for researchers due to their substantial physicochemical properties. IL's associated with significant vapour pressures prevent the purification of ILs through common distillation methods. Researchers should select an appropriate method to purify and recover IL's based on their physicochemical properties. (Ishak, I. *et al.*, 2017)

The recyclability of ionic liquids in transesterification reactions was carried out by almost all researchers in their studies, as we will see in section 5.4, in which its stability as a catalyst and its excellent reuse in reactions are confirmed, demonstrating its high potential in environmental protection. It should be one of the options for future researchers with the purpose of feeding diesel engines for transportation, operational simplicity and a friendly catalyst for the purpose of scaling up. In return, this can serve as an opportunity to pave the way for this green catalytic process and feed the prospects of becoming economically viable in the near future (Ishak, I. *et al.*, 2017).

4. EXPERIMENTAL DESCRIPTION

4.1. Reagents and materials

The raw materials used in biodiesel production were oleic acid (tech. 90%), obtained from Alfa Aesar (Germany), waste cooking oil, obtained from restaurants in the region of Bragança, Portugal. The ionic liquid 1-methylimidazolium hydrogen sulfate (+ 95%) was obtained from Sigma Aldrich Chemistry (Switzerland) and methanol (+99.8%) obtained from Riedel-de-Haën (Germany). The standard mixture of 37 FAME was obtained from Supelco (USA) and boron trifluoride dihydrate (96 %) obtained from Sigma-Aldrich (Germany)

The reagents utilized for characterization and analysis of raw materials and biodiesel were diethyl ether (+99.8%), borax (+99.5%) and the red methyl indicator, all obtained from Riedel-de-Haën (Germany). N-heptane (+99%) and anhydrous sodium sulphate (Na_2SO_4) (+99.6%) were obtained from Carlo Erba Reagents (France). Sodium chloride (NaCl) obtained from Honeywell (Germany), potassium hydroxide (KOH) (85%) and phenolphthalein indicator (+99%) were obtained from Panreac Quimica (Spain). Methyl heptadecanoate (+97%), used as an internal standard, was purchased from Sigma-Aldrich (Switzerland) and ethanol (+96%) from Chem-Lab (Belgium). Hydrochloric acid (HCl) (37%) was obtained from Fisher Chemical (UK).

4.2. Equipment

The biodiesel production reaction takes place in a 100 mL round bottom flask. For heating the reaction mixture, an automatic heating plate with magnetic stirring was used (IKA, model C-MAG HS4 digital), connected to a condenser for the reflux of methanol. Weights of sample masses were made on an analytical balance (AE, model ADA 210/C). For phase separation, a 100 mL separating funnel and a centrifuge (EPPENDORF, model 5810 R) were used. The samples resulting from biodiesel production were dried in a vacuum oven at 110 ºC (SCIENTIFIC, series 9000).

The content of fatty acid methyl esters in the biodiesel samples was determined by gas chromatography, GC-FID, using a Shimadzu brand equipment (Nexis, model GC-2030) and the ionic liquid analysis was performed by FTIR (Fourier Transform Infrared Spectroscopy) using a Perkin Elmer brand spectrophotometer (UATR Two model).

4.3. Methodology

4.3.1. Esterification Reaction

The esterification reaction for the production of biodiesel or treatment of waste cooking oil is carried out by adding ionic liquid, oleic acid and waste cooking oil, in that order and in pre-established quantities, in a two-necked 100 mL flask, according to the quantities needed. The flask containing the mixture is immersed in a paraffin bath, with the plate set-point set at 73°C so that the flask remains at a previously established constant temperature of 65°C, under constant magnetic stirring and connected to a reflux condenser. The temperature inside the reactor is measured with an analog thermometer, and when the desired temperature is reached, methanol is added to the mixture (previously heated to 65 ºC) and the reaction time starts counting. Figure 19 shows the scheme of the experimental setup used for the esterification reaction.

At the end of the reaction, the flask is removed from the bath, cooled in water at room temperature and subsequently measured for its mass. The contents contained in the flask are transferred to a 100 mL separating funnel to promote phase separation for 24 hours. After separating the upper phases, containing the biodiesel, and the lower one, containing the ionic liquid, water and methanol in excess, as shown in Figure 20, the masses of the two phases are measured again and then transferred to centrifuge tubes and taken centrifuge at 3000 rpm for 30 minutes for more efficient separation. With the aid of a Pasteur pipette, the phases obtained by centrifugation are again separated, their masses measured and placed in identified flasks, as shown in Figure 21. Both phases are placed in a vacuum oven at a temperature of 110 ºC for approximately 48 hours for evaporation of water and methanol still present in the samples. Finally, the vials containing the light and heavy phases are stored at 4°C for further analysis.

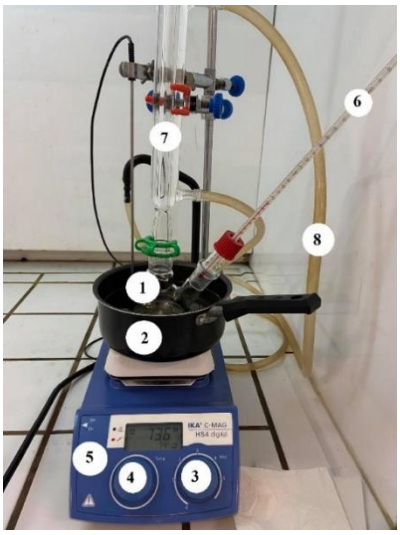

Figure 19 - Scheme of the experimental setup for the reaction. 1-two-neck reaction flask; 2-pot with paraffin bath; 3-agitation control; 4-temperature control; 5- heating plate; 6- thermometer; 7- condenser; 8-water outlet.

Figure 20 - Phase separation using a decanting funnel. 1- heavy phase; 2-light phase.

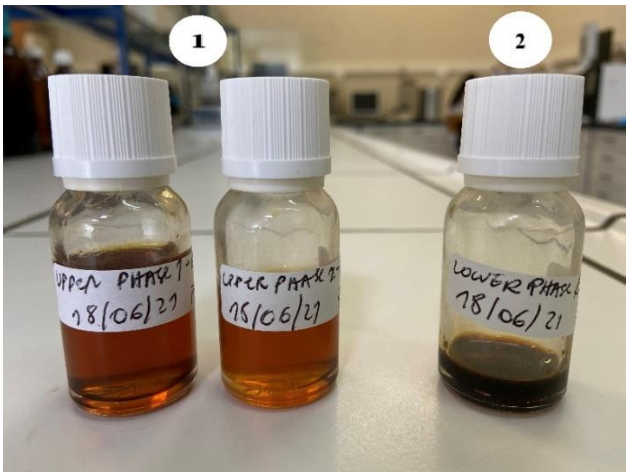

Figure 21 - Separation and storage of phases in 15 mL vials. 1-ligth phase; 2-heavy phase.

4.3.2. Determination of acidity index and conversion

The acidity of the light phase is determined according to European Standard EN 14104/2003. The procedure consists of rigorously adding 1 g of biodiesel, measured on an analytical balance, 25 mL diethyl ether/ethanol (1:1 v/v) and 5 drops of phenolphthalein in a 250 mL Erlenmeyer flask. This solution is then titrated with a methanolic potassium hydroxide solution with a standard concentration of approximately 0.1 mol/L, placed in a 25 mL burette, until a first pink hue appears. The KOH solution is periodically titrated with a standard HCl solution to check its concentration, which is approximately 0.1 mol/L. The standard HCl solution is also titrated, using sodium tetraborate (borax) and methyl red as a visual indicator. The acidity value (AV) is calculated by Equation 1, being expressed in mg of KOH per g of sample. This same procedure is used to determine the acidity of the raw material used.

$$AV\left(\frac{mgKOH}{g_{sample}}\right) = \frac{V_{KOH} \times C_{KOH} \times M_{KOH}}{m_{sample}} \quad (1)$$

Where in the equation, AV corresponds to the acidity of the sample (mg KOH/g sample), V_{KOH} is the volume of KOH standard solution needed to titrate the sample (mL), C_{KOH} is the concentration of the potassium hydroxide standard solution (mol/L), M_{KOH} is the molar mass of KOH (g/mol), and m_{sample} is the measured mass of sample (g).

The conversion (X), in terms of acidity reduction, is calculated by comparing the initial acidity, that is, the acidity of the raw material used, and the final acidity, that is, the acidity of the biodiesel. The calculation is done using Equation 2.

$$X\ (\%) = \frac{AV_{initial} - AV_{final}}{AV_{initial}} \times 100 \quad (2)$$

Where in the equation, $AV_{initial}$ is the acidity index of the raw material used and AV_{final} is the acidity index of the biodiesel sample, both in mg KOH/g

4.3.3. Determination of Yield

The Yield in terms of final mass of FAME's converted in relation with the initial FAME mass is given by the Equation 3.

$$X\ (\%) = \frac{m_{liht\ phase\ (final)} \times \%\ FAME}{m_{raw\ material}} \times 100 \quad (3)$$

Where in the equation, $m_{upper\ phase\ (final)}$ is the final mass (g) of the raw material in the end of the reaction described in section 4.3.1, and $m_{raw\ material}$ is the initial mass of the raw material used for biodiesel production.

4.3.4. Determination of FAME content in biodiesel samples

The analysis by gas chromatography is performed in order to determine the content of fatty acid methyl esters present in the biodiesel produced and for this, the procedure of standard EN14103:2003 is followed.

To prepare the samples for analysis in the GC-FID, about 250 mg of the light phase is weighed into a 15 mL bottle and then added with a micropipette, 5 mL of a standard concentration solution of methyl heptadecanoate approximately 10 mg. mL^{-1}. In order to ensure that there is no trace of water present in the samples, a microspatula of anhydrous sodium sulfate (Na_2SO_4) is added. Afterwards, shake the bottle well to facilitate the water removal process. Once this process is done, the samples must be placed at rest, allowing the Na_2SO_4 to settle at the bottom of the flask and then with a micropipette, 1mL is added from the top in 1.5 mL flasks to be taken for analysis in the GC-FID. The sample volume injected into the chromatograph is 1 μL.

As operational conditions in the GC-FID analyses, a helium flow of 1 mL/min was used, initial temperature of 50 °C (1 min), ramp at 25 °C/min to a temperature of 200 °C followed by a second ramp at 3 °C /min up to 230°C. The total analysis time is 20 minutes for each sample. The temperature in the injector is 250 °C, a split ratio of 1:25 is used, with the detector at a temperature of 250 °C. Figure 22 shows the GC-FID equipment with an automatic sampler.

Figure 22 - GC-FID used to determine FAME's content by gas chromatography.

The identification of each compound, fatty acid methyl esters, present in the biodiesel samples was determined by comparing the retention times of each FAME obtained with the retention times obtained in the analysis of a standard mixture of 37 FAME's purchased from Supelco and analyzed with the GC-FID Shimadzu.

The chromatogram displayed on Figure 23 from Supelco was obtained with a similar packing and the same dimensions as the column used in this work, which allows comparison of the results obtained in both. Figure 24 shows the chromatogram obtained using the same operating conditions as the standard mixture of 37 FAME's published by Supelco, in which the peaks are identified based on signal intensity and retention times, and this will serve as a comparison for the determination of the FAME's present in the biodiesel samples.

Table 9 shows the elution order, compound name, compound ID, retention time and the obtained chromatographic area, for the analysis of the Supelco 37 compound FAME mix used in this work and presented in Figure 24. This table is used to identify each FAME peak in the analyzed samples. These peaks are subsequently selected for the estimation of the individual FAME contents, and the total FAMEs content, in the biodiesel samples.

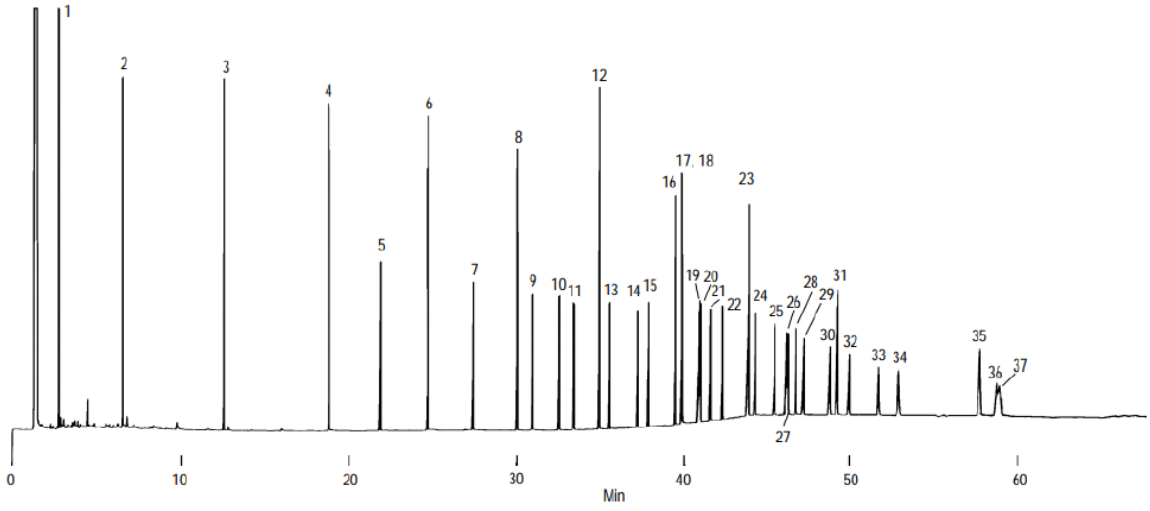

Figure 23 - Chromatogram of the standard mixture of 37 FAMEs obtained by Supelco.

Adapted Source: Supelco (Supelco, Bulletin 907 – Comparison of 37 Component FAME Standard on Four Capillary GC Columns)

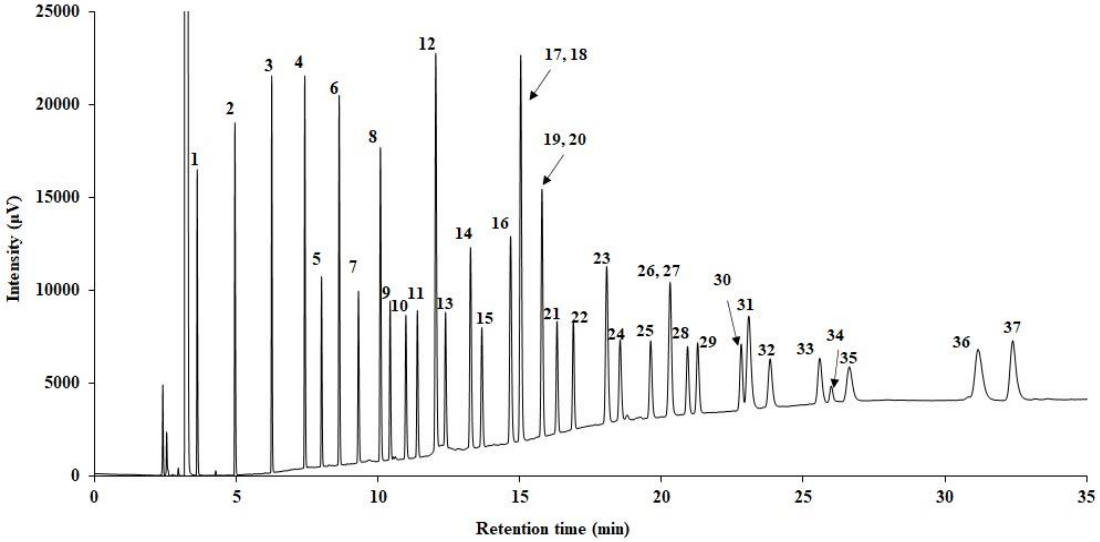

Figure 24 - Chromatogram for the mixture of 37 Supelco FAMEs obtained from the LQA GC-FID.

Table 9 - Elution order, compound name, compound ID and retention time for the 37 compounds.

Elution Order	Peak name	Peak ID	Retention time (min)	Area (µV)
1	Butyric acid methyl ester	C4:0	3.621	30583
2	Caproic acid methyl ester	C6:0	4.953	37694
3	Caprylic acid methyl ester	C8:0	6.250	42455
4	Capric acid methyl ester	C10:0	7.416	45648
5	Undecanoic acid methyl ester	C11:0	8.007	23521
6	Lauric acid methyl ester	C12:0	8.629	48399
7	Tridecanoic acid methyl ester	C13:0	9.310	24745
8	Myristic acid methyl ester	C14:0	10.084	50129
9	Myristoleic acid methyl ester	C14:1	10.427	24033
10	Pentadecanoic acid methyl ester	C15:0	10.982	25267
11	cis-10-Pentadecanoic acid methyl ester	C15:1	11.389	25247
12	Palmitic acid methyl ester	C16:0	12.036	82633
13	Palmitoleic acid methyl ester	C16:1	12.381	28309
14	Heptadecanoic acid methyl ester	C17:0	13.263	45323
15	cis-10-Heptadecanoic acid methyl ester	C17:1	13.662	25536
16	Stearic acid methyl ester	C18:0	14.677	52918
17, 18	Oleic acid methyl ester, Elaidic acid methyl ester	C18:1n9 (c+t)	15.033	92760
19, 20	Linoleic acid methyl ester, Linolelaidic acid methyl ester	C18:2n6 (c+t)	15.784	59824
21	gamma-Linolenic acid methyl ester	C18:3n6	16.315	25316
22	alpha-Linolenic acid methyl ester	C18:3n3	16.891	25721
23	Arachidic acid methyl ester	C20:0	18.068	52296
24	cis-11-Eicosenoic acid methyl ester	C20:1n9	18.541	25933
25	cis-11,14-Eicosadienoic acid methyl ester	C20:2	19.618	25832
26, 30	cis-8,11,14-Eicosatrienoic acid methyl ester, Henicosanoic acid methyl ester	C20:3n6, C21:0	20.304	51710
27	cis-11,14,17-Eicosatrienoic acid methyl ester	C20:3n3	20.920	22562
28	Arachidonic acid methyl ester	C20:4n6	21.276	24669
29	cis-5,8,11,14,17-Eicosapentaenoic acid methyl ester	C20:5n3	22.811	24184
31	Behenic acid methyl ester	C22:0	23.080	53019
32	Erucic acid methyl ester	C22:1n9	23.832	25793
33	cis-13,16-Docosadienoic acid methyl ester	C22:2	25.582	24786
34	cis-4,7,10,13,16,19-Docosahexanoic acid methyl ester	C22:6n3	25.989	6549
35	Tricosanoic acid methyl ester	C23:0	26.629	25197
36	Lignoceric acid methyl ester	C24:0	31.164	49429
37	Nervonic acid methyl ester	C24:1n9	32.393	47595

The FAMEs present in the biodiesel samples are identified by comparing the retention time of the peaks present in the chromatogram, with the retention time of the FAMEs obtained by analyzing the standard mixture. After identifying the FAMEs present in the biodiesel sample, the conversion is calculated by Equation 4, using the individual area of each compound, the area of methyl heptadecanoate, used as an internal standard, and the sum of all areas of all compounds identified as FAMEs.

$$C(\%) = \left(\frac{\sum A_{FAMEs} - A_{IS}}{A_{IS}}\right) \times \frac{C_{IS} \times V_{IS}}{m_{sample}} \times 100 \quad (4)$$

Where in the equation, $\sum A_{FAMEs}$ corresponds to the sum of the areas of the FAMEs, in µV, A_{IS} is the area corresponding to the internal standard, in µV, C_{IS} is the concentration of the methyl heptadecanoate solution, in mg/mL, V_{IS} is the volume used of the methyl heptadecanoate solution, in mL, and the m_{sample} is the sample mass, in mg.

In order to quantify the conversion into FAMEs of each ester (C_n) in relation to the total content, Equation 5 is used.

$$C_n(\%) = \frac{A_{FAME}(n)}{A_{IS}} \times \frac{C_{IS} \times V_{IS}}{m_{sample}} \times 100 \quad (5)$$

Where in the equation, n is the analyzed FAME and $A_{FAME}(n)$ is the FAME area in question.

4.3.5. Preparation of methyl heptadecanoate solution

The internal standard method was performed to quantify the FAME content (wt.%) present in the biodiesel samples produced. To prepare the solution, 500 mg of methyl heptadecanoate was measured and transferred to a volumetric flask of 50 mL. Then n-heptane was used to fill the remaining volume in order to reach a final concentration of 10 mg. mL^{-1}.

4.3.6. Derivatization of fatty acids by BF_3

In order to determine the maximum theoretical conversion that can be obtained, the derivatization, using BF_3, of the raw materials used in the production of biodiesel was carried out to determine the composition of present fatty acids. With this derivatization, the fatty acids

and triglycerides present in the samples are transformed into methyl esters and these compounds are subsequently identified and quantified by gas chromatography.

The procedure consists of adding approximately 25 mg of raw material sample and 2.5 mL of KOH solution (0.05 mol/L) in a 15 mL bottle. Then, this bottle is closed and placed for 10 minutes in an oven at 90°C. After this period, the flask is removed from the oven and allowed to cool to room temperature. Then, 2 mL of BF_3 in methanol solution (10% wt) is added, the bottle being closed again and placed for another 30 minutes in the oven at 90°C. After this second period, the flask is removed from the oven and allowed to cool to room temperature. Then 3 mL of internal standard solution is added, and the mixture is vortexed. 2 ml of saturated sodium chloride solution are then added, and the mixture is again subjected to the same homogenization process. The sample is centrifuged for 5 minutes at 3000 rpm for phase separation.

After centrifugation, 2 mL are removed from the upper phase and transferred to a 15 mL flask. Then anhydrous sodium sulfate is added to remove all moisture present in the sample. Then, 1 mL is transferred to a 2 mL flask, taking care not to transfer Na_2SO_4, in order to carry out the analysis by gas chromatography.

4.3.7. Recovery of ionic liquid

The ionic liquid's recovery is investigated to determine the maximum number of recovery cycles that can be applied without significantly lowering the reaction yield.

Following the removal of the heavy phase, the sample is washed with an appropriate solvent, in this case distilled water, due to the hydrophilic properties of the ionic liquid, at a mass ratio of 1:3 sample/solvent. Following that, the contents of the flask are transferred to the decanting funnel for 24h, for separation of the aqueous phase from the impurities, as can be seen in Figure 25. After separation, the upper phase may contain traces of light phase and unreacted raw material, and the lower phase contains the ionic liquid, methanol and water. The upper phase is transferred to a flask and stored, to be analyzed by Fourier Transform Infrared Spectroscopy (FT-IR) to study its composition and identify the origin of the residue, while the lower phase is transferred to a flask and placed for 24 hours in an oven at 110 ºC. After this period, the sample, containing the ionic liquid, is removed from the oven, cooled to room temperature, weighed and can be used again. At the end of the recovery study, the IL is analyzed by FT-IR to verify the correspondence of the obtained spectrum with the spectrum of the commercial IL.

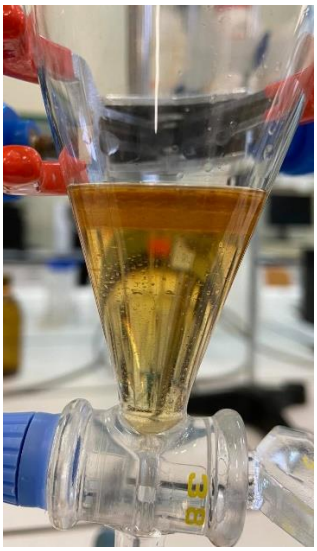

Figure 25 - Separation of the ionic liquid after washing.

4.3.8. Qualitative Analysis using FT-IR

Fourier transform infrared spectroscopy analysis is used to qualitatively assess the compounds present in a sample by identifying the vibrations of each of their functional groups. FT-IR analyses were performed for several samples, from reagents to products, to analyze the compounds present in the samples by identifying each functional group vibration. FT-IR spectra were recorded using a Fourier transform infrared spectrophotometer, operating from 400 to 4500 cm^{-1} in a resolution of 4 cm^{-1} and 4 cumulative scans. Recovered IL is also analyzed to obtain a correspondence with the commercial IL, used initially, in order to assess the efficiency of the recovery process. The equipment used is shown in Figure 26.

Figure 26 - Equipment used for FTIR analysis.

4.3.9. Experimental Design

Four factors were studied in order to estimate the optimal conditions for biodiesel production. The chosen factors were reaction time (h), the molar ratio between methanol and simulated oil (oleic acid incorporated in waste cooking oil) (mol/mol), the amount of catalyst added to the system (% wt) and the amount of incorporation of the oleic acid (wt %). A response surface methodology (RSM) was employed, known as Box-Behnken Design (BBD) (Box & Behnken, 1960). Table 10 describes the 4 parameters chosen, the code applied, and the 3 levels used.

Table 10 - Levels chosen for Box-Behnken Design.

Parameters	**Code**	**Levels**		
		-1	**0**	**1**
Time (h)	**A**	2	4	6
Catalyst Dosage (% wt)	**B**	5	10	15
Molar Ratio MeOH/Oil (mol/ mol)	**C**	5	10/1	15
OA incorporation (%wt)	**D**	20	40	60

The intended methodology estimates that 27 runs are needed to understand the behavior of each factor in the response. The design matrix in coded and actual values is shown in Table 11. Each run was performed according to the generic esterification procedure presented in section 4.3. Three responses were evaluated: the influence of the incorporation of oleic acid in the waste cooking oil, the FAME content according to the procedure described in section 4.3.4. and the Yield according to the procedure described in section 4.3.3

The methodology allows adjusting a quadratic mathematical model that exposes the relationship between the parameters and each response. The generic formula of the mathematical model is given by Equation 6.

Table 11 - Experimental conditions applied for each run, in coded values and in real values.

Run	Parameters							
	Code Values				Real Values			
	A	B	C	D	Time (h)	Catalyst Dosage (wt %)	Molar Ratio WCO/MeOH	OA incorporation (wt %)
					A	B	C	D
1	0	1	0	1	4	15	1/10	60
2	-1	0	1	0	2	10	1/15	40
3	0	-1	0	-1	4	5	1/10	20
4	-1	0	0	1	2	10	1/10	60
5	0	-1	0	1	4	5	1/10	60
6	-1	-1	0	0	2	5	1/10	40
7	0	0	0	0	4	10	1/10	40
8	0	0	1	-1	4	10	1/15	20
9	0	1	-1	0	4	15	1/5	40
10	1	0	-1	0	6	10	1/5	40
11	0	0	-1	1	4	10	1/5	60
12	0	1	0	-1	4	15	1/10	20
13	1	0	0	-1	6	10	1/10	20
14	-1	0	-1	0	2	10	1/5	40
15	1	1	0	0	6	15	1/10	40
16	0	1	1	0	4	15	1/15	40
17	1	0	0	1	6	10	1/10	60
18	0	-1	-1	0	4	5	1/5	40
19	-1	0	0	-1	2	10	1/10	20
20	0	0	1	1	4	10	1/15	60
21	0	0	-1	-1	4	10	1/5	20
22	1	0	1	0	6	10	1/15	40
23	1	1	0	0	6	15	1/10	40
24	0	0	0	0	4	10	1/10	40
25	0	0	0	0	4	10	1/10	40
26	-1	1	0	0	2	15	1/10	40
27	0	-1	-1	0	4	5	1/5	40

$$Y = \beta_0 + \sum_{i=1}^{4} \beta_i X_i + \sum_{i=1}^{4} \beta_{ii} X_i^2 + \sum_{j<i} \beta ji X_j X_i \qquad (6)$$

Where Y is the response, in this case, acidity reduction, the FAME content or the Yield, is the intercept coefficient. By maximizing the equation, it is possible to obtain the optimal conditions for each response separately.

5. RESULTS AND DISCUSSION

5.1. Feedstock Characterization

Waste cooking oil (WCO), oleic acid (OA) and simulated oil (20 % wt, 40% wt e 60% wt of oleic acid) were analyzed by gas chromatography to determine the distribution of fatty acids, as described in Section 4.4.3. The fatty acids were identified by comparison with fatty acid methyl esters using retention time.

The acidity index of the raw materials was determined in triplicate and the results are shown in Table 12.

Table 12 - Acidity index of raw materials.

Samples	m_{sample} (g)	V_{KOH} (mL)	C_{KOH} (mol/L)	AV (mg_{KOH}/g_{sample})	$Av_{average}$ (mg_{KOH}/g_{sample})	Standard deviation
OA	0.5007	15.50	0.09391	163.09	162.40	0.4900
	0.5008	15.40		162.01		
	0.5005	15.40		162.10		
WCO	10.0204	1.27		0.6677	0.6608	0.0069
	10.0281	1.24		0.6514		
	10.0076	1.26		0.6633		
SIMULATED OIL$_{20\% wt OA}$	1.0143	6.60		34.2809	34.1263	0.1113
	1.0127	6.55		34.0749		
	1.0065	6.50		34.0231		
SIMULATED OIL$_{40\% wt OA}$	1.0343	12.50		63.6705	63.5789	0.4113
	1.0038	12.20		64.0306		
	1.0280	12.30		63.0357		
SIMULATED OIL$_{60\% wt OA}$	1.0197	18.75		96.8732	96.9493	0.0761
	1.0026	18.20		95.6353		
	1.0181	18.75		97.0254		

The acidity index determined for oleic acid was 162.40 mg KOH/g, while for waste cooking oil it was 0.66 mg KOH/g. These values were periodically checked, verifying that they did not vary significantly over time, with a variation less than or equal to 1%. As the acid index indicates the amount of free fatty acids in a sample, the high acidity index value found for oleic acid is consistent as it is composed of free fatty acids. Compared with WCO, oleic acid has a much higher AI, so OA is used to increase the acidity of the waste oil, simulating an oil with high acidity.

The raw materials were also characterized by derivatization by BF_3 (Section 4.3.6), and analyzed by gas chromatography, identifying the methyl esters formed, and thus, the fatty acid profile present in the samples. Analyzes were performed in duplicate. Table 13 shows the amount of each FAME present in the oleic acid, after its derivatization, showing the values for each run and the average value of them. It can be seen that the sample of OA is constituted by 59.01 % of the methyl ester of oleic acid, and about 25.29 % of other methyl esters. The

percentage of oleic acid methyl ester present is much lower than the 90 % value described by the manufacturer with 59.01 %.

Table 13 - Profile of FAMEs after derivatization of the oleic acid.

Compounds	Structure	FAMEs (%)		
		1	2	**Average**
Palmitic acid methyl ester	C16:0	1.88	1.73	1.81
Stearic acid methyl ester	C18:0	3.08	2.52	2.80
Oleic acid methyl ester, Elaidic acid methyl ester	C18:1(c+t)	57.72	60.30	59.01
Linoleic acid methyl ester, Linolelaidic acid methyl ester	C18:2(c+t)	3.69	4.05	3.87
gamma-Linolenic acid methyl ester	C18:3n6	6.28	5.96	6.12
cis-11-Eicosenoic acid methyl ester	C20:1	6.71	7.99	7.35
	TOTAL	79.37	82.54	**80.95**

The chromatograms obtained for the derivatization of oleic acid is shown in Figure 27, in which the distribution of the formed FAMEs can be qualitatively verified.

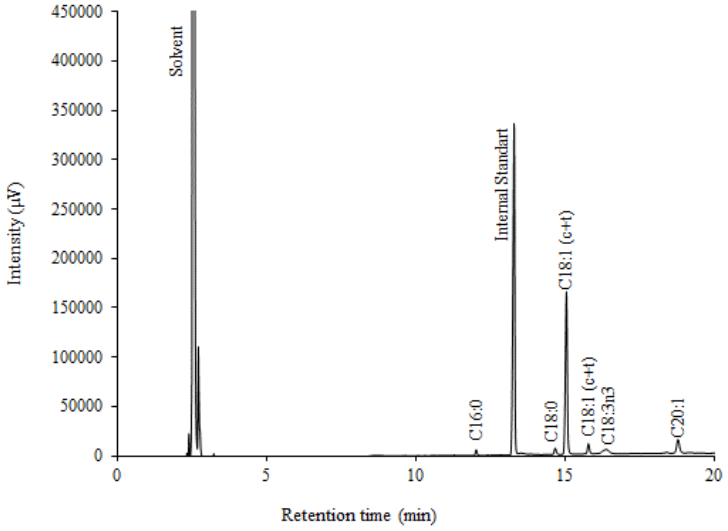

Figure 27 - Chromatogram obtained by GC-FID after A and B oleic acid derivatization.

The amount of each FAME present in the waste cooking oil sample after its derivatization can be seen in Table 14, showing low values for the two oils samples (1 and 2) and for the average value. It is observed that WCO consists essentially of 30.87 % of linoleic acid methyl ester and linolelaidic acid methyl ester 18.58 % of oleic acid methyl ester, and 11.79% from other esters with an average total of 60.80 % in FAMEs.

Table 14 - Profile of FAMEs obtained after the derivatization of the waste cooking oil.

Compounds	Structure	FAMEs (%)		
		1	2	**Average**
Palmitic acid methyl ester	C16:0	8.12	6.79	7.45
Stearic acid methyl ester	C18:0	2.96	2.52	2.74
Oleic acid methyl ester, Elaidic acid methyl ester	C18:1(c+t)	20.89	16.27	18.58
Linoleic acid methyl ester, Linolelaidic acid methyl ester	C18:2(c+t)	27.73	34.01	30.87
Linolenic acid methyl ester	C18:3n3	1.36	0.96	1.16
	TOTAL	61.06	60.54	**60.80**

Figure 28 shows the chromatogram obtained by the derivatization of FAMEs from waste cooking oil.

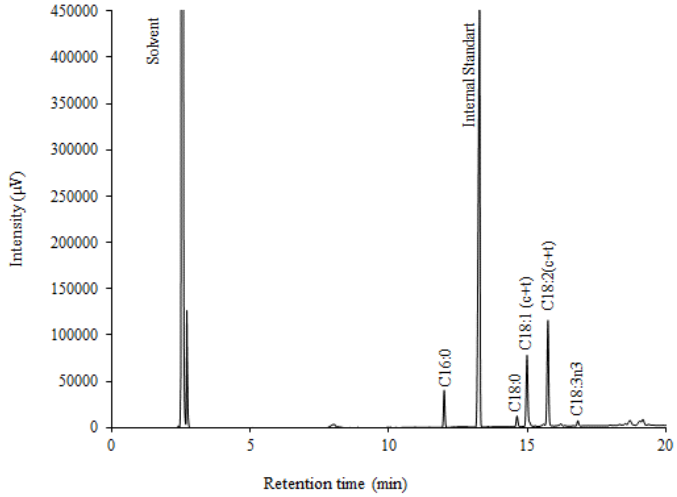

Figure 28 - Chromatogram obtained by GC-FID after the waste cooking oil derivatization.

5.2. Experimental Design

The optimization of the biodiesel production reaction was performed based on the Total Factorial Design 3^4, four factors with three levels. For a design with four variables and three levels, a complete factorial would require 81 runs, while for the same situation, the Box-Behnken Design requires only 27. Replicates in the central point are necessary to estimate pure errors. Those factors were chosen based on previously done investigations in IPB and also based on several papers found on the literature (Diniz H., 2020) (Goes H., 2018) (Roman F., *et al*., 2019).

The parameters chosen as control factors were: reaction time (A), catalyst dosage (B), oil/methanol molar ratio (C) and percentage of OA incorporated in the WCO (D), with all factors adjusted at 3 levels (-1, 0, +1). Three response variables were studied: R1, conversion of the simulated oil based on the reduction of acidity, and R2, content in FAME and R3, yield in terms of final mass of FAME's converted in relation with the initial FAME mass. Table 15

describes the conditions applied in each run, both the design matrix and the actual values and their respective responses.

The evaluation of the responses was made separately. A different model was developed for each of the responses and different optimal conditions were estimated for the biodiesel production reaction. The conversion was determined by the variation between the initial acidity of the raw material (simulated oil) and the final acidity of the biodiesel produced, according to the procedure described in section 4.3.2. The FAME content was determined by gas chromatography analysis of the biodiesel produced, according to the procedure in section 4.3.4.

Table 15 - Experimental design, real conditions and experimental responses of Experimental Design.

Run	Experimental Design				Real Conditions				Experimental Results		
	Time (h)	Catalyst Dosage (wt %)	Molar Ratio MeOH/WCO (mol/mol)	OA incorporation (wt %)	Time (h)	Catalyst Dosage (% wt)	Molar Ratio WCO/MeOH (mol/mol)	OA incorporation (% wt)	Conversion (%)	FAME (%)	Yield (%)
	A	B	C	D	A	B	C	D	R1	R2	R3
1	0	1	0	1	4	15	1/10	60	45.65	27.96	27.04
2	-1	0	1	0	2	10	1/15	40	52.62	24.92	24.12
3	0	-1	0	-1	4	5	1/10	20	53.33	12.84	12.41
4	-1	0	0	1	2	10	1/10	60	34.64	17.7	17.07
5	0	-1	0	1	4	5	1/10	60	46.12	31.54	30.91
6	-1	-1	0	0	2	5	1/10	40	28.82	16.16	15.73
7	0	0	0	0	4	10	1/10	40	45.92	21.28	20.53
8	0	0	1	-1	4	10	1/15	20	78.35	15.87	14.04
9	0	1	-1	0	4	15	1/5	40	23.09	13.68	12.81
10	1	0	-1	0	6	10	1/5	40	27.90	13.12	12.32
11	0	0	-1	1	4	10	1/5	60	26.65	19.29	18.27
12	0	1	0	-1	4	15	1/10	20	53.74	13.28	12.91
13	1	0	0	-1	6	10	1/10	20	63.44	16.9	16.35
14	-1	0	-1	0	2	10	1/5	40	13.46	10.47	9.53
15	1	1	0	0	6	15	1/10	40	52.75	28.34	27.62
16	0	1	1	0	4	15	1/15	40	69.55	30.46	29.76
17	1	0	0	1	6	10	1/10	60	52.50	37.77	36.94
18	0	-1	-1	0	4	5	1/5	40	21.09	10.96	10.27
19	-1	0	0	-1	2	10	1/10	20	36.77	9.2	8.74
20	0	0	1	1	4	10	1/15	60	62.79	35.29	34.55
21	0	0	-1	-1	4	10	1/5	20	25.38	6.94	6.43
22	1	0	1	0	6	10	1/15	40	75.97	36.83	35.69
23	1	1	0	0	6	15	1/10	40	55.93	29.41	28.63
24	0	0	0	0	4	10	1/10	40	45.51	20.4	19.56
25	0	0	0	0	4	10	1/10	40	46.32	19.65	18.89
26	-1	1	0	0	2	15	1/10	40	39.98	17.94	17.31
27	0	-1	-1	0	4	5	1/5	40	60.74	24.15	23.15

5.2.1. Analysis for the conversion response (R1) – ANOVA Table

5.2.1.1. ANOVA Table

The primary principle behind the ANOVA is to compare the variation in the response due to statistical treatment, which is defined as a change in the level of the variables, with the variation due to random errors in the response measurement. It is feasible to determine whether the suggested regression is adequate while considering the experimental imperfections related with the procedure using this method (Bezerra, Santelli, Oliveira, Villar, & Escaleira, 2008).

Table 16 shows the ANOVA table for the conversion calculated from the reduction of acidity of the simulated oil, according to Equation 2, whose value was calculated with the aid of the software Design Expert 11.

Table 16 - ANOVA Table for R1.

Source	Sum of squares	df	Mean Square	Calculated F-value	Tabulated F- value	p-value	
Model	7495.56	14	535.40	218.70	2.637	3.21×10^{-12}	significant
Residual	29.38	12	2.45				
Lack of Fit	29.05	10	2.90	17.74	19.40	0.0545	not significant
Pure Error	0.33	2	0.16				
Cor Total	7524.94	26					

To evaluate the significance of the regression, the **F-value calculated** must be determined, by dividing the Mean Square of the Model by the Mean Square of the Residuals. Taking into consideration the degrees of freedom from both the regression and the residual, this number must be compared to the **F-value tabulated**, giving by the Fisher distribution table. If the calculated value is greater than the tabulated one, the regression is statistically significant, indicating that the model is well fitted to the data with a 95% confidence level.

Considering the ANOVA analysis for the response R1 in Table 16, it can be seen that the determined F-value calculated for the regression is 218.70. The F-value tabulated was determined by considering the degrees of freedom of the regression (df1 = 14) and the degrees of freedom of the residual (df2 = 12) and checking the Fisher's distribution table for the critical value of $F_{14,12,0.05}$ (α equal to 0.05), giving a tabulated F-value of 2.637, concluding that the model is reliable because F-value calculated is much higher than the tabulated one.

The significance of the model can also be seen by checking the **lack of fit** evaluated by the F-value tabulated and the calculated one, but in this case must considering the degrees of

freed of the lack of fit and the pure error. The F distribution shows that for a $F_{10,2,0.05}$, the value is 19.396, while the calculated F-value is 17.74, meaning that the lack of fit is not significant, and this is the expected response that we want. It means that the model errors are due to random and inherent errors of the system rather than a problem with the data fit.

Another way to check the significance of the model is by evaluating the **p-value,** which is related to the null hypothesis's strength of evidence. Low p-values allow the null hypothesis to be rejected, which in this case is that the model is irrelevant or that the factors have no effect on the answer. If the null hypothesis is rejected, the alternative hypothesis must be correct, implying that the model and factors are significant. Treatments with p-values less than a pre-determined significance level, in this case 0.05, are statistically significant. For this current model, the p-value is statistically relevant, and the lack of fit is not.

5.2.1.2. Residual Analysis for the conversion

The reliability of the model adjustment was also assessed by the analysis of the determination coefficient, which was estimated as R^2= 0.9961 and the $R^2_{adjusted}$= 0.9915, showing that the observed and predicted values are close and concluding that the model can be used to predict responses. The absence of residues in the analysis is indicated by the close proximity of these values because residues are calculated by subtracting the observed response from the expected response. The data should be dispersed normally along a straight diagonal line, with no residue occurring too far away from the line. There are no outliers, or points that detract from the model's suitability for the experimental data. Figure 29 depicts the normally distributed set of experimental data in question.

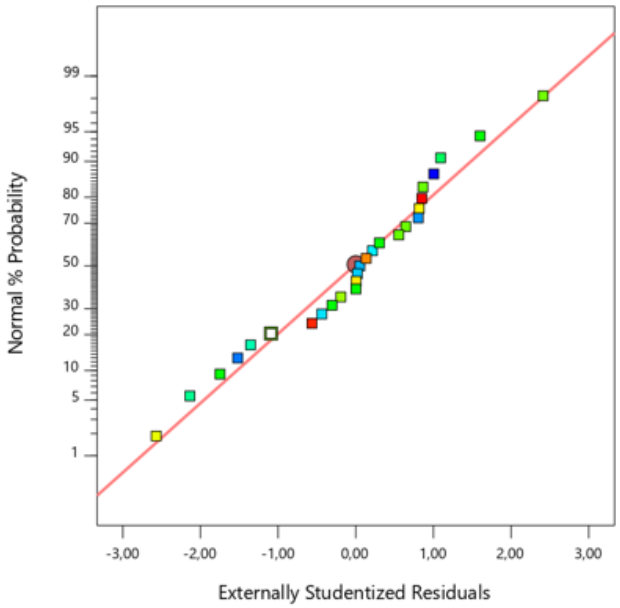

Figure 29 - Normal plot of Residuals

Figure 30 shows the residuals vs expected plot, which may be used to see if the residuals are close to 0 and if the residuals are unrelated to the variable levels. Both conditions are met because the residuals are close to the black line indicating no special pattern, such as a funnel, emerges as the predict response grows.

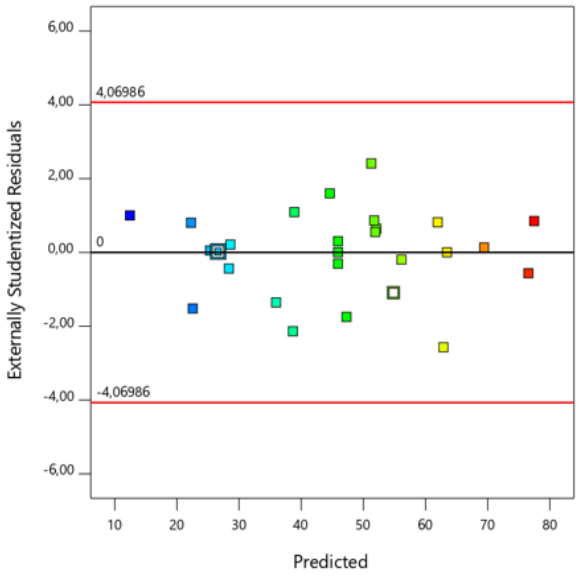

Figure 30 - Residuals versus predicted values.

Any values outside the red line in Figure 30 should be considered outliers, which by definition are runs with very large residuals that should be discarded from the statistical evaluation and the experiment or response measurements should be repeated.

5.2.1.3. Factor effect on the conversion

The ANOVA analysis can also be built to analyze the influence of each factor, as well as the interactions between them and their quadratic effect on the response, applying the same logic when the model regression was evaluated, taking into consideration the degrees of freedom of each factor and the degree of freedom of the residuals, showed in Table 17. The calculated F-value is higher than the tabulated one for the following parameters: A (reaction time), B (catalyst dosage), C (molar ratio oil: methanol), D (incorporation of oleic acid), AB, AC, AD, CD, A^2, C^2, D^2 and the remaining terms are not significant. It is important to say that the interactions involving parameter B proved to be insignificant for the model except the interaction AB. How significant each factor is, is given by the *p-value* in which the lowest it is, the highest is it's influence on the response. In this way, the order of importance is C > A > D > CD > D^2> AB> A^2 > AC > AD > C^2.

Table 17 - ANOVA analysis for the parameters influencing the response R1.

Source	Sum of squares	df	Mean Square	Calculated F-value	Tabulated F- value	p-value
A-Reaction Time	1244.64	1	1244.64	508.41	4.965	3.4×10^{-11}
B-Catalyst Dosage	29.26	1	29.26	11.95	4.965	0.0047
C-Molar Ratio oil:methanol	5740.75	1	5740.75	2344.96	4.965	3.9×10^{-15}
D-Oleic Acid incorporation	151.70	1	151.70	61.96	4.965	4.4×10^{-6}
AB	51.43	1	51.43	21.01	4.965	0.0006
AC	19.83	1	19.83	8.10	4.965	0.0147
AD	19.43	1	19.43	7.94	4.965	0.0155
BC	11.61	1	11.61	4.74	4.965	0.0501
BD	0.19	1	0.19	0.08	4.965	0.7850
CD	70.84	1	70.84	28.94	4.965	0.0002
A^2	21.29	1	21.29	8.70	4.965	0.0122
B^2	0.00	1	0.0002	0.00	4.965	0.9936
C^2	14.47	1	14.47	5.91	4.965	0.0317
D^2	68.17	1	68.17	27.85	4.965	0.0002

For each combination of associated factor levels, the cube chart gives expected mean values for response R1. Figure 31 shows the adjusted averages of the experimental conversion findings for the low and high levels of (A) reaction time, (B) catalyst dosage, (C) molar ratio oil:methanol.

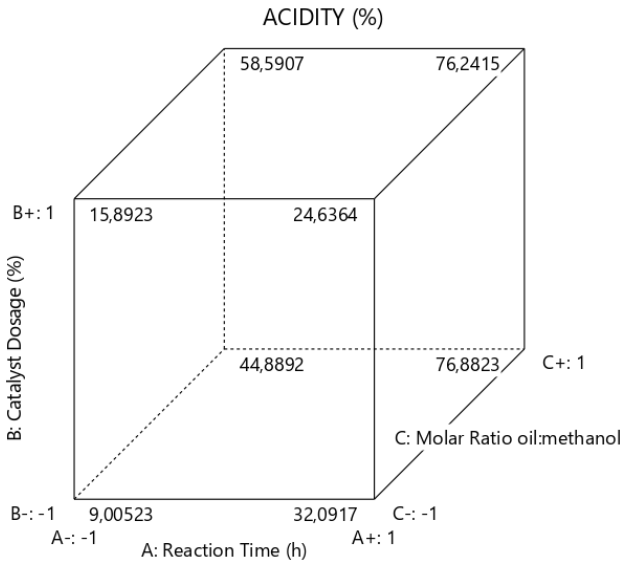

Figure 31 - Cube chart for response R1 (Incorporation of oleic acid (D) = 0)

The effects of the parameters are shown in Figure 32, where the deviation of the adjusted means between the levels can be seen, and when the factor has a positive effect, the conversion is expected to increase as this factor is changed to a value higher and opposite also applies, when the factor has a negative effect, the conversion increases as the factor value decreases.

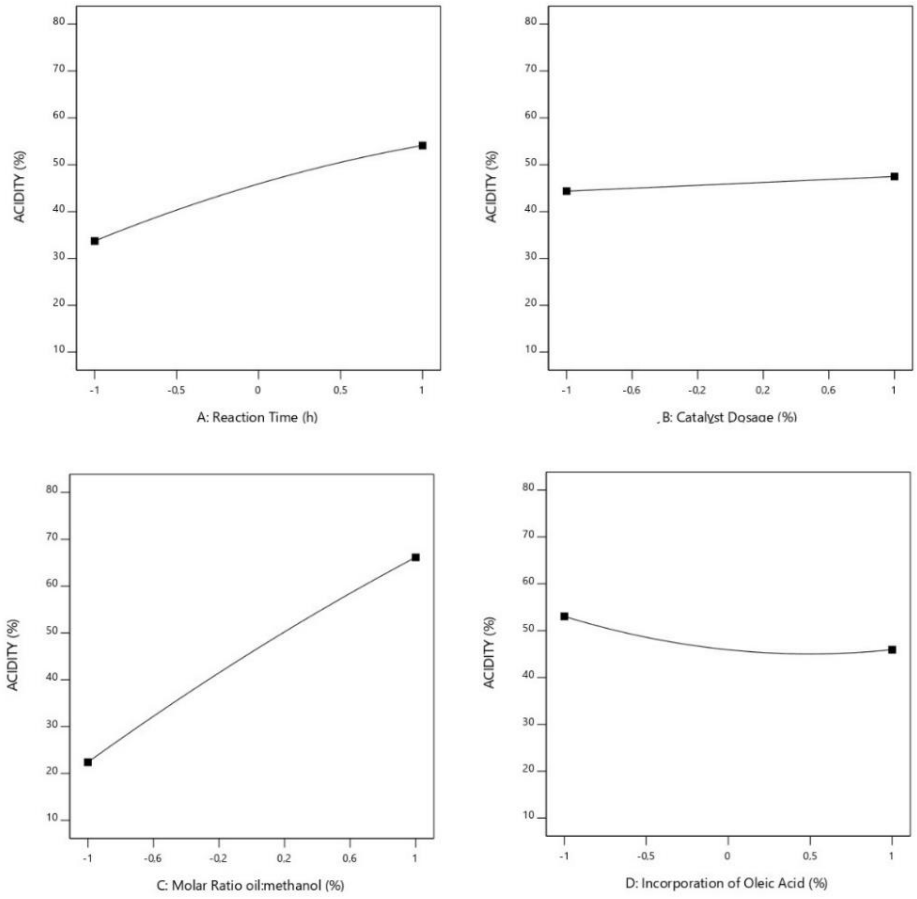

Figure 32 - Effects for each factor on the response R1.

Factor D has a negative effect due to the reduction in conversion, when the factor of the lower level is changed to the higher one, presenting a negative slope. On the other hand, factors A, B and C have a positive effect, because the response it increases as it changes from the lowest to the highest level, with factor B having little influence on the response. Parameters A and C have lines with greater slopes than parameter B, which means that they induce larger changes in the conversion values when changed.

The response surface graph is an important statistical analysis tool because it displays the interaction plots for several pairs of variables and their corresponding influences on the response R1, as showed in Figure 33 to 38.

Figure 33 shows the response surface relating to the influence of the variables: reaction time (A) and catalyst dosage (B), and the interaction graph for these two variables.

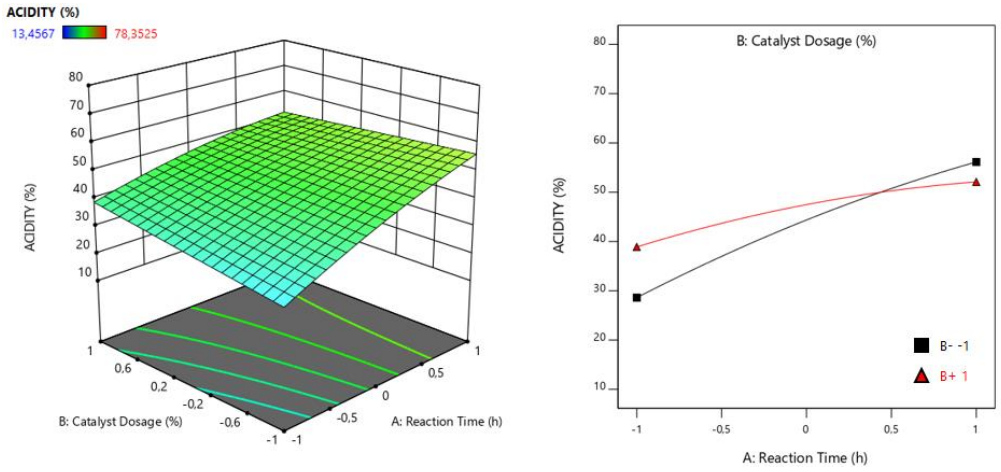

Figure 33 - Response surface for the acidity reduction in function of reaction time (A) and catalyst dosage (B) and the interaction plot of those variables (Molar ratio oil: methanol (C) = 0; Oleic acid incorporation (D) = 0).

The response surface plot shows that there is a difference in the slopes corresponding to the two factors, in which the factor A has a greater influence on the conversion response than the factor B, observing that there is a significant variation in the surface along axis A in fixed point in B, while the surface hardly changes along the axis B, concluding then, that factor A has a greater influence on the conversion response than factor B.

The interaction graph helps understand how one factor influences another. If the interaction graph displays two parallel lines, the conclusion is that the effect of one factor does not depend on the level of the other factor. If the lines are not parallel, it means that the effect exhibited by one factor depends on the level of the other factor, that is, a factor not only influences the response by itself, but also influences the other variable, changing the effect of this second variable on the response between minimum (-1) and maximum (+1) levels. For example, put a fixed point at level -1, in relation to reaction time (A), that is, 2 hours, it can be seen that, higher values in terms of conversion are obtained for the maximum level of factor B, that is, for the catalyst dosage 15%, but this fact is not observed, if placed the fixed point for the time at its maximum (+1), equivalent to 6 hours, it is observed that factor B, at its minimum level (-1), 5% , gives higher values in terms of conversion. One of the main conclusions given by the interaction plot, is that the variables have influence in one another, by checking the two non-parallels lines, and another conclusion, is that use the minimum level of the catalyst dosage, higher values for the conversion can be obtained. It is also concluded that the interaction between these two factors is significant, since the calculated F-value is higher than the tabulated one, and the *p-value* is less than 0.05 (α= 5%), given in Table 17.

Figure 34 shows the response surface relating to the influence of the variables: reaction time (A) and molar ratio oil: methanol (C), and the interaction graph for these two variables.

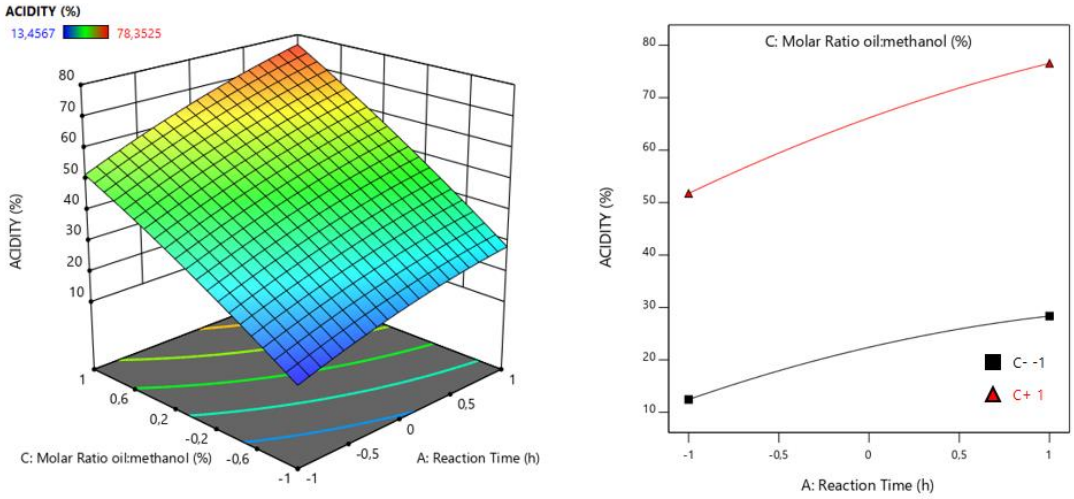

Figure 34 - Response surface for the acidity reduction in function of reaction time (A) and molar ratio oil:methanol (C) and the interaction plot of those variables (Catalyst dosage (B) = 0; Oleic acid incorporation (D) = 0).

The response surface plot shows that there is a difference in the slopes corresponding to the two factors, in which the factor C has a greater influence on the conversion response than the factor A, observing that there is more significant variation in the surface along axis C when compared to the surface variation along the axis A, concluding then, that factor C has a greater influence on the conversion response than factor A.

The interaction plot shows two non-parallel lines, indicating that the variables have influence on one another. If we put a fixed point at level -1, in relation to reaction time (A), that is, 2 hours, it can be seen that, higher values in terms of conversions are obtained for the maximum level of factor C, that is, for the molar ratio oil: methanol 15%, and the same happens if placed the fixed point for the time at its maximum (+1), equivalent to 6 hours, observing that factor C, at its maximum (+1), 15%, gives higher values in terms of conversion, concluding that factor C at a fixed point in A gives the highest conversions on his maximum level. It is also concluded that the interaction between these two factors is significant to the model, since the F-calculated > F-tabulated, and *p-value* < 0.05, given in Table 17.

Figure 35 shows the response surface relating to the influence of the variables: reaction time (A) and incorporation of oleic acid (D), and the interaction graph for these two variables.

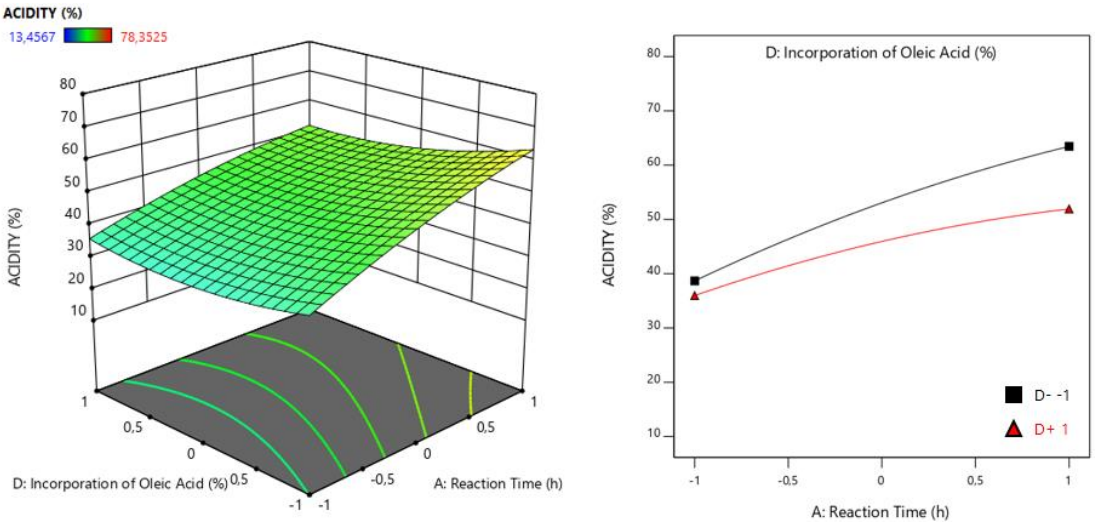

Figure 35 - Response surface for the acidity reduction in function of reaction time (A) and incorporation of oleic acid (D) and the interaction plot of those variables (Catalyst dosage (B) = 0; Molar ratio oil: methanol (C) = 0).

The response surface plot shows that there is a difference in the slopes corresponding to the two factors, in which the factor A has a greater influence on the conversion response than the factor D, observing that there is more significant variation in the surface along axis A when compared to the other, concluding then, that factor A has a greater influence on the conversion response than factor D.

The interaction plot shows two non-parallel lines, indicating that the variables have influence on each other. If we put a fixed point at level -1, in relation to reaction time (A), that is, 2 hours, it can be seen that higher values in terms of conversions are obtained for the minimum level of factor D, that is, for the incorporation of oleic acid of 20 %, and the same happen if placed the fixed point for the time at its maximum (+1), equivalent to 6 hours, it is observed that factor D, at its minimum (-1), 20 % , gives higher values in terms of conversion, concluding that the factor D at a fixed point in A, give the highest conversions on his minimum level. It is also concluded that the interaction between these two factors is significant to the model, since the F-calculated > F-tabulated and the *p-value* < 0.05, given in Table 17.

Figure 36 shows the response surface relating to the influence of the variables: catalyst dosage (B) and molar ratio oil: methanol (C), and the interaction graph for these two variables.

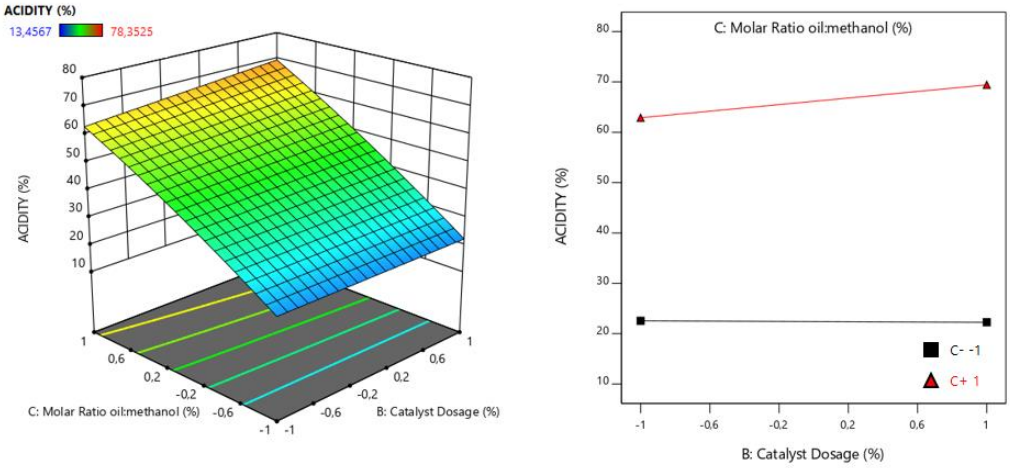

Figure 36 - Response surface for the acidity reduction in function of catalyst dosage (B) Molar ratio oil: methanol (C) and the interaction plot of those variables (Reaction Time (A) = 0; Incorporation of oleic acid (D) = 0).

The response surface plot shows that there is a difference in the slopes corresponding to the two factors, in which the factor C has a greater influence on the conversion response while the factor B is clearly not important for the model, observing that there is a more positive variation in the surface along axis C when compared to the surface variation along the axis C.

The interaction plot shows two non-parallel lines, indicating that the variables have influence on each another. With a fixed point at level -1, in relation to catalyst dosage (B), that is, 5 %, it can be seen that, higher values in terms of conversions are obtained for the maximum level of factor C, that is, for the molar ratio oil methanol of 15 % and the same happens if we place the fixed point for the catalyst dosage at its maximum (+1), equivalent to 15%, it is observed that factor C, at its maximum (+1), 15 % , gives higher values in terms of conversion, concluding that the factor C at a fixed point in B, give the highest conversions on his maximum level. The interaction between these two factors is not significant to the model, since the F-calculated < F-tabulated, and the *p-value* > 0.05, given in Table 17.

Figure 37 shows the response surface relating to the influence of the variables: catalyst dosage (B) and incorporation of oleic acid (D), and the interaction graph for these two variables.

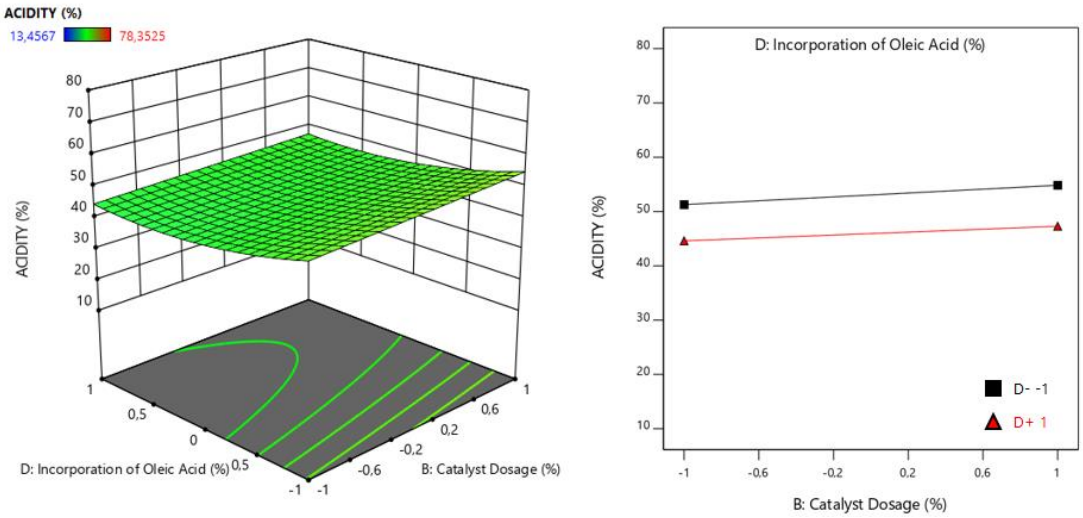

Figure 37 - Response surface for the acidity reduction in function of catalyst dosage (B) and incorporation of oleic acid (D) and the interaction plot of those variables (Reaction Time (A) = 0; Molar ratio oil: methanol (C) = 0).

The response surface plot shows that there is a similarity in the slopes corresponding to the two factors, in which both factors do not have significant effect on the conversion response.

The interaction plot shows two parallel lines, indicating that the variables do not influence on each another. With a fixed point at level -1, in relation to catalyst dosage (B), that is, 5 %, it can be seen that, higher values in terms of conversions are obtained for the minimum level of factor D, that is, incorporation of oleic acid of 20 % and the same happens if placed the fixed point for the catalyst dosage at its maximum (+1), equivalent to 15%, it is observed that factor D, at its minimum (+1). One of the main conclusions through this plot, is that for both levels of B, use the minimum level of D, gives higher values in terms of conversion. The interaction between these two factors is the least significant to the model, since the F-calculated < F-tabulated, and the *p-value* > 0.05, given in Table 17.

Figure 38 shows the response surface relating to the influence of the variables: molar ratio oil: methanol (C) and incorporation of oleic acid (D), and the interaction graph for these two variables.

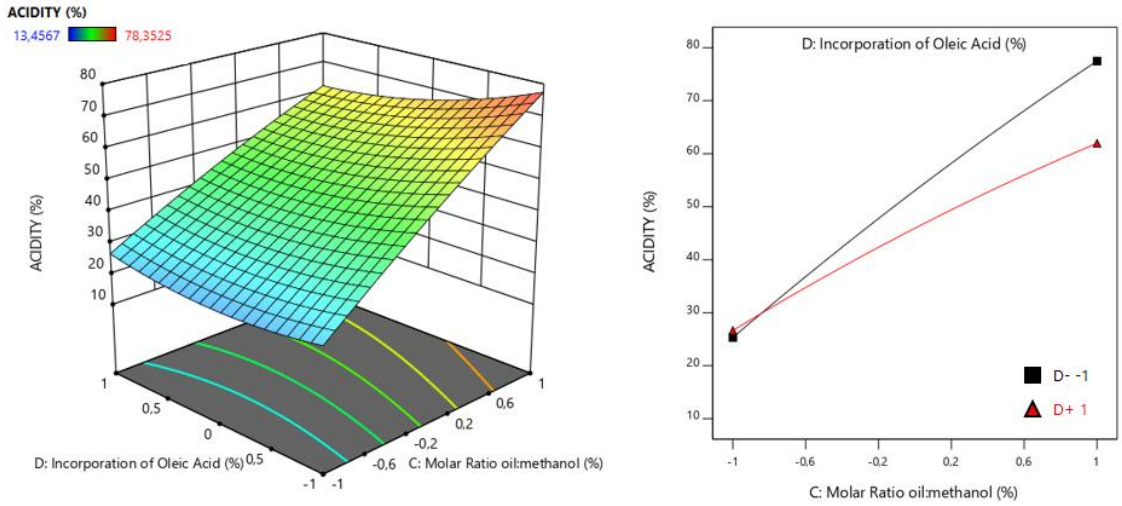

Figure 38 - Response surface for the acidity reduction in function of molar ratio oil: methanol (C) and incorporation of oleic acid (D) and the interaction plot of those variables (Reaction Time (A) = 0; Catalyst dosage (B) = 0).

The response surface plot shows that there is a difference in the slopes corresponding to the two factors, in which the factor C has a greater influence on the conversion response than the factor D, observing that there is more significant variation in the surface along axis C when compared to the surface variation along the axis D, concluding then, that factor C has a greater influence on the conversion response than factor D.

The interaction plot shows two non-parallel lines, indicating that the variables have influence on one another. If we put a fixed point at level -1, in relation to molar ratio oil:methanol (C), that is, 5:1, we can see that we have higher values in terms of conversions for the maximum level of factor C, that is, for the molar ratio oil: methanol 1:15, but it's a small difference to the minimum level, while if we place the fixed point for the molar ratio at its maximum (+1), 15:1, it is observed that factor D, at its minimum, 20%, gives higher values in terms of conversion. It concluded that the interaction between these two factors is the most significant for the model for the response R1, given by the *p-value* 0.002, in Table 17.

5.2.1.4. Optimal conditions for the response R1

The construction of a quadratic equation given by the Equation 4 presented in section 4.3.8 allow the determination of the optimal combination of a set of parameters.

Table 18 displays the coefficients determined by regression of the data set in the software Design Expert 11. Using the information of the coefficients, it is possible to construct the equation that best fits the region studied, as displayed by Equation 7. The equation is constructed using coded values.

Table 18 - Coefficients for the quadratic equation for the response R1.

Coefficient	Coded Factor
Interception	+45.92
A	+10.18
B	+1.56
C	+21.87
D	-3.56
AB	-3.59
AC	+2.23
AD	-2.20
BC	+1.70
BD	-0.2183
CD	-4.21
A^2	-2.00
B^2	+0.0055
C^2	-1.65
D^2	+3.58

$$Y = 45.92 + 10.18A + 1.56B + 21.87C - 3.56D - 3.59AB + 2.23AC - 2.20AD + 1.70BC - 0.2183BD - 4.21CD - 2.00A^2 + 0.0055B^2 - 1.65C^2 + 3.58D^2 \quad (7)$$

Using a statistical tool from EXCEL, named Solver, that allows several types of simulations, being used especially for sensitivity analysis with more than one variable and with parameter restrictions, it was possible to determine which values for the set of parameters studied would lead to the highest conversion in terms of acidity reduction, which is displayed on Table 19, both in coded values and in real values.

Table 19 - Optimal values for the response R1.

Factor	Factor Name	Coded Value	Real Value
A	Time	1	6h
B	Catalyst Dosage	-1	5%
C	Molar ratio MeOH/Oil	1	15/1
D	Incorporation of oleic acid	-1	20%

Two confirmation runs were performed with the optimal values which are displayed in Figure 39. The average obtained for the two runs is 76.70 %. The real values are not very dispersed from the predicted one, indicating that the model is well fitted and accurate (predicted value for acidity reduction content: 80.21 %).

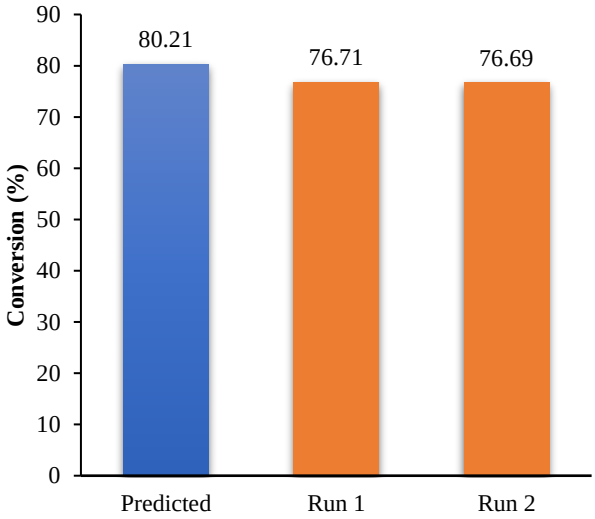

Figure 39 - Predicted value and confirmation runs for the conversion in terms of acidity reduction.

5.2.2. Analysis for the FAME response (R2) – ANOVA Table

5.2.2.1. ANOVA Table

The ANOVA analysis was built in the same way as it was built for the response R1. The ANOVA table for the FAME content evaluation displayed on Table 20 indicates that the model is significant, with a calculated F-value higher than the tabulated one. Also, the lack of fit is not significant with calculated F-value lower than the tabulated one.

Table 20 - ANOVA Table for R2.

Source	Sum of squares	df	Mean Square	Calculated F-value	Tabulated F-value	p-value	
Model	1941.39	14	138.67	22.13	2.637	2×10^{-6}	significant
Residual	75.21	12	6.27				
Lack of Fit	73.88	10	7.39	11.10	19.396	0.0854	not significant
Pure Error	1.33	2	0.67				
Cor Total	2016.60	26					

5.2.2.2. Residual Analysis for the response R2

The reliability of the model adjustment was also assessed by the analysis of the determination coefficient, which was estimated as R^2= 0.9627 and the $R^2_{adjusted}$= 0.9192, showing that the observed and predicted values are close and concluding that the model can be used to predict responses. There are no relevant outliers, or points that significantly detract from

the model's suitability for the experimental data. Figure 40 depicts the normally distributed set of experimental data in question.

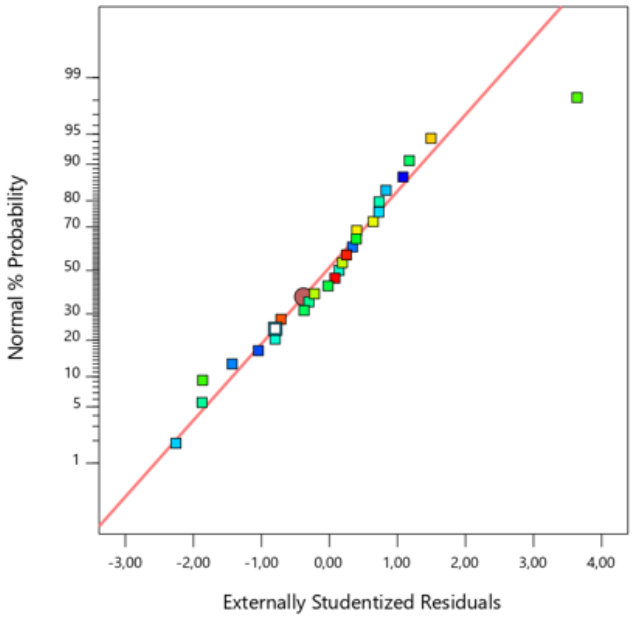

Figure 40 - Normal plot of Residuals.

Figure 41 allows verifying that the residuals are independent of the level of the known variables and that they are practically close to the black line, since the residuals are distributed within the red lines and more or less close to the 0 line.

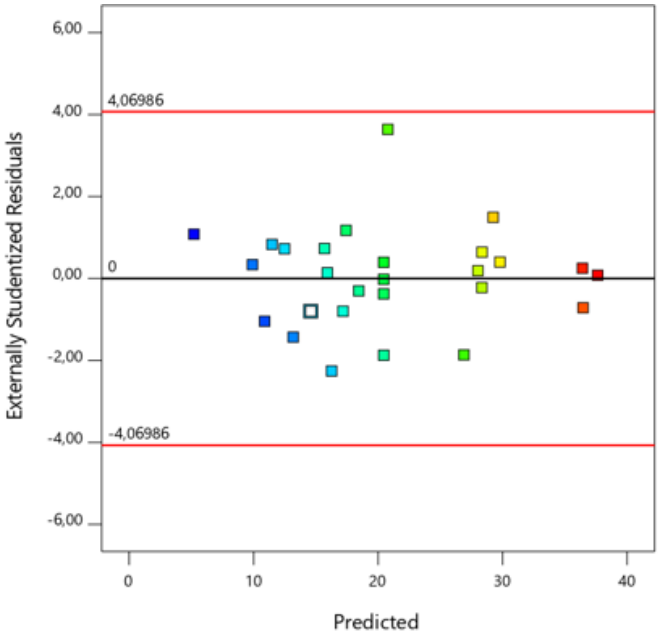

Figure 41 - Residuals versus predicted values.

5.2.2.3. Factor effect on the response R2

Analyzing the influence of each factor, as well as the interactions between them and their quadratic effect on the response, applying the same logic in response R1, the ANOVA

table can also be built, showed in Table 21. The calculated F-value is higher than the tabulated one for the following parameters: A, B, C, D, AD and the remaining terms are not significant. The interactions involving parameter B, proved to be the least significant for the model. Determining the p-value it's possible to see how significant each factor is, and by that, the order of importance is: D > C > A > AD > B.

Table 21 - ANOVA analysis for the parameters influencing the response R2.

Source	Sum of squares	df	Mean Square	Calculated F-value	Tabulated F- value	p-value
A-Reaction Time	362.78	1	362.78	57.88	4.965	6.3×10^{-6}
B-Catalyst Dosage	3.63	1	3.63	0.58	4.965	0.4613
C-Molar Ratio oil:metanol	721.68	1	721.68	115.15	4.965	1.7×10^{-7}
D-Oleic Acid incorporation	744.50	1	744.50	118.79	4.965	1.4×10^{-7}
AB	2.03	1	2.03	0.32	4.965	0.5797
AC	21.44	1	21.44	3.42	4.965	0.0892
AD	38.25	1	38.25	6.10	4.965	0.0295
BC	3.22	1	3.22	0.51	4.965	0.4871
BD	4.04	1	4.04	0.64	4.965	0.4377
CD	12.50	1	12.50	1.99	4.965	0.1833
A^2	8.30	1	8.30	1.32	4.965	0.2722
B^2	5.25	1	5.25	0.84	4.965	0.3779
C^2	3.85	1	3.85	0.61	4.965	0.4482
D^2	1.47	1	1.47	0.23	4.965	0.6369

Figure 42 shows the adjusted averages of the experimental conversion findings for the low and high levels of (A) reaction time, (B) catalyst dosage, (C) molar ratio oil:methanol.

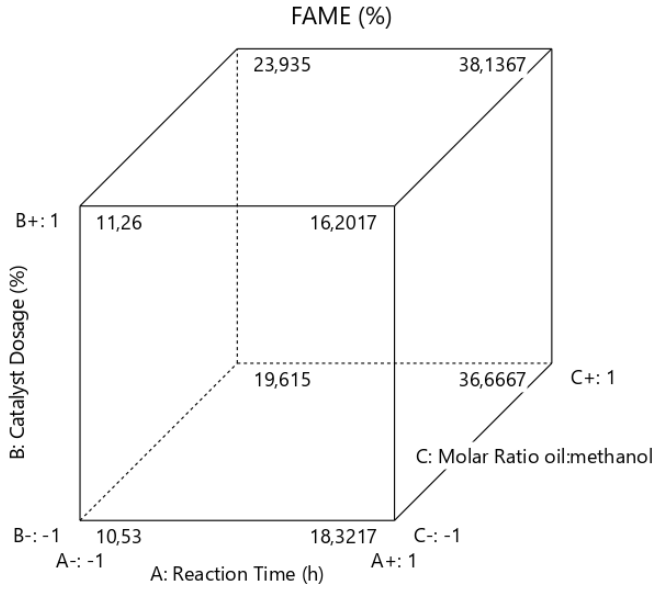

Figure 42 - Cube chart for response R2 (Incorporation of oleic acid (D) = 0).

The effects of each parameters are shown in Figure 43, where the deviation of the adjusted means between the levels can be seen.

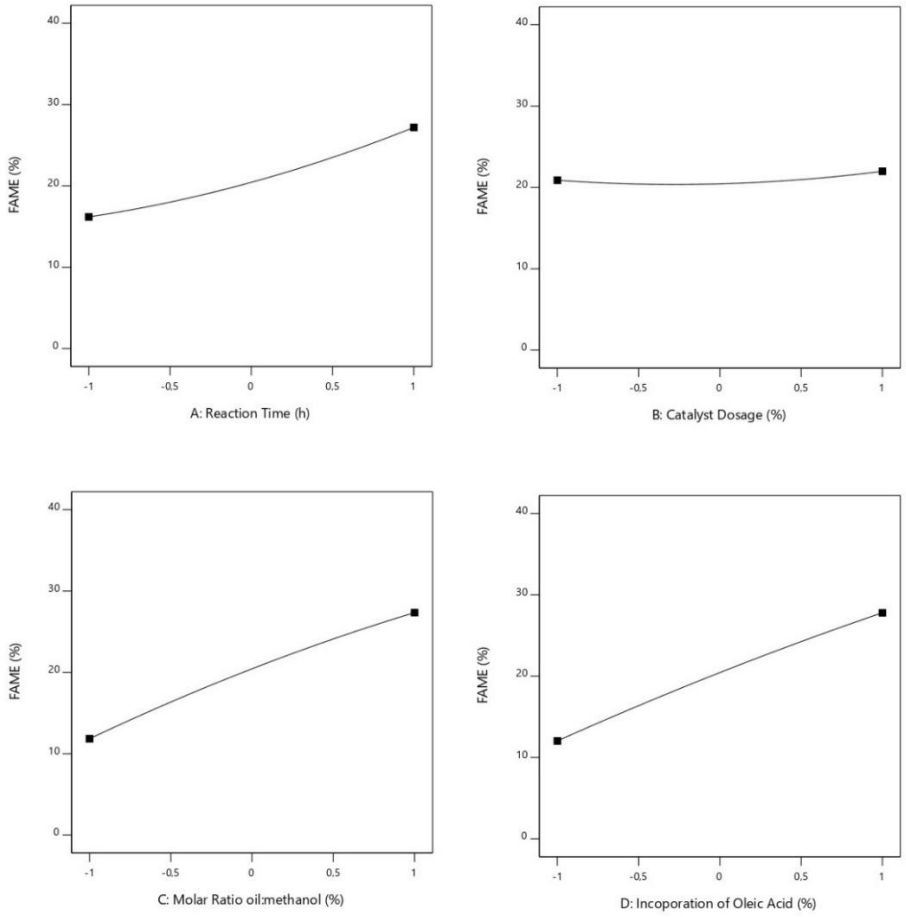

Figure 43 - Effects for each factor on the response R2.

Factors A, C and D have a positive effect, because the response increases as it changes from the lowest to the highest level, with factor B having insignificant influence on the response. Parameters A, C and D have lines with greater slopes than parameter B, inducing larger changes in the FAME content when changed.

Figure 44 shows the response surface in relation to the influence of variables, reaction time (A) and catalyst dosage (B), and the respective interaction graph.

The response surface indicates that variable B has a low influence on the FAME content results. Observing the variation along axis B at a fixed point in A, only a small change between the levels of the factor is noticed and making the same analysis for variable A at a fixed point in B, it is possible to verify that the response increases significantly when the levels of the factor vary, concluding that Factor A has a greater influence on FAME content than factor B. The interaction plot shows two non-parallel lines, indicating that the variables have influence on one another. The main conclusion is that use 5 % or 15 % of catalyst dosage (B), it's not

significant for the response variation because at a maximum level of reaction time (A), the interaction plot shows that the minimum level of catalyst dosage (B) has greater values in terms of FAME than the maximum level of B. The interaction of these two variables is insignificant to the model, given by the F-calculated < F- tabulated and by the *p-value* > 0.05, showed in Table 21.

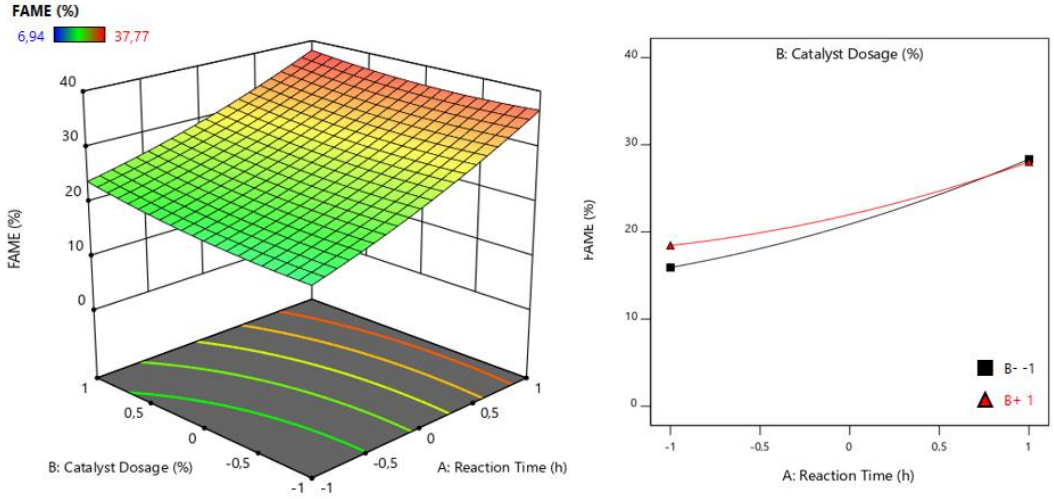

Figure 44 - Response surface for the FAME content in function of reaction time (A) and catalyst dosage (B) and the interaction plot of those variables (Molar ratio oil: methanol (C) = 0; Oleic acid incorporation (D) = 0).

Figure 45 shows the response surface in relation to the influence of variables, reaction time (A) and molar ratio oil: methanol (C), and the respective interaction graph.

The response surface indicates that variable A, this time, has a lower influence on the FAME content results. Observing the variation along axis A at a fixed point in C, only a small change between the levels of the factor is noticed, making the same analysis for variable C at a fixed point in A, it is possible to verify that the response increases significantly when the levels of the factor vary, concluding that Factor C has a greater influence on FAME content than factor A. The interaction plot shows two non-parallel lines, indicating that the variables have influence on one another. One of the main conclusions is that the molar ratio oil: methanol at its maximum level, give highest values in terms of the FAME content. The interaction of these two variables is insignificant to the model, given by the F-calculated < F- tabulated and by the *p-value* > 0.05, showed in Table 21.

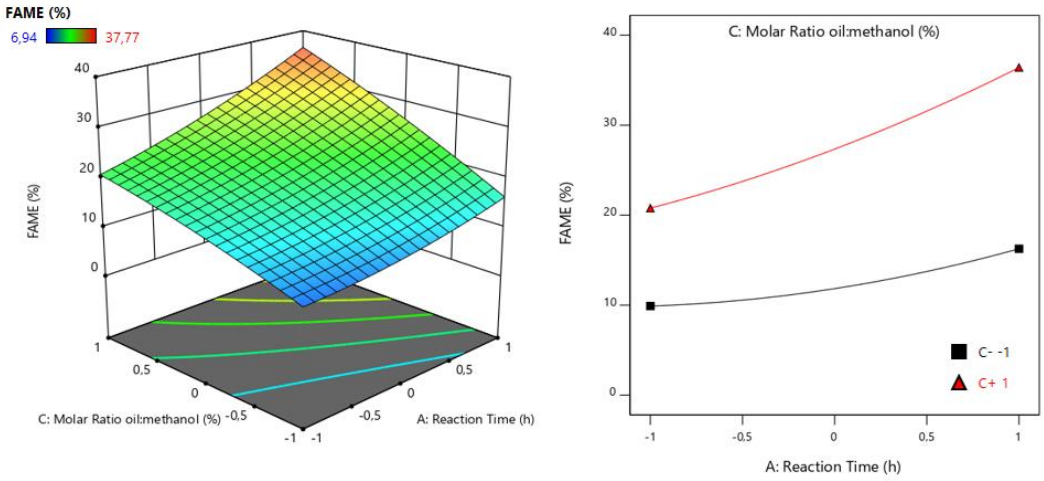

Figure 45 - Response surface for the FAME content in function of reaction time (A) and molar ratio oil: methanol (C) and the interaction plot of those variables (Catalyst dosage (B) = 0; Oleic acid incorporation (D) = 0).

Figure 46 shows the response surface in relation to the influence of variables, reaction time (A) and incorporation of oleic acid (D), and the respective interaction graph.

The response surface is very similar to the variables AC, indicating that variable A, has a lower influence on the FAME content results. Observing the variation along axis A at a fixed point in D, only a small change between the levels of the factor is noticed, making the same analysis for variable D, it is possible to verify that the response increases significantly when the levels of the factor vary, concluding that Factor D has a greater influence on FAME content than factor A. The interaction plot shows two non-parallel lines, indicating that the variables have influence on one another. One of the main conclusions, is that the incorporation of oleic acid at its maximum level, give highest values in terms of the FAME content. The interaction of these two variables is the most significant to the model, given by the F-calculated > F-tabulated and by the *p-value* < 0.05, showed in Table 21.

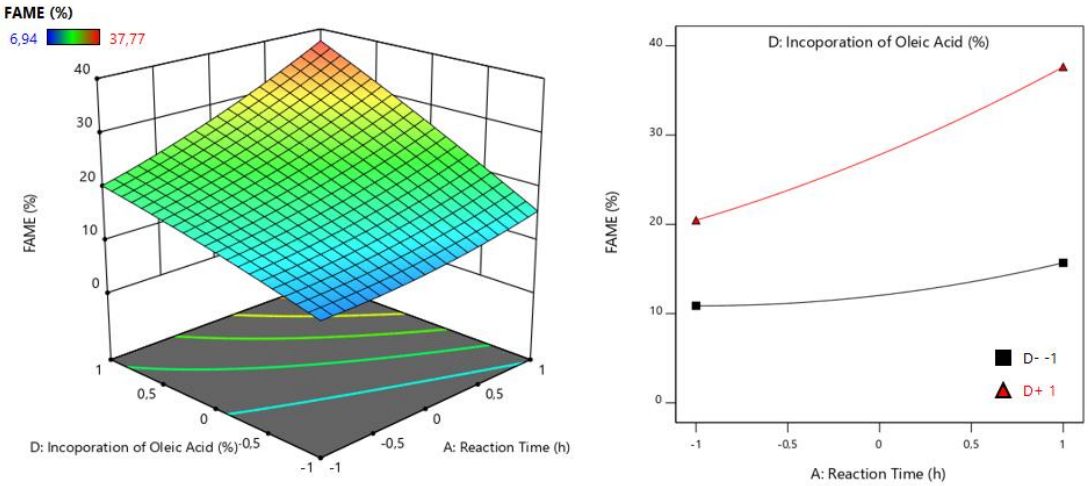

Figure 46 - Response surface for the FAME content being in function of reaction time (A) and incorporation of oleic acid (D) and the interaction plot of those variables (Catalyst dosage (B) = 0; Molar ratio oil: methanol (C) = 0).

Figure 47 shows the response surface in relation to the influence of variables, catalyst dosage (B) and molar ratio oil: methanol (C), and the respective interaction graph.

The response surface indicates that variable B, has a lower influence on the FAME content results. Observing the variation along axis B at a fixed point in C, only a small change between the levels of the factor is noticed, making the same analysis for variable C, it is possible to verify that the response increases significantly when the levels of the factor vary, concluding that Factor C has a greater influence on FAME content than factor A. The interaction plot shows two non-parallel lines, indicating that the variables have influence on one another. The main conclusion is that at maximum level of C, use 5 % or 15 % of catalyst (B), hardly changes the response in terms of FAME content. The interaction of these two variables is one of the most insignificant to the model, given by the F-calculated < F- tabulated and by the *p-value* > 0.05, showed in Table 21.

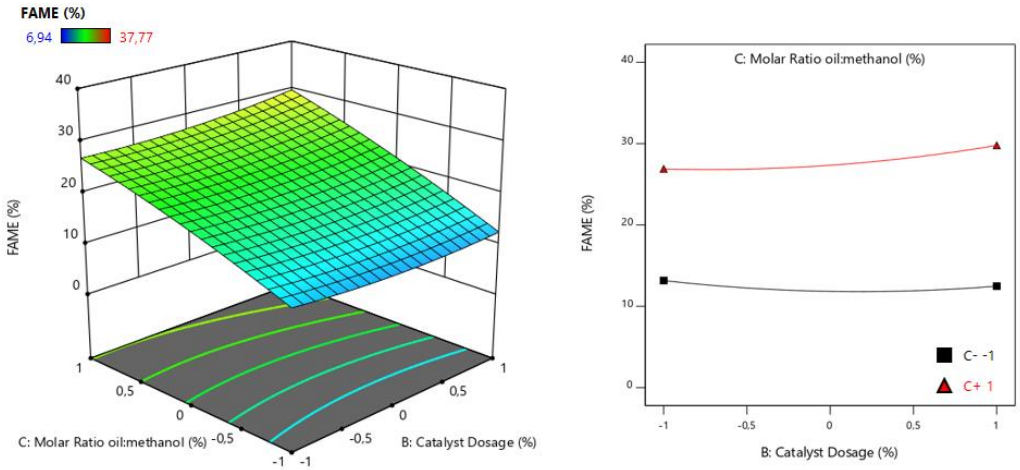

Figure 47 - Response surface for the FAME content in function of catalyst dosage (B) Molar ratio oil: methanol (C) and the interaction plot of those variables (Reaction Time (A) = 0; Incorporation of oleic acid (D) = 0).

Figure 48 shows the response surface in relation to the influence of variables, catalyst dosage (B) and incorporation of oleic acid (D), and the respective interaction graph.

The same behavior is observed in Figure 46, it's observed to for the Figure 47, but this interaction is even more insignificant to the response, given by the F-calculated < F- tabulated and by the *p-value* > 0.05, showed in Table 21.

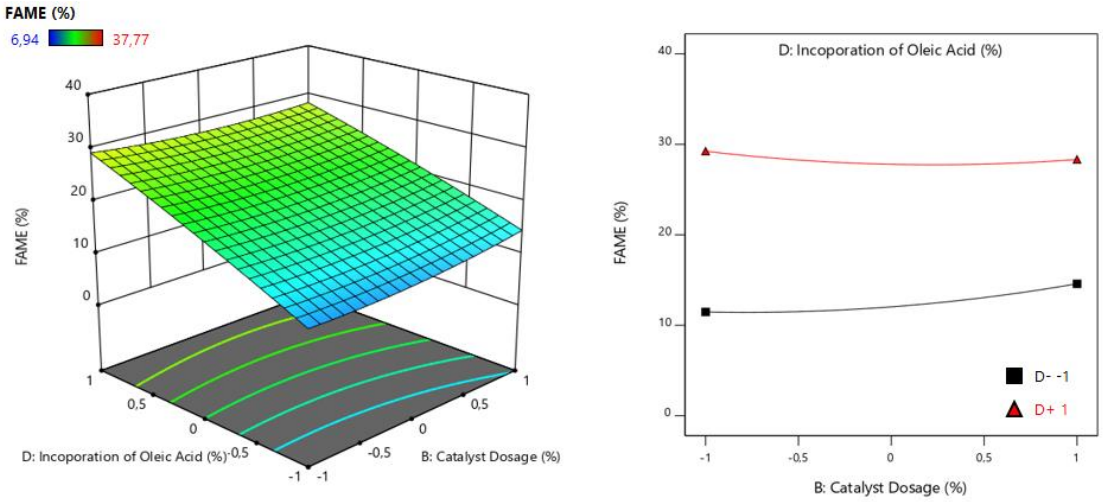

Figure 48 - Response surface for the FAME content in function of catalyst dosage (B) and incorporation of oleic acid (D) and the interaction plot of those variables (Reaction Time (A) = 0; Molar ratio oil: methanol (C) = 0).

Figure 49 shows the response surface in relation to the influence of variables, reaction time (C) and incorporation of oleic acid (D), and the respective interaction graph.

The response surface indicates that both variables have a huge influence on the FAME content results. Observing the variation along axis C at a fixed point in D, a large change between the levels of the factor is noticed and the same change happen making the same analysis for variable C at a fixed point in A, it is possible to verify that the response increases significantly when the levels of the factor vary, concluding that both factors have a greater influence on FAME content. The interaction plot shows two non-parallel lines (almost parallels), indicating that the variables have influence on one another (almost don't have influence in one another). One of the main conclusions is that factor at their maximum levels, give highest values in terms of FAME content. The interaction of these two variables is insignificant to the model, given by the F-calculated < F-tabulated and by the *p-value* > 0.05, showed in Table 21.

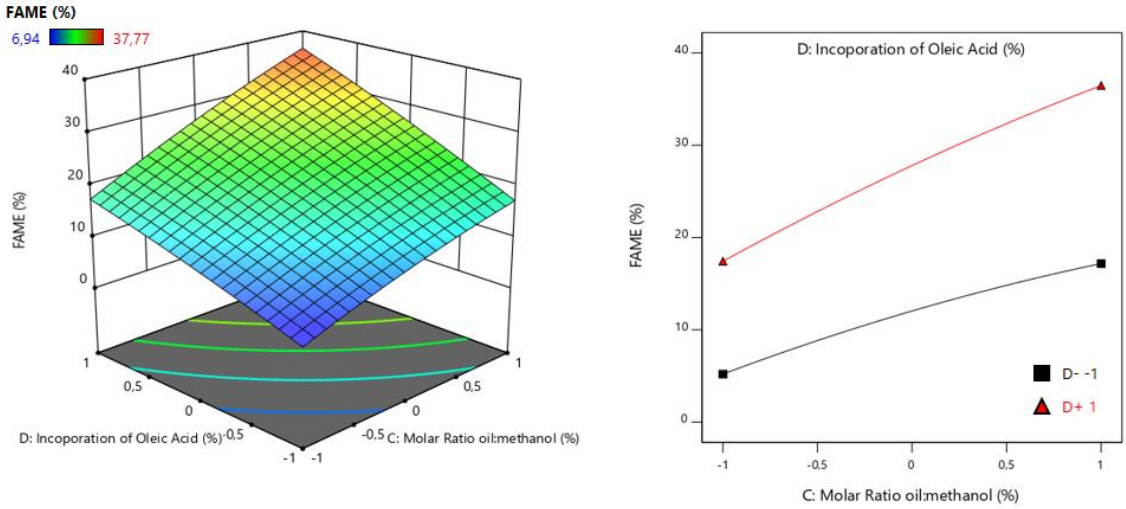

Figure 49 - Response surface for the FAME content in function of molar ratio oil: methanol (C) and incorporation of oleic acid (D) and the interaction plot of those variables (Reaction Time (A) = 0; Catalyst dosage (B) = 0).

5.2.2.4. Optimal conditions for the response R2

Table 18 displays the coefficients determined by regression of the data set in the software Design Expert 11. Using the information of the coefficients, it is possible to construct the equation that best fits the region studied, as displayed by Equation 8. The equation is constructed using coded values.

Table 22 - Coefficients for the quadratic equation for the response R2.

Coefficient	Coded Factor
Interception	+20.44
A	+5.50
B	+0.5500
C	+7.76
D	+7.88
AB	-0.7125
AC	+2.31
AD	+3.09
BC	+0.8975
BD	-1.00
CD	+1.77
A^2	+1.25
B^2	+0.9925
C^2	-0.8500
D^2	-0.5250

$$Y = 20.44 + 5.50 + 0.5500B + 7.76C + 7.88D - 0.7125AB + 2.31AC + 3.09AD + 0.8975BC - 1.00BD + 1.77CD + 1.25A^2 + 0.9925B^2 - 0.8500C^2 - 0.5250D^2 \quad (8)$$

Using Solver, it was possible to determine which values for the set of parameters studied would lead to the highest conversion in terms of FAME content, which is displayed on Table 19, both in coded values and in real values. New runs must be carried out with the purpose to confirm the predicted result and the model.

Table 23 - Optimal values for the response R2.

Factor	Factor Name	Coded Value	Real Value
A	Time	1	6h
B	Catalyst Dosage	-1	5%
C	Molar ratio MeOH/Oil	1	15/1
D	Incorporation of oleic acid	1	60%

With a 95% confidence level, the predicted response in terms of FAME, is 50.01 %.

Goes H., 2018 found that the most favorable reaction conditions for the FAME content response correspond to an incorporation of 40 % oleic acid in waste cooking oil, reaction time of 8 h, molar ratio oil/methanol 1:20, temperature of 90 ºC and a catalyst dosage ([HIM][HSO_4]) of 10 % wt, with an average content of 36.5 %.

Diniz H., 2020 found that using ionic liquid [HIM][HSO_4] to catalyze the esterification reaction of a simulated oil with methanol, the highest content in FAME was 24.1 %, under the follow optimal conditions: temperature of 65 °C, reaction time of 4 hours, molar ratio 1:10 of raw material/methanol and 10 % wt catalyst.

Two confirmation runs were performed with the optimal values which are displayed in Figure 50. The average obtained for the two runs is 42.52 %. The real values are not very far from the predicted one, indicating that the model is well fitted and accurate (predicted value for acidity reduction content: 50.01 %).

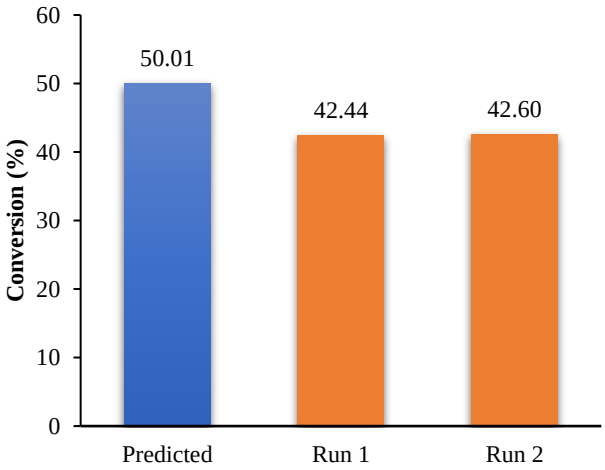

Figure 50 - Predicted value and confirmation runs for the FAME content.

5.2.3. Analysis for the Yield response (R3) – ANOVA Table

5.2.3.1. ANOVA Table

The ANOVA analysis was built in the same way as it was built for the response R1 and R2. The ANOVA for the Yield content displayed on Table 24 indicates that the model is significant, with a calculated F-value higher than the tabulated one. Also, the lack of fit is not significant with calculated F-value lower than the tabulated one.

Table 24 - ANOVA Table for R3.

Source	Sum of squares	df	Mean Square	Calculated F-value	Tabulated F-value	p-value	
Model	1911.66	14	136.55	21.03	2.637	2.7×10^{-6}	significant
Residual	77.93	12	6.49				
Lack of Fit	76.57	10	7.66	11.29	19.396	0.0840	not significant
Pure Error	1.36	2	0.68				
Cor Total	1989.59	26					

5.2.3.2. Residual Analysis for the response R3

The reliability of the model adjustment was assessed by the analysis of the determination coefficient and its very similar to the response R2, which was estimated as R^2= 0.9608 and the $R^2_{adjusted}$= 0.9151, showing that the observed and predicted values are close and concluding that the model can be used to predict responses. There are no relevant outliers, or points that significantly detract from the model's suitability for the experimental data. Figure 51 depicts the normally distributed set of experimental data in question.

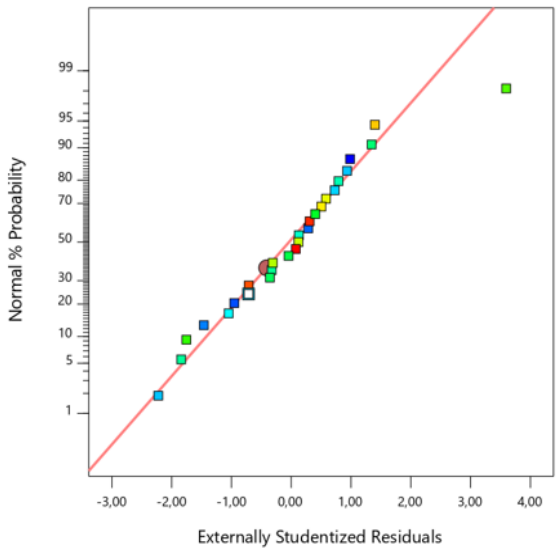

Figure 51 - Normal plot of Residuals.

Figure 52 allows verifying that the residuals are independent of the level of the known variables and that they are practically close to the black line, since the residuals are distributed within the red lines and more or less close to the 0 line.

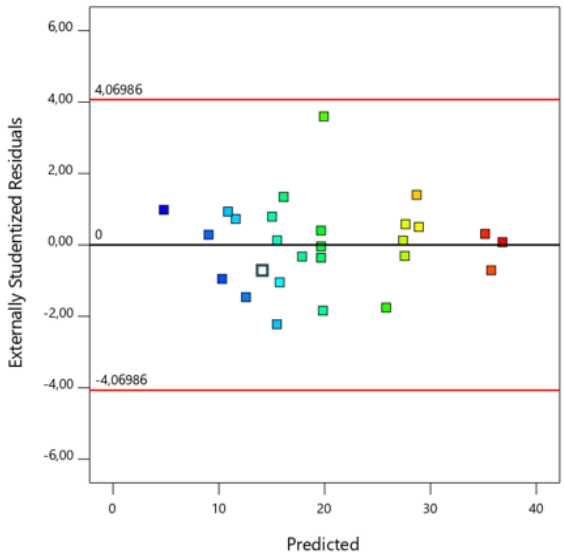

Figure 52 - Residuals versus predicted values.

5.2.3.3. Factor effect on the response R3

Analyzing the influence of each factor, as well the interactions between them and their quadratic effect on the response, applying the same logic in response R1 and R2, the ANOVA was built, showed in Table 25. It is very similar to the response R2, in which the calculated F-value is higher than the tabulated one for the following parameters: A, B, C, D, AD and the remaining terms are not significant. As is response R1 and R2, the interactions involving parameter B, proved to be least significant for the model. Determining the p-value it's possible to see how significant each factor is, and by that, the order of importance is: D > C > A > CD > B.

Table 25 - ANOVA analysis for the parameters influencing the response R3.

Source	Sum of squares	df	Mean Square	Calculated F-value	Tabulated F-value	p-value
A-Reaction Time	352.6298	1	352.6298	54.30	4.965	8.63×10^{-6}
B-Catalyst Dosage	3.372508	1	3.372508	0.52	4.965	0.4849
C-Molar Ratio oil : metanol	700.46	1	700.46	107.86	4.965	2.38×10^{-7}
D-Oleic Acid incorporation	734.92	1	734.92	113.17	4.965	1.83×10^{-7}
AB	1.67	1	1.67	0.26	4.965	0.6208
AC	19.28	1	19.28	2.97	4.965	0.1106
AD	37.55	1	37.55	5.78	4.965	0.0332
BC	4.13	1	4.13	0.64	4.965	0.4409
BD	4.78	1	4.78	0.74	4.965	0.4075
CD	18.76	1	18.76	2.89	4.965	0.1150
A^2	9.25	1	9.25	1.42	4.965	0.2557
B^2	6.84	1	6.84	1.05	4.965	0.3251
C^2	6.14	1	6.14	0.94	4.965	0.3502
D^2	1.232043	1	1.232043	0.19	4.965	0.6709

The response surfaces and the interaction plots allow to see that the most relevant variable is reaction time (A), molar ratio oil: methanol (C) and incorporation of oleic acid (D), as in the response R2. By increasing the level of the reaction time, molar ratio oil: methanol and the incorporation of oleic acid, a clear and strong effect in the response is observed. The least relevant variable is the catalyst dosage by observing the hard change of the factor B along the axis. AD is the most relevant interaction for the response R3, given by the *p-value* < 0.05 and by looking to the Figure 55 it is possible to see that both variables have a strong and positive effect when both are in their maximum level. Interaction AB reveals to be the least significant interaction for the response R3 given by the Figure 56 that shows a hardly change into the response when both are in their minimum and maximum levels.

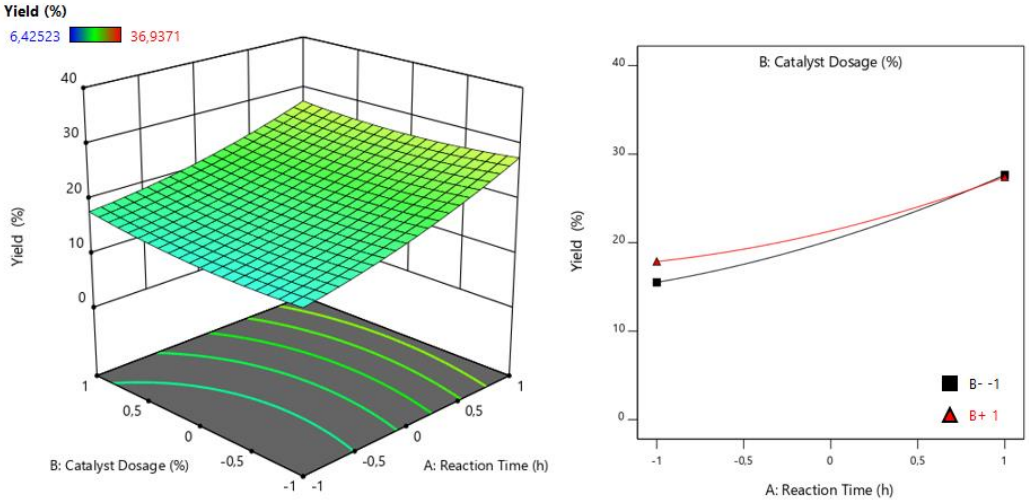

Figure 53 - Response surface for the Yield in function of reaction time (A) and catalyst dosage (B) and the interaction plot of those variables (Molar ratio oil:methanol (C) = 0; Oleic acid incorporation (D) = 0).

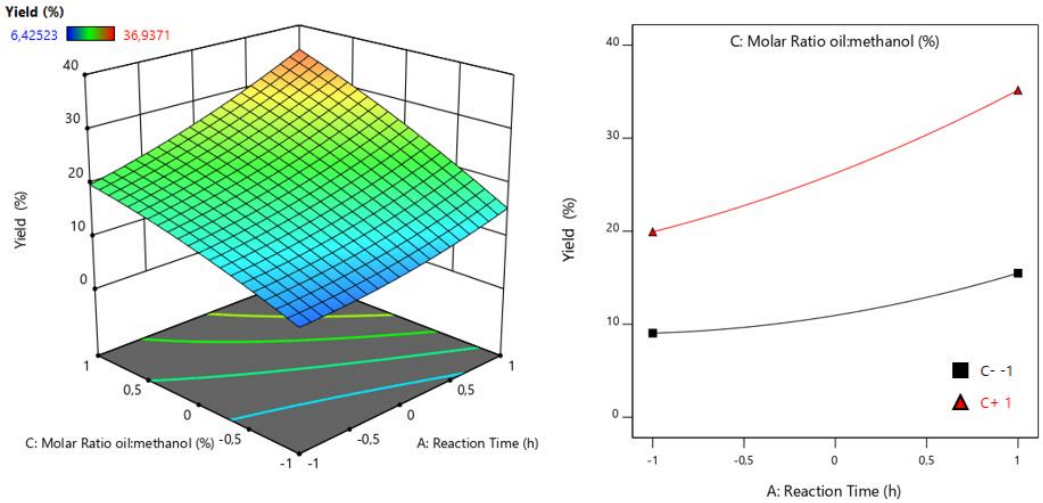

Figure 54 - Response surface for the Yield in function of reaction time (A) and molar ratio oil: methanol (C) and the interaction plot of those variables (Catalyst dosage (B) = 0; Oleic acid incorporation (D) = 0).

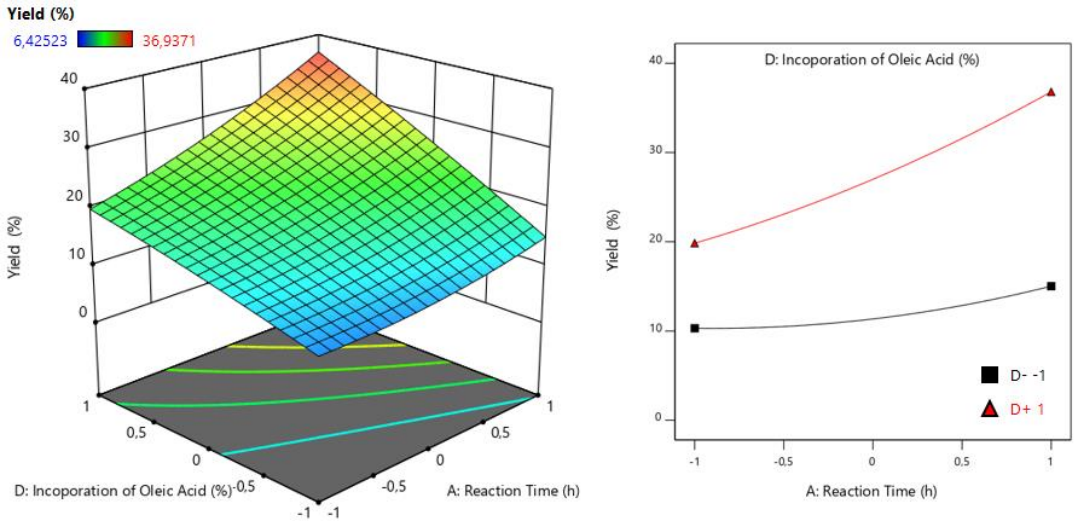

Figure 55 - Response surface for the Yield in function of reaction time (A) and incorporation of oleic acid (D) and the interaction plot of those variables (Catalyst dosage (B) = 0; Molar ratio oil: methanol (C) = 0).

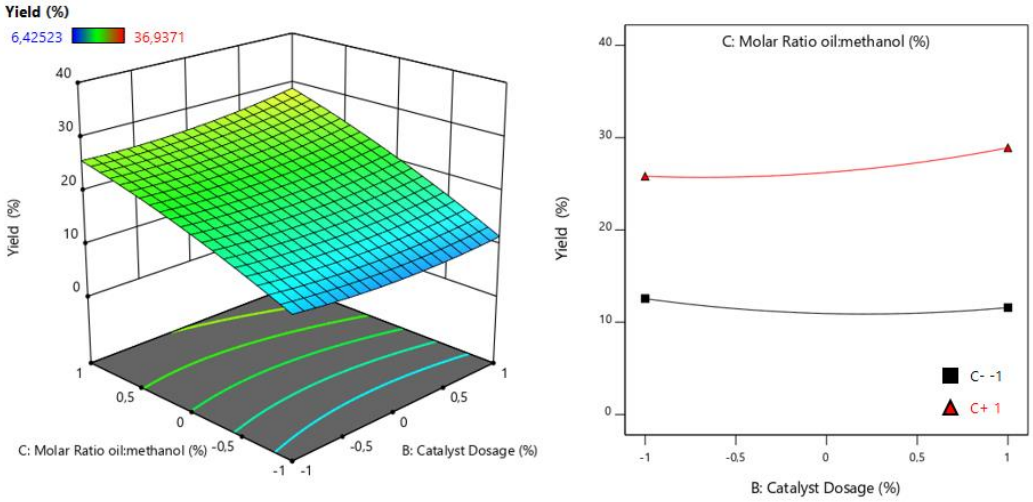

Figure 56 - Response surface for the Yield in function of catalyst dosage (B) Molar ratio oil: methanol (C) and the interaction plot of those variables (Reaction Time (A) = 0; Incorporation of oleic acid (D) = 0).

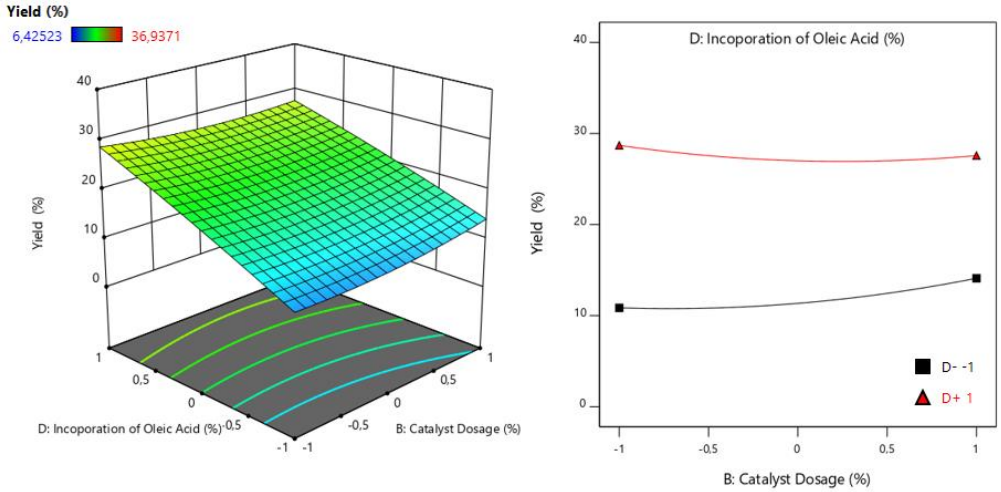

Figure 57 - Response surface for the Yield in function of catalyst dosage (B) and incorporation of oleic acid (D) and the interaction plot of those variables (Reaction Time (A) = 0; Molar ratio oil: methanol (C) = 0).

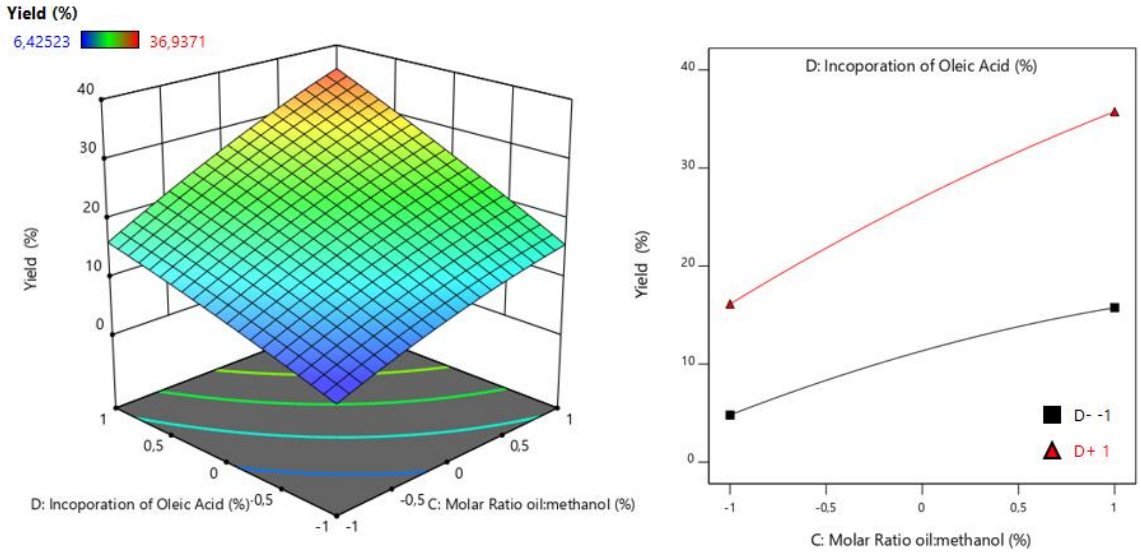

Figure 58 - Response surface for the Yield in function of molar ratio oil: methanol (C) and incorporation of oleic acid (D) and the interaction plot of those variables (Reaction Time (A) = 0; Catalyst dosage (B) = 0).

5.2.3.4. Optimal conditions for the response R3

Table 26 displays the coefficients determined by regression of the data set in the software Design Expert 11. The equation that best fits the region studied is displayed by Equation 9, constructed using coded values.

Table 26 - Coefficients for the quadratic equation for the response R3.

Coefficient	Coded Factor
Interception	+19.66
A	+5.42
B	+0.5301
C	+7.64
D	+7.83
AB	-0.6471
AC	+2.20
AD	+3.06
BC	+1.02
BD	-1.09
CD	+2.17
A^2	+1.32
B^2	+1.13
C^2	-1.07
D^2	-0.4806

$$Y = 19.66 + 5.42\mathrm{A} + 0.5301B + 7.64\mathrm{C} + 7.83D - 0.6471AB + 2.20AC + 3.06AD + 1.02BC - 1.09BD + 2.17CD + 1.32A^2 + 1.13B^2 - 1.07C^2 - 0.4806D^2 \quad (9)$$

Whit Solver, it was possible to determine which values for the set of parameters studied would lead to the highest conversion in terms of Yield content, which is displayed on Table 27, both in coded values and in real values.

Table 27 - Optimal values for the response R3.

Factor	Factor Name	Coded Value	Real Value
A	Time	1	6h
B	Catalyst Dosage	-1	5%
C	Molar ratio MeOH/Oil	1	15/1
D	Incorporation of oleic acid	1	60%

Two confirmation runs were performed which are displayed in Figure 59. The average obtained for the two runs is 37.70 %. This value is not far from the estimated by the model, indicating it is well fitted and accurate (predicted value for the yield content: 48.98 %).

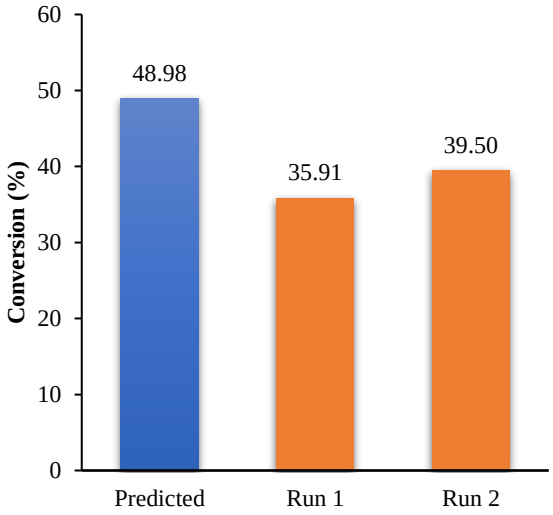

Figure 59 - Predicted value and confirmation runs for the Yield content.

5.3. FT-IR Qualitative Analysis

The chemical composition of selected raw materials and the produced biodiesel was determined using infrared spectrophotometry (FT-IR), revealing if the conversion of free fatty acids to esters truly occurred. The FT-IR spectrum obtained with a sample of waste cooking oil, used as raw material, is shown in Figure 60.

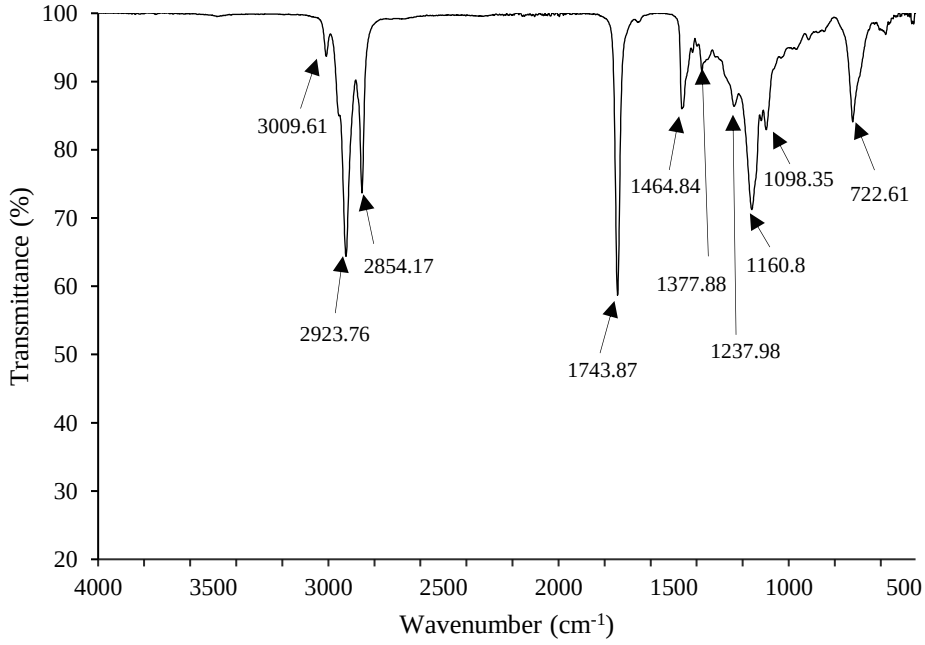

Figure 60 - FT-IR spectrum of the waste cooking oil.

Triglycerides, which are esters, make up the majority of the oil. The bands 2923.76 and 2854.17 cm^{-1} correspond to the asymmetric and symmetrical elongation of the aliphatic C-H bonds with sp^3 hybridization, respectively, as in the oleic acid spectrum (Roman, *et al.*, 2019)

(Pavia, L. *et al.*, 1989). The C=O stretch, which is also characteristic of esters, occurs in the range of 1750 to 1735 cm^{-1} in this sample, with a value of 1743.87 cm^{-1}. The folding of the CH_2 bond is represented by the band 1464.84 cm^{-1}, while the folding of the CH_3 bond is represented by the band 1377.88 cm^{-1}. In the range of 1300 to 1000 cm^{-1}, the C-O stretch shows as two or more bands, one of which is the strongest and widest. The link appears at 1160.8 and 1098.35 cm^{-1} in this case. *Rocking* movement associated with four or more CH_2 groups in an open chain occurs at 722.61 cm^{-1}, as seen in the oleic acid spectrum (Pavia, L. *et al.*, 1989).

The FT-IR spectrum obtained with a sample of oleic acid is shown in Figure 61.

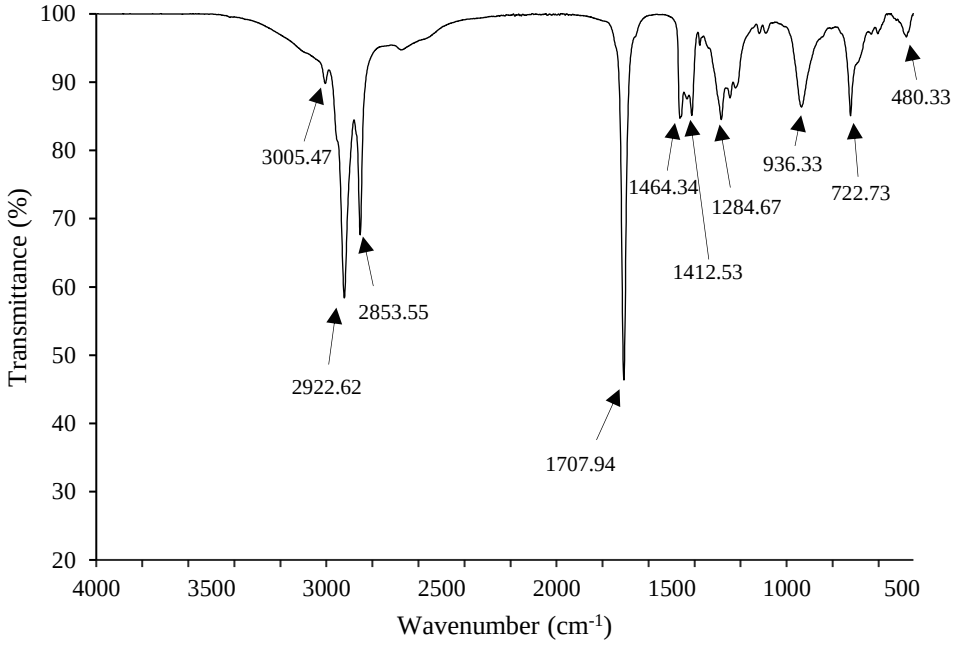

Figure 61 - FT-IR spectrum of the oleic acid.

Carboxylic acids contain a broad band that spans 3400 to 2400 cm^{-1}, with a peak at 3000 cm^{-1}, which symbolizes the O-H bond strongly connected by hydrogen bonding. Normally, this band overlaps the C-H absorptions. This band, centered at 3005.47 cm^{-1}, may be seen in the FT-IR spectrum of oleic acid (Goes H., 2018) (Pavia, L. *et al.*, 1989). The asymmetric and symmetrical elongation of the aliphatic C-H bonds with sp^3 hybridization are connected with the 2922.62 and 2853.55 cm^{-1} bands that overlap the O-H bond, respectively. Carboxylic acids also exhibit C=O stretching, which occurs between 1730 and 1700 cm^{-1}. This band appears at 1707.94 cm^{-1} in the OA spectrum, and it is the strongest and sharpest band in the spectrum. The folding of the CH_2 bond is represented by the band 1464.34 cm^{-1}, and the folding of the C-O-H bond is represented by the band 1412.53 cm^{-1}, which appears as a broad and weak peak between 1440 and 1220 cm^{-1}. The C-O stretch, which is also a feature of the OA, occurs in the region of

1320 to 1210 cm^{-1} and is of medium strength. The connection appears to be at 1284.67 cm^{-1} in this case. An out-of-plane angular distortion of the O-H bond causes the band at 936.33 cm^{-1}. The rocking movement associated with four or more CH_2 groups in an open chain occurs at around 720 cm^{-1}, and in this sample, it appears at 722.73 cm-^{1} (Roman, *et al.*, 2019) (Pavia, L. *et al.*, 1989).

Figure 62 shows the FTIR spectrum of 1-methylimidazolium hydrogensulfate ionic liquid ([HMIM][HSO_4]).

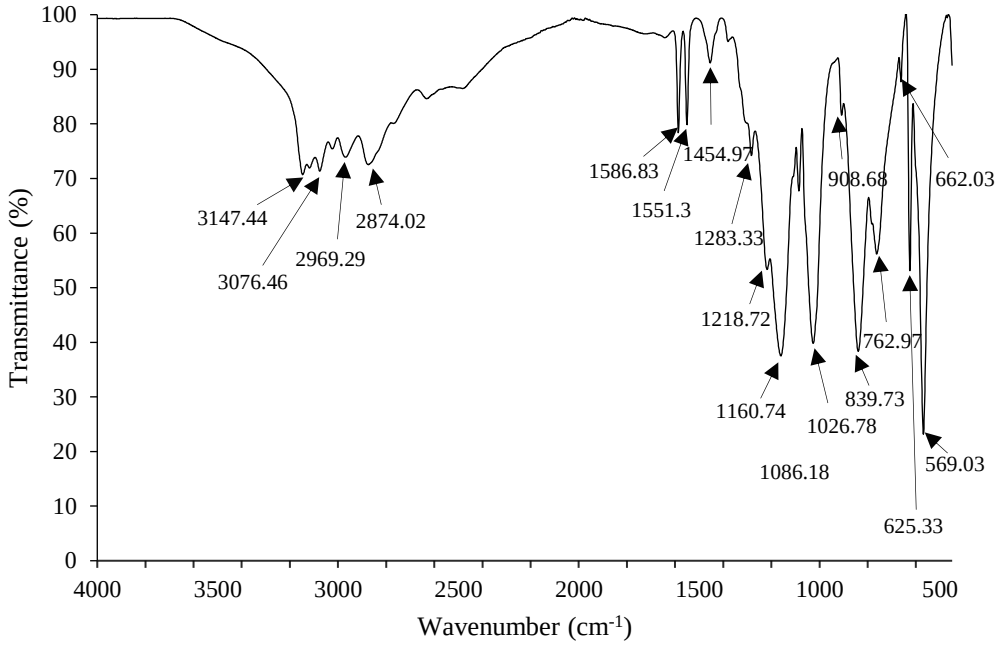

Figure 62 - FT-IR spectrum of the commercial ionic liquid [HMIM][HSO_4].

The C-H bond for nitrogen-containing heteroaromatic rings occurs at roughly 3180-3090 cm^{-1}, hence the bands 3147.44 and 3076.46 cm^{-1} can be attributed to the cation's elongation vibration of the C-H bonds. The symmetrical and asymmetrical stretching of the CH_3 bond is shown by the bands 2969.29 and 2874.02 cm^{-1}, respectively. Bands 1586.83, 1551.3, and 1454.9 cm^{-1} are related to the ring present on the imidazolium cation. Heterocyclic compounds with a five-membered ring and two double bonds have three ring vibrations around 1590, 1490, and 1400 cm^{-1}, so bands 1586.83, 1551.3, and 1454.9 cm^{-1} are related to the ring present on the imidazolium cation. The absorption bands of the HSO_4^- group are 1190-1160 cm^{-1} for the asymmetric SO_3^{-2} group and 1080-1015 cm^{-1} for the symmetric SO_3^{-2} group. The anion is represented by bands 1160.74 and 1026.78 cm^{-1}. Furthermore, in the 900-700 cm^{-1} range, most five-membered rings with an unsubstituted CH=CH group display considerable

hydrogen absorption. As a result, this vibration is responsible for the bands 839.73 and 762.97 cm^{-1} (Roman, *et al.*, 2019) (Pavia, L. *et al.*, 1989).

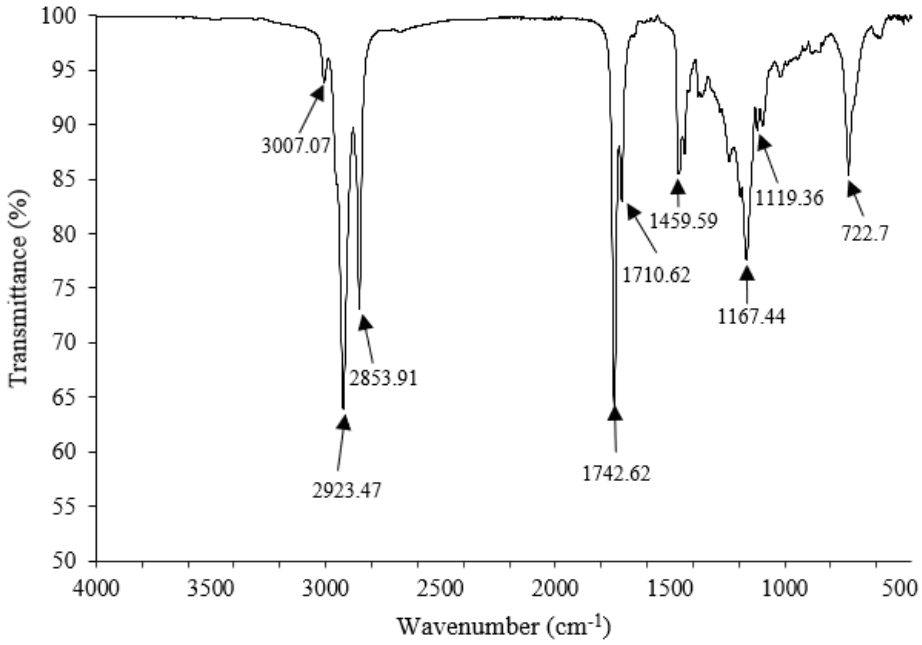

Figure 63 - FT-IR spectrum of final produced biodiesel.

Bands 2923.47 and 2853.91 cm^{-1} correspond to the asymmetric and symmetrical elongation, respectively, of the aliphatic C-H bonds with sp^3 hybridization. The differences with oleic acid are related to the disappearance of the broad band centered at 3005.47 cm^{-1} and the band corresponding to the folding of the COH bond in 1412.53 cm^{-1}, and the displacement in the absorption of the C=O bond, which occurs in the esters range from 1750 to 1735 cm^{-1}, and now appears at 1742.62 cm^{-1}. However, it is still possible to visualize the band 1710.62 cm^{-1}, but at a lower intensity, which is related to the C=O bond present in oleic acid. Therefore, it can be concluded that not all free fatty acids were converted to esters. Band 1459.59 cm^{-1} correspond to the folding of the CH_2 bond. The elongation vibration CO appears with two or more bands in the region from 1300 to 1000 cm^{-1}, with the band in the range 1300-1150 cm^{-1} referring to the carbonyl group and the other band, generally weaker than the first, appears in the range 1150-1000 cm^{-1}. Thus, band 1167.47 cm^{-1} correspond to the C-O elongation. The rocking movement associated with four or more CH_2 groups in an open chain occurs at 722.7 cm^{-1} (Roman, *et al.*, 2019) (Pavia, L. *et al.*, 1989).

5.4. Recovery of the ionic liquid

The recovery of the ionic liquid was studied for the optimal point of responses R2 and R3, described in section 5.3.1.4 and 5.3.2.4, respectively. The ionic liquid was recovered and

reused, for only two cycles, in order to confirm the recoverability and reuse of IL, without significantly altering its initial composition. Thus, in cycle one commercial ionic liquid is used, and in the next, IL recovered from the previous reaction was used.

Table 28 presents the initial and recovered masses of ionic liquid and the percentage of IL mass recovery (relative to the initial mass used) for the reactions performed.

Table 28 - Ionic liquid recovery masses.

Cycle	Initial IL mass (g)	Recovered IL mass (g)	Recovered IL mass (%)
1	1.5020	1.3396	88.19
2	1.3396	1.1410	85.17

Through Table 28, it is possible to observe that it was possible to recover and reuse the IL for the next reaction, obtaining in the last cycle a mass corresponding to 75.97% of the initial mass used in the first reaction.

FT-IR analyses were used to see if the ionic liquid recovered at the end of each round of reactions still matched its beginning structure. The spectra of the commercial ionic liquid used in the first reaction and the ionic liquid recovered from the last reaction are shown in Figure 60. The spectra have a 99.40 % correlation, which means that the structure of the initial IL and the recovered LI are very similar.

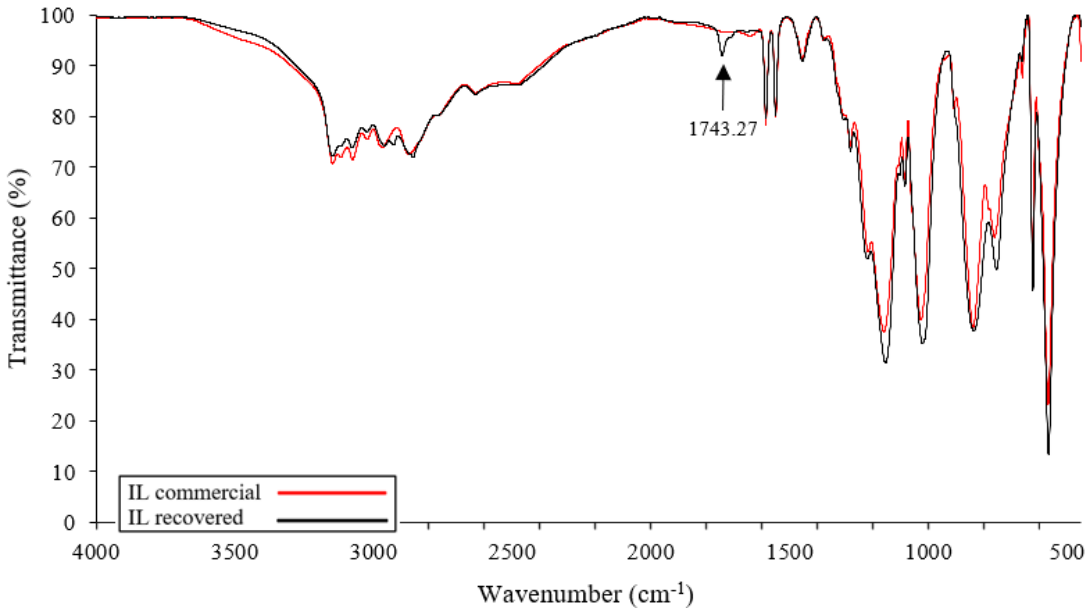

Figure 64 - Comparison of the FTIR spectra of the ionic liquid recovered from the last reaction and the commercial ionic liquid.

In Figure 64, it can be seen that the most significant difference between the two FT-IR spectra is the band 1743.27 cm^{-1}, but this absorption vibration is not present in the spectra of

oleic acid, used cooking oil and biodiesel. Therefore, it may be due to the presence of some impurity from the biodiesel production process or from the recovery of the ionic liquid.

Figure 65 shows the behavior of the conversion in terms of acidity reduction (R1), FAME content (R2) and Yield (R3) along the two reaction cycles. The conversion for the three responses, remains practically constant, with minor changes.

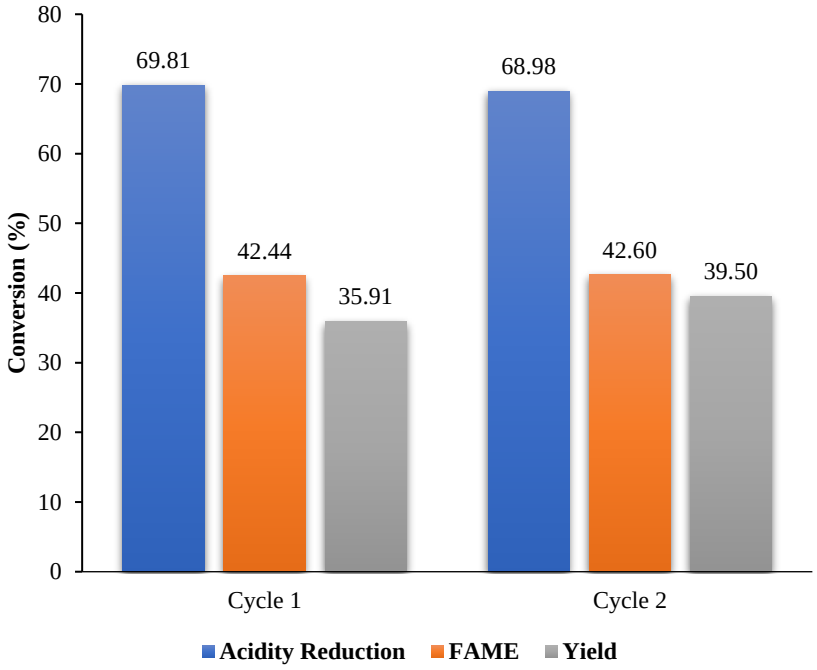

Figure 65 - Conversion in terms of acidity reduction, FAME content and Yield for the ionic liquid recovery cycles.

6. CONCLUSIONS

In this work, the production of biodiesel using methanol as alcohol and the ionic liquid 1-methylimidazolium hydrogen sulfate ([HIM][HSO_4]) as catalyst in the esterification reactions of a waste cooking oil with incorporation of oleic acid was studied.

One of the objectives of this work was the use of waste cooking oils for the production of biodiesel, given its enormous potential to reduce the cost associated with the product, making it competitive with the petrochemical market.

The Response Surface Methodology applied, allowed to understand how each factor (time, catalyst dosage, molar ratio oil/methanol and incorporation of oleic acid) influences the three responses chosen, the conversion in terms of acidity reduction (R1), the FAME content of the obtained biodiesel samples when [HMIM][HSO_4] was used as catalyst (R2) and the Yield in terms of FAME mass formed in relation to the initial one contained in the simulated oil (R3).

For the response R1, the most significant factor for the conversion was the molar ratio oil/methanol, followed by the reaction time and then by the OA incorporation, while for the responses R2 and R3, the most relevant factor was the incorporation of OA, followed by the molar ratio oil/methanol and finally by the reaction time. For all the responses, the least significant factor was the catalyst dosage. There were defined the ideal conditions that led to the highest possible conversion in terms of acidity reduction, the highest possible FAME content and Yield. The ideal conditions for acidity reduction were reaction time at 6 h, catalyst dosage at 5 % wt, molar ratio oil/methanol for 1:20 and 20 % wt OA incorporation, leading to a conversion of 76.70 %. The optimal conditions, which leads to the highest FAME content and highest Yield, of 42.02 % wt and 37.71 %, respectively, was estimated at 6 h of reaction time, 15 % wt of catalyst dosage, molar ratio oil/methanol for 1:20 and 60 % wt of OA incorporation.

The ionic liquid recovery process was studied for the optimal points of the R2 and R3 response, only for two cycles, in order to evaluate its recoverability and reuse efficiency, without observing significant yield losses in terms of reaction mass and without profound changes in the structure of the recovered IL in relation to the initial used. The washing method used for IL [HMIM][HSO_4] was with distilled water at a mass ratio of 1:3 IL/solvent. This recovery process proved to be efficient, as the correspondence of the IL recovered at the end of the two cycles with the commercial IL was 99.9 %.

The reaction conversion in terms of acidity reduction remains practically constant in the two recovery cycles, with a slight decrease from 69.81 % to 68.98 %. The content in FAME also remains practically constant, with a slight increase from 42.44 % to 42.60 %. The same happens for Yield, in which there is a small increase, from 35.91 % to 39.50 %. The ionic liquid

can be recovered and reused for at least two cycles, without significantly decreasing the reaction yield. In conclusion, [HMIM][HSO_4], was not able to promote the transesterification reaction, but presented excellent results as a catalyst for the esterification reaction. Its use can be applied as a preliminary treatment for non-edible commercial oils with high FFA content, that is, acid oils. The preliminary treatment may increase the cost of biodiesel production, but recovery of ionic liquid is an advantage to reduce process costs.

6.1. Suggestions for future works

Some studies are still necessary in order to fully evaluate the suitability of the ionic liquid 1-methylimidazolium hydrogen sulfate for biodiesel production. The suggestions for future work are:

- The study of biodiesel production using a two-stage conversion process. The first stage with [HMIM][HSO_4] ionic liquid as a catalyst for the esterification of the FFAs present in the waste oil and the second stage in a consecutive reaction with a basic catalyst such as NaOH and KOH, for the promotion of the transesterification reaction;
- The improvement of the recovery of [HMIM][HSO_4] IL with liquid-liquid extraction by screening a wide range of different organic solvents.

BIBLIOGRAPHY

Ajala, O. E., Aberuagba, F., Odetoye, T. E., & Ajala, A. M. (2015). Biodiesel: Sustainable Energy Replacement to Petroleum-Based Diesel Fuel – A Review. *ChemBioEng Reviews, 2*(3), 145-156. doi:https://doi.org/10.1002/cben.201400024

Alajmi, F. S., Hairuddin, A. A., Adam, N. M., & Abdullah, L. C. (2017). Recent trends in biodiesel production from commonly used animal fats. *International Journal of Energy Research, 42*(3), 885-902. doi:https://doi.org/10.1002/er.3808

Ambat, I., Srivastava, V., & Sillanpää, M. (2018). Recent advancement in biodiesel production methodologies using various feedstock: A review. *Renewable and Sustainable Energy Reviews, 90*, 356-369. doi:https://doi.org/10.1016/j.rser.2018.03.069

Banerjee, A., & Chakraborty, R. (2009). Parametric sensitivity in transesterification of waste cooking oil for biodiesel production—A review. *Resources, Conservation and Recycling, 53*(9), 490-497. doi:https://doi.org/10.1016/j.resconrec.2009.04.003

Banković-Ilić, I. B., Stamenković, O. S., & B., V. V. (2012). Biodiesel production from non-edible plant oils. *Renewable and Sustainable Energy Reviews, 16*, 3621-3647. doi:https://doi.org/10.1016/j.rser.2012.03.002

Bezerra, M. A., Santelli, R. E., Oliveira, E. P., Villar, L. S., & Escaleira, L. A. (2008). Response surface methodology (RSM) as a tool for optimization in analytical chemistry. *Talanta, 76*(5), 965-977. doi:https://doi.org/10.1016/j.talanta.2008.05.019

Bian, Y., Shan, Q., Guo, C., Liu, C., & Zhang, J. (2021). Biodiesel Production Over Esterifcation Catalyzed by a Novel Poly(Acidic Ionic Liquid)s. *Catalysis Letters*. doi:https://doi.org/10.1007/s10562-021-03592-x

Bian, Y., Zhang, J., Liu, C., & Zhao, D. (2019). Synthesis of Cross-Linked Poly Acidic Ionic Liquids and its Application in Biodiesel Production. *Catalysis Letters, 150*, 969–978. doi:https://doi.org/10.1007/s10562-019-02988-0

Bölük, S., & Sönmez, Ö. (2020). Microwave-Assisted Esterification of Oleic Acid Using an Ionic Liquid Catalyst. *Chemical Engineering & Technology, 43*(9), 1792-1801. doi:https://doi.org/10.1002/ceat.202000045

Box, G. E., & Behnken, D. W. (1960). Some New Three Level Designs for the Study of Quantitative Variables. *Technometrics, 2*, 455-475. doi:10.1080/00401706.1960.10489912

Cai, D., Zhan, G., Xiao, j., Zhou, S.-F., & Qiu, T. (2021). Design and synthesis of novel amphipathic ionic liquids for biodiesel production from soapberry oil. *Renewable Energy, 168*, 779-790. doi:https://doi.org/10.1016/j.renene.2020.12.051

Chang, F., & Zhou, Q. (2020). Facile Preparation of β-Cyclodextrin-Fe3O4 Magnetic-Brønsted Acidic Ionic Liquid for Biodiesel Production. *Waste and Biomass Valorization, 11*, 983–1988. doi:https://doi.org/10.1007/s12649-018-0506-4

Demirbas, A. (2008). *Biodiesel – A Realistic Fuel Alternative for Diesel Engines.* London: Springer-Verlag London Limited. doi:10.1007/978

Ding, H., Ye, W., Wang, Y., Wang, X., Li, L., Liu, D., . . . Ji, N. (2018). Process intensification of transesterification for biodiesel production from palm oil: Microwave irradiation on

transesterification reaction catalyzed by acidic imidazolium ionic liquids. *Energy, 144*, 957-967. doi:https://doi.org/10.1016/j.energy.2017.12.072

Diniz, H. O. (2020). *Valorização de óleos alimentares usados através de processos de conversão em biodiesel catalisados por líquidos iónicos.* Diniz, Heloísa Oliveira Resende. Obtido de https://bibliotecadigital.ipb.pt/handle/10198/23534

EN14214, E. C. (2003). *Automotive Fuels - Fatty acid methyl ester (FAME) engines - Requirements and teste methods.* EUROPEAN COMMITTEE FOR STANDARDIZATION.

Fan, M., Liu, H., & Zhang, P. (2018). Ionic liquid on the acidic organic-inorganic hybrid mesoporous material with good acid-water resistance for biodiesel production. *Fuel, 215*, 541-550. doi:https://doi.org/10.1016/j.fuel.2017.11.085

Fauzi, A. H., Saidina, N. A., & Amin. (2012). An overview of ionic liquids as solvents in biodiesel synthesis. *Renewable and Sustainable Energy Reviews, 16*(8), 5770-5786. doi:https://doi.org/10.1016/j.rser.2012.06.022

Freemantle, M. (2010). *An Introduction to Ionic Liquids.* Royal Society of Chemistry. Obtido de https://books.google.pt/books?id=kvM2YEftV2cC&dq=%E2%80%A2%09Freemantle+M.,+An+Introducion+to+Ionic+Liquids,+2010.&lr=&hl=pt-PT&source=gbs_navlinks_s

GAIN. (2017). *Portugal Biofuel Market Outlook 2017.* GAIN. Obtido de https://apps.fas.usda.gov/newgainapi/api/report/downloadreportbyfilename?filename=Portugal%20Biofuel%20Market%20Outlook%20_Madrid_Portugal_6-21-2017.pdf

Goes, H. H. (2018). *Estudo da produção de biodiesel por transesterificação catalisada por líquidos iónicos.* Goes, Higgor Henrique Dias. Obtido de https://bibliotecadigital.ipb.pt/handle/10198/19238

Gupta, J., Agarwal, M., & Dalai, A. (2016). Optimization of biodiesel production from mixture of edible and nonedible vegetable oils. *Biocatalysis and Agricultural Biotechnology, 8*, 112-120. doi:https://doi.org/10.1016/j.bcab.2016.08.014

Hoekman, S. K., Broch, A., Robbins, C., Ceniceros, E., & Natarajan, M. (2012). Review of biodiesel composition, properties, and specifications. *Renewable and Sustainable Energy Reviews, 16*(1), 143-169. doi:https://doi.org/10.1016/j.rser.2011.07.143

Ishak, Z. I., Sairi, N. A., Aroua, M. K., & Yusoff, R. (2017). A review of ionic liquids as catalysts for transesterification reactions of biodiesel and glycerol carbonate production. *Catalysis Reviews*, 44-93. doi:10.1080/01614940.2016.1268021

Johnston, M., & Holloway, T. (2007). A Global Comparison of National Biodiesel Production Potentials. *Environ. Sci. Technol., 41*(23), 7967–7973. doi:https://doi.org/10.1021/es062459k

Koel, M. (2008). *Ionic Liquids in Chemical Analysis.* Taylor & Francis Group, LLC. Obtido de https://books.google.pt/books?hl=pt-PT&lr=&id=y8d9F7NG60cC&oi=fnd&pg=PP1&dq=%E2%80%A2%09Koel+M.,+Ionic+Liquids+in+Chemical+Analysis,+Analytical+Chemistry,+2008.+&ots=R2NM-bNESZ&sig=sIE-mq6pXXSNa5GSKQgVRcGE4N0&redir_esc=y#v=onepage&q=%E2%80%A2%09Koel%20M.%

Lam, M. K., Lee, K. T., & Mohamed, A. R. (2010). Homogeneous, heterogeneous and enzymatic catalysis for transesterification of high free fatty acid oil (waste cooking oil) to biodiesel: A review. *Biotechnology Advances, 28*(4), 500-518. doi:https://doi.org/10.1016/j.biotechadv.2010.03.002

Leung, D. Y., Wu, X., & Leung, M. (2010). A review on biodiesel production using catalyzed transesterification. *Applied Energy, 87*(4), 1083-1095. doi:https://doi.org/10.1016/j.apenergy.2009.10.006

Li, Q., Du, W., & Liu, D. (2008). Perspectives of microbial oils for biodiesel production. *Applied Microbiology and Biotechnology, 80*, 749–756. doi:10.1007/s00253-008-1625-9

Lin, Y.-C., Yang, P.-M., Chen, S.-C., & Lin, J.-F. (2013). Improving biodiesel yields from waste cooking oil using ionic liquids as catalysts with a microwave heating system. *Fuel Processing Technology, 115*, 57-62. doi:https://doi.org/10.1016/j.fuproc.2013.04.00

Lôbo, I. P., Ferreira, S. L., & Cruz, R. S. (2009). Biodiesel: quality parameters and analytical methods. *Química Nova, 32*, 1596-1608. doi:10.1590/S0100-40422009000600044

Mahlia, T., Syazmi, Z., Mofijur, M., Pg Abas, A., Bilad, M. O., & Silitonga, A. (2020). Patent landscape review on biodiesel production: Technology updates. *Renewable and Sustainable Energy Reviews, 118*, 1364-0321. doi:https://doi.org/10.1016/j.rser.2019.109526

Mohammad, A., & Inamuddin. (2012). *Green Solvents II - Properties and Applications of Ionic Liquids.* Springer, Dordrecht. doi:https://doi.org/10.1007/978-94-007-2891-2

Mohammadi, F., Rahimi, M., Parvareh, A., & Feyzi, M. (2018). Biodiesel production from soybean oil using ionic liquid as a catalyst in a microreactor. *Iranian Journal of Chemical Engineering (IJChE), 15*(1), 102-114. Obtido de http://www.ijche.com/article_63151_f41b09ac3165a57095799e3516e643df.pdf

Muriell, G. (2009). *Produção de biodiesel através de catálise enzimática em líquido iônico.* doi:https://www.lume.ufrgs.br/bitstream/handle/10183/18402/000718412.pdf?sequence=1&isAllowed=y

Pavia, D. L., Lampman, G. M., Kriz, G. S., & Vyvyan, J. A. (1989). *Spectral data for structure determination of organic compounds.* Berlin: Springer-Verlag. Obtido de https://books.google.pt/books?hl=pt-PT&lr=&id=N-zKAgAAQBAJ&oi=fnd&pg=PP1&dq=Pavia+DL,+Lampman+GM,+Kriz+GS.+Introduction+to+Spectroscopy.+2nd+Edition.+Orlando:+Saunders+College+Publishing%3B+1979.&ots=XfihbZjQYD&sig=bsZbjY0_yk5xGtHZl9ckp4-4_4s&redir_esc=y#

Plechkovaa, N. V., & Seddonab, K. R. (2007). Applications of ionic liquids in the chemical industry. *The Royal Society of Chemistry*. doi:10.1039/b006677j

Ramos, L. P., Silva, F. R., Mangrich, A. S., & Cordeiro, C. S. (2011). Tecnologias de Produção de Biodiesel. *Revista Virtual de Quimica, 3*, 385-405. Obtido de http://www.uff.br/rvq

REN21. (2021). *RENEWABLES 2021 - GLOBAR STATUS REPORT.* REN21. Obtido de https://www.ren21.net/wp-content/uploads/2019/05/GSR2021_Full_Report.pdf

Roman, F. F., Ribeiro, A. E., Queiroz, A., Lenzi, G. G., Chaves, E. S., & Brito, P. (2019). Optimization and kinetic study of biodiesel production through esterification of oleic acid applying ionic liquids as catalysts. *Fuel, 239*, 1231-1239. doi:https://doi.org/10.1016/j.fuel.2018.11.087

Ruhul, A. M., Kalam, M. A., Masjuki, H. H., Fattah, I. M., Rehama, S. S., & Rasheda, M. M. (2015). State of the art of biodiesel production processes: a review of the heterogeneous catalyst. *RSC Advances*, 4-53. Obtido de https://pubs.rsc.org/en/content/getauthorversionpdf/C5RA09862A

Sahar, Sadaf, S., Iqbal, J., Ullah, I., Bhatti, H. N., Nouren, S., . . . Nisar, J. (2018). Biodiesel production from waste cooking oil: An efficient technique to convert waste into biodiesel. *Sustainable Cities and Society, 41*, 220-226. doi:https://doi.org/10.1016/j.scs.2018.05.037

Sajjadi, B., Raman, A. A., & Arandiyan, H. (2016). A comprehensive review on properties of edible and non-edible vegetable oil-based biodiesel: Composition, specifications and prediction models. *Renewable and Sustainable Energy Reviews, 63*, 62-92. doi:https://doi.org/10.1016/j.rser.2016.05.035

Santori, G., Nicola, G., Moglie, M., & Polonara, F. (2012). A review analyzing the industrial biodiesel production practice starting from vegetable oil refining. *Applied Energy, 92*, 109-132. doi:https://doi.org/10.1016/j.apenergy.2011.10.031

Shaterian, H., & Mohammadnia, M. (2013). Acidic Brønsted Ionic Liquids Catalyzed the Preparation of 1-((Benzo[d]thiazol-2-ylamino)(aryl)-methyl)naphthalen-2-ol Derivatives 1-[(1,3-Benzothiazol-2-ylamino)(aryl)methyl]-2-naphthol. *S. Afr. J. Chem, 66*, 60–63. Obtido de https://www.ajol.info/index.php/sajc/article/view/123101

Silva, J. (2008). *Caracterização de Materiais Catalíticos.* Obtido de http://mtc-m16c.sid.inpe.br/attachment.cgi/sid.inpe.br/mtc-m18@80/2008/07.08.15.19/doc/publicacao.pdf

Singh, S. K., & Savoy, A. W. (2020). Ionic liquids synthesis and applications: An overview. *Journal of Molecular Liquids, 297*, 112038. doi:https://doi.org/10.1016/j.molliq.2019.112038

Tabatabaei, M., & Aghbashlo, M. (2018). *Biodiesel - From Production to Combustion.* Springer Nature Switzerland AG. doi:10.1007/978

Tran, D.-T., Chang, J.-S., & Lee, D.-J. (2017). Recent insights into continuous-flow biodiesel production via catalytic and non-catalytic transesterification processes. *Applied Energy, 185*, 376-409. doi:https://doi.org/10.1016/j.apenergy.2016.11.006

U.S Department of Energy. (2016). *Biodiesel Handling and Use Guide (Fifth Edition).* U.S Department of Energy. Obtido de https://www.nrel.gov/docs/fy17osti/66521.pdf

UFOP. (2021). *REPORT ON GLOBAL MARKET SUPPLY 2020/2021.* UFOP. Obtido de https://www.ufop.de/files/7216/1649/5848/UFOP_SupplyReport_2020-2021__120321.pdf

Ullah, Z., Bustam, M. A., & Man, Z. (2015). Biodiesel production from waste cooking oil by acidic ionic liquid as a catalyst. *Renewable Energy, 77*, 521-526. doi:https://doi.org/10.1016/j.renene.2014.12.040

Ullah, Z., Bustam, M. A., Man, Z., Khan, A. S., Muhammad, N., & Sarwomo, A. (2017). Preparation and kinetics study of biodiesel production from waste cooking oil using new functionalized ionic liquids as catalysts. *Renewable Energy, 114*, 755-765. doi:https://doi.org/10.1016/j.renene.2017.07.085

Ullah, Z., Khan, A. S., Muhammad, N., Ullah, R., Alqahtani, A. S., Shah, S. N., . . . Man, Z. (2018). A review on ionic liquids as perspective catalysts in transesterification of different feedstock oil into biodiesel. *Journal of Molecular Liquids, 266*, 673-686. doi:https://doi.org/10.1016/j.molliq.2018.06.024

Wei, X., Xiao-dong, G., Xiu-hua, Y., & Rong, S. (2015). Optimization of methyl ricinoleate synthesis with ionic liquids as catalysts using the response surface methodology. *Chemical Engineering Journal, 275*, 63-70. doi:https://doi.org/10.1016/j.cej.2015.04.035

Wu, Q., Chen, H. M., Wang, D., & Wang, J. (2007). Transesterification of Cottonseed Oil Catalyzed by Brønsted Acidic Ionic Liquids. *Ind. Eng. Chem. Res., 46, 24*, 7955–7960. doi:https://doi.org/10.1021/ie070678o

Yaakob, Z., Mohammad, M., Alherbawi, M., Alam, Z., & Sopian, K. (2013). Overview of the production of biodiesel from Waste cooking oil. *Renewable and Sustainable Energy Reviews*, 184-193.

Yue, S., Lei, L., TieQiang, R., QingDong, Q., & Qiang, L. (2015). Synthesis of oleic acid methyl oleate catalyzed by acidic ionic liquid [Hmim] HSO4. *China Oils and Fats, 40*, 68-71. doi:https://www.cabdirect.org/globalhealth/abstract/20153201483

APENDIX A - XXVII National Meeting of Portuguese Chemical Society

XXVII ENCONTRO NACIONAL
Sociedade Portuguesa de Química

Braga, 14-16 julho 2021

Abstract Certificate

This is to certify that

Fábio Júlio Santos Monteiro

presented the Comunicação em Painel entitled

Valorization of used cooking oils through ionic liquid catalyzed biodiesel conversion processes

at the XXVII Encontro Nacional da Sociedade Portuguesa de Química - in Universidade do Minho, Braga, from 14 a 16 julho 2021

The Organizing Committee

XXVII ENCONTRO NACIONAL
Sociedade Portuguesa de Química

Braga, 14-16 julho 2021

Participation Certificate

This is to certify that

Fábio Júlio Santos Monteiro

attended the XXVII Encontro Nacional da Sociedade Portuguesa de Química which was held in Universidade do Minho, Braga, from 14 a 16 julho 2021

The Organizing Committee